



National Library
of Canada

Bibliothèque nationale
du Canada

Acquisitions and
Bibliographic Services Branch

Direction des acquisitions et
des services bibliographiques

395 Wellington Street
Ottawa, Ontario
K1A 0N4

395, rue Wellington
Ottawa (Ontario)
K1A 0N4

Your file *Votre référence*

Our file *Notre référence*

NOTICE

The quality of this microform is heavily dependent upon the quality of the original thesis submitted for microfilming. Every effort has been made to ensure the highest quality of reproduction possible.

If pages are missing, contact the university which granted the degree.

Some pages may have indistinct print especially if the original pages were typed with a poor typewriter ribbon or if the university sent us an inferior photocopy.

Reproduction in full or in part of this microform is governed by the Canadian Copyright Act, R.S.C. 1970, c. C-30, and subsequent amendments.

AVIS

La qualité de cette microforme dépend grandement de la qualité de la thèse soumise au microfilmage. Nous avons tout fait pour assurer une qualité supérieure de reproduction.

S'il manque des pages, veuillez communiquer avec l'université qui a conféré le grade.

La qualité d'impression de certaines pages peut laisser à désirer, surtout si les pages originales ont été dactylographiées à l'aide d'un ruban usé ou si l'université nous a fait parvenir une photocopie de qualité inférieure.

La reproduction, même partielle, de cette microforme est soumise à la Loi canadienne sur le droit d'auteur, SRC 1970, c. C-30, et ses amendements subséquents.

Canada

UNIVERSITY OF ALBERTA

HYDROCRACKING OF ATHABASCA BITUMEN

by



ALAN AYASSE

A THESIS

SUBMITTED TO THE FACULTY OF GRADUATE STUDIES AND RESEARCH
IN PARTIAL FULFILLMENT OF THE REQUIREMENTS FOR THE DEGREE
OF MASTER OF SCIENCE

DEPARTMENT OF CHEMICAL ENGINEERING

EDMONTON, ALBERTA

FALL, 1994



National Library
of Canada

Acquisitions and
Bibliographic Services Branch

395 Wellington Street
Ottawa, Ontario
K1A 0N4

Bibliothèque nationale
du Canada

Direction des acquisitions et
des services bibliographiques

395, rue Wellington
Ottawa (Ontario)
K1A 0N4

Your file *Voire référence*

Our file *Notre référence*

The author has granted an irrevocable non-exclusive licence allowing the National Library of Canada to reproduce, loan, distribute or sell copies of his/her thesis by any means and in any form or format, making this thesis available to interested persons.

L'auteur a accordé une licence irrévocable et non exclusive permettant à la Bibliothèque nationale du Canada de reproduire, prêter, distribuer ou vendre des copies de sa thèse de quelque manière et sous quelque forme que ce soit pour mettre des exemplaires de cette thèse à la disposition des personnes intéressées.

The author retains ownership of the copyright in his/her thesis. Neither the thesis nor substantial extracts from it may be printed or otherwise reproduced without his/her permission.

L'auteur conserve la propriété du droit d'auteur qui protège sa thèse. Ni la thèse ni des extraits substantiels de celle-ci ne doivent être imprimés ou autrement reproduits sans son autorisation.

ISBN 0-315-95000-5

Canada

UNIVERSITY OF ALBERTA

RELEASE FORM

NAME OF AUTHOR: ALAN AYASSE

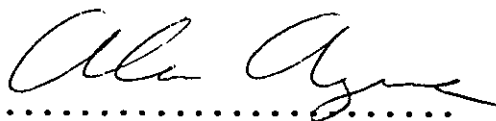
TITLE OF THESIS: HYDROCRACKING OF ATHABASCA BITUMEN

DEGREE: MASTER OF SCIENCE

YEAR THIS DEGREE GRANTED: 1994

Permission is hereby granted to the University of Alberta Library to reproduce single copies of this thesis and to lend or sell such copies for private, scholarly or scientific research purposes only.

The author reserves all other publication and other rights in association with the copyright in the thesis, and except as hereinbefore provided neither the thesis nor any substantial portion thereof may be printed or otherwise reproduced in any material form whatever without the author's prior written permission.



.....

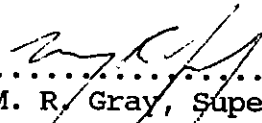
Alan Ayasse
32 Burnham Ave
St. Albert, AB
T8N 0A7

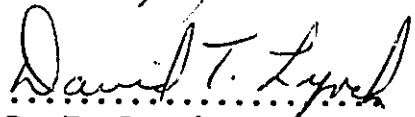
Aug. 9, 1994
.....

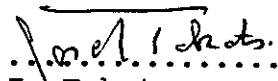
UNIVERSITY OF ALBERTA

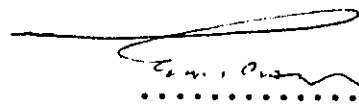
FACULTY OF GRADUATE STUDIES AND RESEARCH

The undersigned certify that they have read, and recommend to the Faculty of Graduate Studies and Research for acceptance, a thesis entitled **HYDROCRACKING OF ATHABASCA BITUMEN** submitted by **ALAN AYASSE** in partial fulfillment of the requirements for the degree of **MASTER OF SCIENCE**.


.....
M. R. Gray, Supervisor


.....
D. T. Lynch


.....
J. Takats


.....
E. Chan

Date: *Aug. 9, 1994*
.....

DEDICATION

I would like to dedicate this thesis to my family for their support during the entire process.

ABSTRACT

The kinetics for the hydrocracking of Athabasca bitumen were investigated using a one litre CSTR. Reactions were done at 430 °C with a total pressure of 13.7 MPa for residence times between 0.4 and 1.9 h. A fixed annular catalyst basket was used with 78 g of industrial hydrocracking catalyst. Further runs were done at a residence time of 0.96 h with crushed catalyst, down to approximately 600 μm spheres, in order to estimate the effectiveness factors for conversion reactions using the aforementioned catalyst. The effect of temperature was investigated, both with and without catalyst, for temperatures between 400 and 450 °C. One run was also done at 10 MPa to investigate the effect of hydrogen concentration on the reactions.

The product was divided into four boiling cuts: naphtha (IBP-177°C), middle distillate (177-343°C), gas oil (343-525°C), and residue (525°C+). Elemental analysis was done for carbon, hydrogen, sulfur and nitrogen on the whole product as well as on each cut. Further analysis were done for pyrrolic nitrogen for all the samples, and also for sulfides on selected samples.

The boiling cut distribution of the product was modelled using lumped first order kinetics. A four parameter model was developed to predict the boiling cut distribution as a function of the residence time.

Residue and micro carbon residue conversion, as well as hydrodesulfurization and hydrodenitrogenation were found to be

approximately first order, with rate constants of 2.22, 1.58, 3.66, and 0.57 h⁻¹, respectively. The thermal contribution to the reactions was determined to be 70, 30, 10 and 0%, respectively. No stoichiometric relationship was found for these constituents.

A more detailed investigation of the product found the added catalyst prevented dehydrogenation of the heavy cuts up to 440 °C. The behaviour of the pyrrolic nitrogen content was consistent with initial cracking of N-substituted chains from the pyrrolic structures. Reaction in the presence of catalyst at high severity gave a significant reduction in the pyrrolic nitrogen content of the residue cut. This was consistent with the occurrence of bridge formation at the nitrogen atom. Evidence was also seen for the significant hydrogenation of the thiophenes to give sulfides.

The effectiveness factor for the residue conversion was found to be approximately 0.3.

ACKNOWLEDGEMENTS

I would like to thank Dr. Murray Gray for his tremendous effort in guiding and supporting the work presented in this thesis. I would also like to thank Syncrude Canada Limited for both their financial and practical support, specifically Dr. Edward Chan, Dave Famulak and Ron Bourassa. Finally I would like to thank my fellow graduate students for making this a sane and enjoyable experience.

TABLE OF CONTENTS

<u>Chapter</u>		<u>Page</u>
	List of Tables	
	List of Figures	
1.	Introduction	1
2.	Literature Review	4
	2.1 Introduction	5
	2.2 Reactions During Hydrocracking	5
	2.3 Reaction Kinetics	6
	2.3.1 Hydrocracking	6
	2.3.2 Hydrogenation	7
	2.3.3 Sulfur	11
	2.3.4 Nitrogen	14
	2.4 Analysis of Sulfides and Pyrroles	15
3.	Materials and Methods	17
	3.1 Selection of Experimental Reactor	18
	3.2 Reactor System	20
	3.2.1 Feed System	20
	A. Bitumen	20
	B. Hydrogen	22
	3.2.2 Reactor	22
	3.2.3 Product System	24
	A. Liquid System	24
	B. Vapor System	24
	3.3 Summary of Operating Procedure	25
	3.4 Analytical Techniques	27
	3.4.1 Distillation	27

3.4.2	Carbon and Hydrogen Analysis	27
3.4.3	Sulfur Analysis	28
3.4.4	Nitrogen Analysis	28
3.4.5	Metals Analysis	28
3.4.6	Micro Carbon Residue Analysis	28
3.4.7	Pyrrolic Nitrogen Analysis	28
3.4.8	Sulfide Analysis	30
3.5	Catalyst	31
4.	Overall Kinetics	32
4.1	Introduction	33
4.2	Overall Kinetics of Residue Conversion	34
4.3	Overall Kinetics of Sulfur Removal	39
4.4	Overall Kinetics of Nitrogen Removal	42
4.5	Removal of Micro Carbon Residue	44
4.6	Stoichiometric Plots	46
4.7	Conclusions	52
5.	Kinetic Model for Hydrocracking of Residue	55
5.1	Introduction	56
5.2	Kinetic Model of Mosby et al.	57
5.3	Modified Model for Hydrocracking	63
5.3.1	Parameter Estimation	66
5.4	Conclusions	82
6.	Sulfide and Pyrrole Analysis	83
6.1	Introduction	84
6.2	Hydrogenation	84
6.3	Nitrogen Types	94
6.4	Sulfur	116

6.4.1	Kinetics of removal of sulfur types	125
6.5	Effectiveness Factor	130
6.6	Conclusions	136
7.	List of References	138
Appendix A:	Summary of Reactor Runs	143
Appendix B:	Metals Content	195
Appendix C:	Arrhenius Plots	198

LIST OF TABLES

<u>Table</u>		<u>Page</u>
3.1	Catalyst Composition	31
4.1	Confirmation of Sulfur Analysis	41
4.2	Summary of Kinetic Data	52
5.1	Summary of Unknown Parameters in Modified Model	64
5.2	Stoichiometric Coefficients for Gas Oil Conversion	67
5.3	Best Fit Parameters	75
5.4	Modified Model, best fit to CANMET data	77
5.5	Stoichiometric Coefficients for Modified Model	81
6.1	Nitrogen Compounds in Hydrocracker Product	100
6.2	Thermal Changes in Nitrogen Compounds with Temperature	109
6.3	Catalytic Changes in Nitrogen Compounds with Temperature	111
6.4	Catalytic to Thermal Sulfur Ratio at 420°C	120
6.5	Mass Percent Sulfide in Cuts	123
6.6	Sulfide to Sulfur Ratio in Cuts	124
6.7	Ratio of Sulfide Formation to Hydrogenolysis in Hydrotreating of Thiophenic Model Compounds over Co-Mo on γ -Alumina Catalyst	128
6.8	Catalyst Effectiveness Factors	131
6.9	Sulfur Content as Related to Residue Conversion	135

LIST OF FIGURES

<u>Figure</u>		<u>Page</u>
2.1	Chemical Structures	9
2.2	Pathways for Dibenzothiophene Conversion	13
3.1	Simplified Schematic for Reactor System	21
4.1	Rate Residue Conversion vs Residue Concentration, Log Plot	37
4.2	Rate Residue Conversion vs Residue Concentration	38
4.3	Rate HDS vs Concentration Sulfur	40
4.4	Rate HDN vs Concentration Nitrogen	43
4.5	Ln MCR Conversion Rate vs Ln Concentration MCR	45
4.6	Rate MCR vs Rate Residue	48
4.7	Rate MCR vs Rate HDS	49
4.8	Rate HDS vs Rate Residue Conversion	50
4.9	Stoichiometric Plot at Different Temperatures	53
5.1	Kinetic Model for Hydrocracking of Residue	58
5.2	Fit of Mosby Model to Data for Hydrocracking of Athabasca Bitumen	62
5.3	Modified Hydrocracking Model	65
5.4	First Order Fit for Residue Conversion, Thermal Data	73
5.5	Fit of Modified Mosby Model to Residence Time Data	74
5.6	Residuals for the Residence Time Data	76
5.7	Residuals for the Thermal Data	78
5.8	Gas Production Rate for the Residence Time Data	80
6.1	H/C Molar Ratio in Product	85

6.2	H/C Molar Ratio vs Temperature	89
6.3	Residue Conversion vs Temperature	93
6.4	Pyrrolic Nitrogen Content vs Time	96
6.5	Nitrogen Content vs Time	98
6.6	Pyrrole Conversion Rate vs Concentration	102
6.7	Nitrogen Content in Boiling Cuts vs Residence Time	103
6.8	Nitrogen to Carbon Molar Ratio	105
6.9	Boiling Cut Composition, Catalytic Runs	112
6.10	Boiling Cut Composition, Thermal Runs	113
6.11	Total Sulfur Concentration vs Residence Time	117
6.12	Sulfur Content for Catalytic Runs	118
6.13	Sulfur Content for Thermal Runs	119
6.14	Sulfur Content vs Residence Time	121
6.15	Theoretical Fit to Sulfur Data	127
6.16	Total N Concentration vs Catalyst Size	132
6.17	Total Sulfur Concentration vs Catalyst Size	134

Chapter 1
Introduction

The upgrading of heavy oil and bitumen to synthetic crude oil contributes approximately 20% of Canada's fuel supply. Hydrocracking is one key processes in the production of synthetic crude oil but, although this process is currently practised at the industrial scale, many questions remain about the chemistry and kinetics of the hydrocracking process. Due to the complexity of the reactions taking place during hydrocracking, measurements of overall kinetics are of limited use for process operating purposes.

Due to environmental considerations and ease of downstream processing, detailed kinetics for the removal of sulfur and nitrogen during hydrocracking are especially important to industry. In order to understand the effects of hydrocracking operating conditions, the intrinsic kinetics for the hydrodesulfurization and hydrodenitrogenation must be determined. Some type of lumping scheme is required in order to deal with the large number of sulfur and nitrogen components associated with the bitumen feedstock and the products from the hydrocracking reactions.

The kinetic measurements were conducted in a one litre CSTR hydrocracking system installed in the Department of Chemical Engineering at the University of Alberta with the assistance of Syncrude Canada Limited. This equipment, along with the procedure for running it and the product analyses, are described in Chapter 3. For analysis, the product was fractionated into four boiling cuts: naphtha, middle

distillate, gas oil and residue. An elemental analysis was performed on the total liquid product as well as on the four distillation cuts. Further analyses for sulfur types (thiophenes vs sulfides), and nitrogen types (pyrroles vs other nitrogen species) were also performed. This data is used in the following three chapters to analyse the kinetics for the whole product, model the cracking reactions, and investigate the sulfide and pyrrole contents in the different boiling cuts. The effects of the different hydrocracking conditions on the kinetics of hydrocracking, heteroatom removal, and the changes in sulfur and nitrogen compound types is the focus of this thesis.

Chapter 2
Literature Review

2.1 Introduction

There is a great deal of literature published on the subject of hydroprocessing reactions. This review will therefore concentrate on the hydrocracking of heavy feedstocks, except in cases where information is only available at milder hydroprocessing conditions. This review is not intended to be exhaustive, but to present relevant previous work from the literature. The review will include modelling of the hydrocracking of a heavy feedstock, sulfide and pyrrole analysis, and reaction kinetics.

2.2 Reactions During Hydrocracking

In order to upgrade bitumen to synthetic crude oil the largest molecules must be reduced in size through cracking of carbon-carbon and carbon-sulfur bonds. In hydrocracking, the hydrogen to carbon ratio is raised through hydrogenation of unsaturated bonds, while heteroatoms such as sulfur and nitrogen are partially removed in gases such as H_2S and NH_3 . The reactions taking place during hydrocracking can generally be divided into thermal and catalytic categories. Miki et al. (1983) asserted that for hydrocracking of heavy oil, the cracking reaction is primarily thermal, hydrodesulfurization (HDS) and hydrogenation are mostly catalytic, and hydrodenitrogenation (HDN) is completely catalytic. They also found that one-third to one-half of the cracking occurred without accompanying hydrogenation. The authors concluded

that the main role of the catalyst was to supply hydrogen to the heavy fractions and prevent carbonization. Khorasheh et al. (1989) found similar results for the hydrocracking of Syncrude coker gas oil at 430°C, with the catalyst active for heteroatom removal but the cracking rate determined thermally.

2.3 Reaction Kinetics

During the processing of hydrocarbons the macroscopic properties of the final product are of great commercial interest. For example, the final heteroatom content or aromaticity of gasoline is very important, and this in turn influences the selection of the various secondary upgrading processes. During operations such as hydrotreating and hydrocracking, kinetic data for HDS and HDN are needed for reactor design and optimization considerations. However, these kinetic analyses are of limited value, as the intrinsic kinetics remain unknown. Work has been done, however, with model compounds in order to try to obtain a better understanding of the reactions involved in these processes.

2.3.1 Hydrocracking

Examination of the detailed kinetics of a complex mixture such as bitumen necessarily involves studying broad structural classes. As each individual structure cannot, for practical reasons, be independently examined, it becomes necessary to lump the compounds into classes which are expected to encompass the behavior of the their components. During

hydrocracking the composition of the liquid phase is changing through a variety of reactions, the most predominant of which is the cracking of large molecules to yield smaller molecules. Although several models do exist for the cracking of light hydrocarbons, very little has been published about the hydrocracking of heavy feedstocks. Koseoglu and Phillips (1988) used a lumping scheme based on SARA (saturates, aromatics, resins and asphaltenes) analysis, but this is not appropriate here as this data was not available. The most obvious lumping scheme for such reactions is through boiling cuts, which roughly divide the mixture by molecular size and can easily be measured by distillation. Mosby et al. (1986) give such a model for hydrocracking of vacuum residue into gas oil, middle distillate and naphtha. The reactions in the network are assumed to be first order, with all the rate constants given relative to one reaction; this reaction network is demonstrated in Figure 5.1. The network was fit to pilot plant data, with one adjustable parameter for different feeds.

2.3.2 Hydrogenation

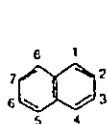
Information pertaining to hydrogenation reactions comes from two main sources: studies involving heavy feedstocks during hydrotreating or hydrocracking, and model compound studies involving aromatic structures.

Sapre and Gates (1981) studied the hydrogenation of four model compounds with sizes between benzene and 2-

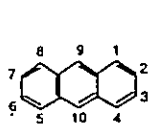
phenylnaphthalene at hydrotreating conditions (325 °C and 75 atm) using a cobalt-molybdenum catalyst. Figure 2.1 gives the structures for a variety of the aromatic hydrocarbons discussed here. They observed pseudo first-order kinetic behavior and found naphthalene, with two fused rings, to be an order of magnitude more reactive than benzene. Hydrogenation of naphthalene did not achieve equilibrium at short residence times.

Girgis and Gates (1991) reviewed the data for hydrogenation of aromatics at hydrotreating conditions. For model compounds with few rings, equilibrium was rapidly achieved at hydrotreating conditions. The hydrogenation of naphthalene was generally an order of magnitude faster than that of tetralin. Wilson et al. (1985), using middle distillate from Athabasca bitumen, only observed the effect of thermodynamic equilibrium above 400 °C. The predominant aromatic species in this distillate were alkylbenzenes, tetralines, benzodicycloparaffins and naphthalenes with concentrations decreasing in that order. Quantitative networks for three or four ring structures are not available (Girgis and Gates), but increasing space times are required to obtain equilibrium hydrogenation, and fully hydrogenating the large ring structures may not be possible at lower pressures. Overall, these observations suggest that thermodynamic limitations are unlikely to be significant in hydrogenation of heavy residues.

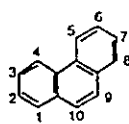
1. Aromatic Hydrocarbons



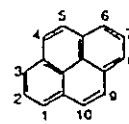
Naphthalene



Anthracene



Phenanthrene

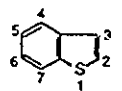


Pyrene

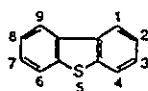
2. Organosulfur Compounds



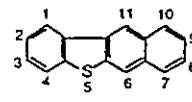
Thiophene



Benzothiophene



Dibenzothiophene

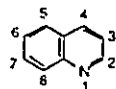


Benzo[b]naphtho[2,3-d]thiophene

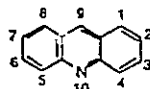
3. Organonitrogen Compounds



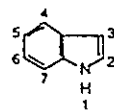
Pyridine



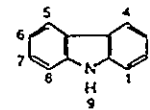
Quinoline



Acridine



Indole



Carbazole

Figure 2.1: Chemical Structures
(Girgis and Gates, 1991)

Hydrogenation information is also available in the form of direct measurements using heavy feedstocks. Beret and Reynolds (1985) used several heavy feedstocks to investigate hydrogen incorporation. They found that with increased processing temperature the proportion of the consumed hydrogen going to cracking increases. Additionally, using a higher boiling cut feed resulted in more of the hydrogen being incorporated by hydrogenation relative to cracking. They found the catalyst to be crucial for this hydrogenation activity. Reynolds and Beret (1989) in a study of the effect of prehydrogenation before hydrotreating of Maya residue measured the hydrogen to carbon molar ratio of the feed and hydrotreating product. It is interesting to note that both with and without the prehydrogenation step the H/C ratio in the product is higher for the higher severity hydrotreating cases, which use a higher temperature. The actual operating conditions were not specified so hydrogen pressure is not known and may also have been changed. In a follow-up paper, Beret and Reynolds (1990) further investigate how the hydrogen is incorporated through ^1H and ^{13}C NMR and a molar balance on the gases and heteroatoms. They show a correlation between the aromaticity and H/C ratio for selected feeds and products, but say this correlation is not accurate enough to predict reactivity. Hydrogen is shown to be incorporated in the liquid by both hydrogenation and cracking reactions, with cracking taking on increased importance as the severity of the

hydrotreating is increased. Steer et al. (1992) used isotope ratio mass spectrometry to follow hydrogen incorporation during the hydrocracking of four Alberta residues at typical hydrocracking conditions. They found more hydrogen incorporation from the gas phase in the light cuts for all four feeds. A net hydrogenation of the residue for the Athabasca and Peace River feeds was seen while a net dehydrogenation of the residue for the Cold Lake and Lloydminster feeds was observed.

2.3.3 Sulfur

The compounds of interest in sulfur removal are the aromatic types, due to their relatively inert nature. Most of the work in the literature focused on thiophene, but, as this is only a single ring structure, it is not the most desirable model compound for bitumen. Some work has, however, been done with dibenzothiophene, which has three rings. As dibenzothiophene is closer to the type of ring structures in bitumen, it makes a better model compound for sulfur removal from heavy feedstocks. Most of the work done with this compound used hydrotreating rather than hydrocracking conditions, with temperatures below 400 °C, and often with lower hydrogen pressure as well (Girgis and Gates, 1991). A reaction network for the desulfurization of dibenzothiophene was proposed by Houalla et al. (1978). In this network there are two pathways for sulfur removal: hydrogenation of one of

the outer rings followed by removal of the sulfur atom, and direct removal of the sulfur from the aromatic structure through hydrogenolysis. Figure 2.2 shows the network proposed by Houalla et al. (1981) and indicates the two pathways for sulfur removal. The authors used pseudo first-order kinetics for all the reactions, and found that with cobalt-molybdenum catalyst and no added hydrogen sulfide the hydrogenolysis pathway is three orders of magnitude faster than the hydrogenation pathway. However, with methyl groups in the four and six positions, or using nickel instead of cobalt catalyst, or with hydrogen sulfide in the reaction mixture the hydrogenation pathway becomes increasingly important. Broderick and Gates (1981) further elucidated this network by using a range of temperatures and hydrogen sulfide concentrations. They found that hydrogen sulfide concentration inhibited hydrogenolysis but not hydrogenation. Girgis and Gates (1991), in reviewing dibenzothiophene HDS, noted that the existence of two types of sites, one for hydrogenation and one for hydrogenolysis, is consistent with the rate equations proposed in the literature.

Some work has also been done with benzonaphthothiophene, a four ring structure, at hydroprocessing conditions. Sapre et al. (1980), concluded that for the same conditions benzonaphthothiophene experiences much more hydrogenation than dibenzothiophene. Vrinat (1983) concluded that in contrast to dibenzothiophene, the hydrogenation pathway for sulfur removal

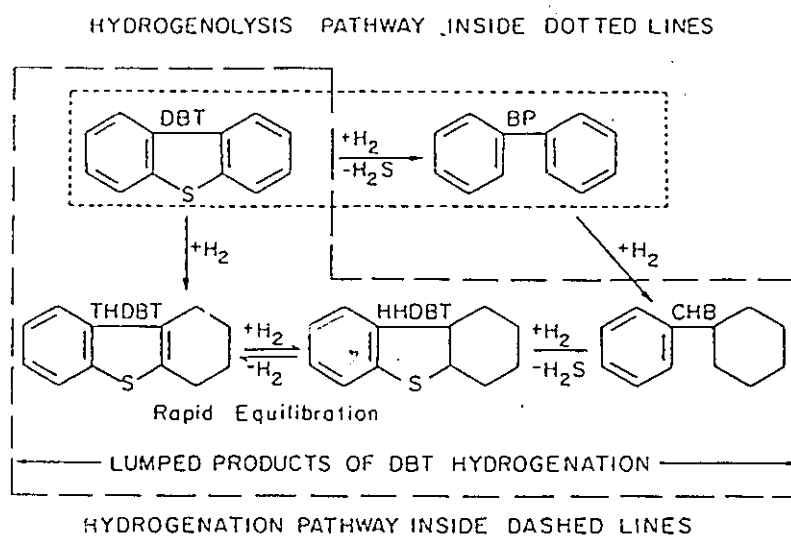


Figure 2.2: Pathways for Dibenzothiophene Conversion
(Houalla et al., 1981)

from benzonaphthathioephene proceeds at approximately the same rate as the hydrogenolysis pathway.

2.3.4 Nitrogen

The model compound studies for hydrodenitrogenation were summarized by Girgis and Gates (1991). They noted that aliphatic amines and nitriles are generally present in very small amounts in typical feedstocks, and these compounds are rapidly converted. Most work has therefore focused on the conversion of aromatic nitrogen structures, which can be basic or neutral. The removal of nitrogen requires the hydrogenation of the nitrogen containing ring, unlike sulfur which can be directly removed. Although higher temperatures favor dehydrogenation, high hydrogen pressure forces the equilibrium toward the hydroprocessing products. HDN is essentially irreversible for the purposes of these model compound studies. Girgis and Gates (1991) summarize the work that has been done with quinoline, a two ring basic structure. A variety of reaction networks have been proposed, with the importance of the dehydrogenation reactions differing between studies. A variety of Langmuir-Hinshelwood rate expressions based on pseudo first-order kinetics were found to be inadequate due to strong inhibition by the nitrogen compounds. Data for the conversion of larger basic structures such as acridine and benzoquinoline is also given, but only in terms of assumed pseudo first-order kinetics.

Girgis and Gates (1991) also discuss the literature for

non-basic nitrogen compounds, mainly for indole. Preferential hydrogenation of the nitrogen containing ring was seen, with dehydrogenation reactions also observed. In addition, they note that Bhide (1979) saw a reaction of indole to higher molecular weight products at 350 °C. Little was said about the conversion of larger ring structures such as carbazole. However, it was noted that during such conversions no amines or anilines were formed in appreciable yields.

2.4 Analysis of Sulfides and Pyrroles

The literature discussed in Section 2.3 indicates that the type of structure containing the sulfur or nitrogen atom is important for the hydrodesulfurization and hydrodenitrogenation reactions. The structural type can cause widely different kinetic behavior, so tracking certain types of sulfur or nitrogen compounds during a reaction may give some insight into the parameters affecting the overall reaction rate. Work has been done in this area for bitumen, where standard combustion techniques are used to determine total sulfur and nitrogen contents. Jacobsen and Gray (1987) used a combination of potentiometric titration, I.R. spectroscopy and ^{13}C -nmr to examine a variety of structural groups, including some nitrogen and sulfur species, in Peace River bitumen. These species included indole and quinoline groups as well as thiophene and sulphide groups. A further

study by Gray et al. (1989) used the same techniques to study thermal conversion of the residual fraction from Athabasca bitumen. They found it difficult to distinguish thiophenes and sulfides in the I.R. spectrum. However, in both cases the pyrrolic nitrogen was distinguishable using I.R., with absorption in the $3455 - 3465 \text{ cm}^{-1}$ range and with an extinction coefficient $B = 0.7 * 10^4 \text{ l mol}^{-1}\text{cm}^{-2}$.

Payzant et al. (1989) developed a technique to oxidize sulfide groups selectively in a bitumen fraction to sulfoxides using tetrabutylammonium periodate so that they could be separated from the thiophenic compounds using a column of silica gel. The sulfoxides were then converted back to sulfides which were quantified and differentiated with GC-FID. A similar procedure was followed for thiophenic compounds through conversion to sulfones. Green et al. (1993) further refined this technique in their study of asphalt by simply oxidizing only the sulfides and then quantifying the sulfoxide peak using I.R. spectrometry. The amount of thiophenic compounds in the original material was then determined by difference. The authors found the technique of Payzant et al. (1989) did not always completely oxidize the sulfides, but overcame this difficulty with their modified technique. They found a molar absorptivity of $245 \text{ L mol}^{-1}\text{cm}^{-1}$ for actual petroleum fractions with I.R. absorbance near 1030 cm^{-1} . Aromatic sulfides were not oxidized with this technique and so were not detected as sulfoxides.

Chapter 3
Materials and Methods

3.1 Selection of Experimental Reactor

A survey was performed to determine which type of bench-scale reactor was suitable for the proposed hydrocracking experiments. Fixed-bed reactors have been used for similar experiments. The differential reactor was eliminated from consideration because of the difficulty in measuring the necessarily small concentration changes across such a reactor, due to the multiple components in the feed. Integral devices, in the form of trickle bed reactors, have been used for similar studies. However, there is little justification but a great deal of criticism for the use of this type of reactor in determining intrinsic kinetics (Schuit and Gates 1973, Weekman 1974, Vrinat 1983, Lee 1985, Whitaker and Cassano 1986, Ammus 1987, DeWind 1988) owing to the formation of concentration and temperature gradients, axial backmixing and incomplete wetting. Adding an external recycle may reduce the temperature gradient across the bed, but the system would be difficult to set up and the wetting problems remain (Ammus 1987).

Spinning basket type reactors have been used successfully for studying intrinsic kinetics of HDS reactions using actual oils (Ammus 1987), and the use of this type of reactor avoids the aforementioned difficulties. As the reactor internals were built in the Department of Chemical Engineering, it was easier to implement a Robinson-Mahoney design with a stationary annular catalyst basket. Details of the design are

provided in the foregoing texts. To ensure that there was good fluid flow through the catalyst basket and no stagnant areas in the reactor, a plexiglass mockup of the reactor vessel was made. The baffles, catalyst basket and impeller from the actual reactor were used in the mockup. The catalyst basket was filled with glass beads, and the mockup test was conducted with water at an impeller speed of 800 rpm. Hydrogen was simulated by air, which was entrained as small bubbles and forced to the bottom of the reactor by the impeller. At the high temperature and pressure of reaction conditions, the reactor liquid would have a similar viscosity to water at room conditions, and the hydrogen would be more easily entrained due to an increased density and a lower surface tension. To check for stagnant areas in the reactor a small amount of dye was dropped into the top of the vessel. The reactor demonstrated good dispersion characteristics as the dye dispersed throughout the reactor in a few seconds. No stagnation zone was observed in the cold flow test.

3.2 Reactor System

The reactor system consisted of three main parts: the feed system, the reactor, and the product system. The purpose of the feed system was to deliver bitumen and hydrogen to the reactor at a controlled and steady rate. The reactor must contact the three phases of gaseous hydrogen, liquid bitumen and solid catalyst in an efficient manner at the desired temperature and pressure. The product system was designed to separate the two-phase product stream into a liquid stream, which could be collected for analysis, and a vapor stream, which could be routed through a gas chromatograph. A simplified schematic of this reactor system is shown in Figure 3.1.

3.2.1 Feed System

3.2.1-A. Bitumen

Due to the high viscosity of the bitumen, pumping it can present many difficulties. Consequently, a piston was used to transfer the bitumen into the reactor. The piston was situated in an oven which could maintain a temperature of 150°C. It was filled with bitumen from a heated feed drum using a Moyno type pump (pm13). The bitumen was fed to the reactor at a set rate by displacing it with a light metering oil (Voltesso). The Voltesso was pumped from a feed drum to the top of the piston with a Milton Roy metering pump (pm-11), driven by a Doerr electric motor.

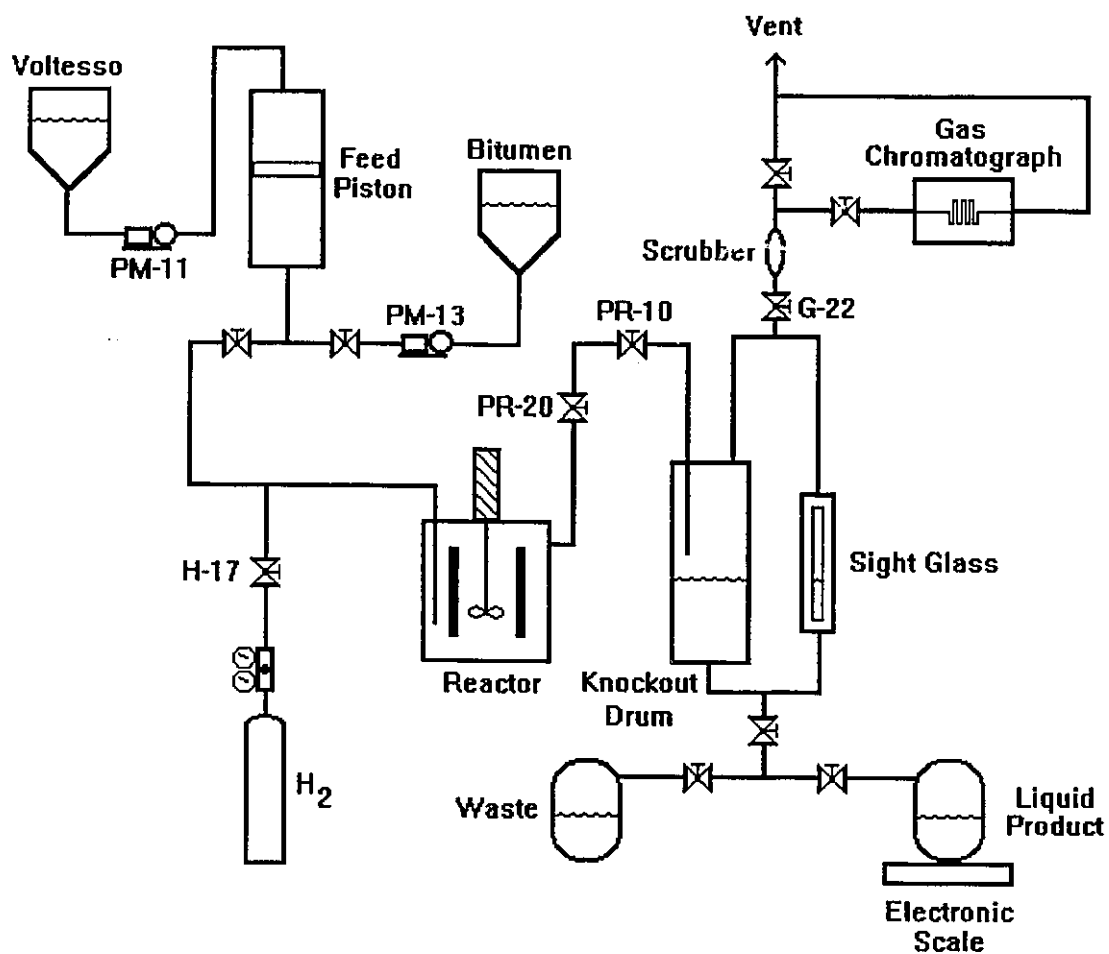


Figure 3.1

Simplified Schematic of Reactor System

3.2.1-B. Hydrogen

Hydrogen was supplied by Canadian Liquid Air Ltd. in either 24000 kPa or 41000 kPa Linde cylinders. A pressure regulator reduced this pressure to about 1400 kPa above the reactor operating pressure. The flow of hydrogen to the reactor was maintained using a mass flow meter, control valve and a digital controller.

3.2.2 Reactor

The reactor used in these experiments was a modified two litre autoclave. The bottom half of the reactor was plugged to give a one litre total volume, with a two to one length to height aspect ratio. An annular catalyst basket with a baffle assembly was added to the reactor when desired. This standard 130 mL basket, made from 16 mesh stainless steel screen with a solid top and bottom, sat in the baffle assembly approximately 1 cm from the bottom of the reactor. The stirrer was designed to force the liquid and bubbles of entrained vapor radially outward through the catalyst basket and then draw it over and under the basket back into the centre. The stirrer was magnetically coupled outside the reactor and was equipped with a variable-speed drive. The reactor was also equipped with a heating element and was surrounded by permanent insulation except at the head, which was covered by a removable insulating jacket. A thermocouple

well descended about three quarters of the way to the bottom of the reactor and a removable bundle of four type K thermocouples were placed in it: the top was a spare, the second to initiate emergency shutdown in case of overheating, the third for the furnace controller and the last thermocouple for the data acquisition system. In the event that the reactor overheated the emergency shutdown system would shut down the furnace, close off the hydrogen supply to the reactor and dump the reactor contents to a holding vessel. The reactor temperature was maintained by a digital controller. A fifth thermocouple penetrated the insulation on the outside of the reactor and gave an estimate of the reactor skin temperature, which was useful to avoid burning out the furnace coil.

The feed hydrogen joined the bitumen through valve H-17 and this two-phase feed then entered near the bottom of the reactor. The two phase product left near the top of the reactor in two streams which immediately joined and went through a manual valve, PR-20, and a control valve, PR-10. The reactor pressure was regulated by a digital controller which maintained the setting by adjusting the outlet flow through PR-10. This arrangement was able to keep the reactor pressure within 200 kPa of the set point, 13.7 MPa.

3.2.3 Product System

After exiting the reactor through control valve PR-10, the two phase product stream entered a knockout drum. This drum had a liquid outlet at the bottom which was directly connected to a sight glass; it also had a vapor outlet at the top which was also directly connected to the sight glass. The pressure in the drum was maintained at 2800 kPa by a digital controller and a valve on the outlet vapor line. The liquid level was maintained manually by inspecting the sight glass and turning a hand valve to drain the liquid from the drum when the level got too high, approximately hourly depending on the flow rates.

3.2.3-A. Liquid System

The liquid drained from the knockout drum could be sent either to a waste drum or to a product collection drum which sat on an electronic scale. The product could then be drained from the collection drum into storage containers and sent for analysis.

3.2.3-B. Vapor System

The off gas from the knockout drum was sent through a water scrubber to remove NH_3 , H_2S and any condensate, and then could either be directly vented or sent to the gas chromatograph for analysis.

3.3 Summary of Operating Procedure

The following is a summary of the operating procedure for a typical reactor run.

1. Fill the catalyst basket with 78 g. of catalyst.
2. Button down the reactor head, close all outlet valves and pressure the system to the desired operating pressure with nitrogen.
3. Check for leaks by observing the system pressure over at least an hour and finding leaky fittings with a soapy solution, "Snoop".
4. Heat the reactor to the operating temperature.
5. Set the hydrogen regulator to 2100 kPa (300 psi) above the desired operating pressure and adjust the flow rate to the desired value, allowing it to flow through the system.
6. Adjust valve PR-20 to maintain the desired pressure in the reactor.
7. Adjust valve G-22 to maintain the desired pressure in the knockout drum, then switch it to automatic.
8. Isolate the bitumen feed drum and feed piston.
9. Start PM-11, pumping Voltesso into the top of the feed piston until the desired reactor operating pressure is reached.
10. Open the line from the feed piston to the reactor.
11. Adjust PM-11 to give the desired bitumen feed rate, as measured using the buret and stop watch.

12. Manually adjust PR-20 to maintain reactor pressure until there is a stable two-phase flow from the reactor, then switch to automatic control with PR-20.
13. Adjust the reactor stirrer to 7.1 (1000 rpm).
14. Every 30 minutes throughout the run check and fine tune the bitumen feed rate.
15. Wait for the temperature to stabilize, then continue to send the liquid product to waste until 3 liquid holdup volumes have flowed through the reactor.
16. Collect the liquid product for analysis, calculating the outlet flow rate with a stopwatch and the electronic scale.
17. Send a gas sample to the gas chromatograph.
18. When sufficient product has been collected for analysis, isolate the reactor by closing the reactor outlet valve PR-10, the bitumen inlet valve, and the hydrogen inlet valve H-17.
19. Turn off the furnace, Voltesso pump and hydrogen at the bottle.
20. When the reactor has cooled to room temperature, unbolt and remove the head unit.
22. Pipet out the remaining liquid in the reactor and measure the liquid holdup with a graduated cylinder.
21. Remove the catalyst basket, chip out the coke from the bottom of the reactor and clean the reactor with methylene chloride.

3.4 Analytical Techniques

When a minimum of 0.5 L of liquid product was collected from a reactor run, it was sent to the Research Department of Syncrude Canada Limited in Edmonton for analysis. The whole product was analyzed for carbon, hydrogen, sulfur, nitrogen and metals. It was then distilled into four cuts: naphtha (IBP - 177°C), middle distillate (177 - 343°C), gas oil (343 - 525 °C), and residue (525+°C). The non-metal elemental analysis was done again on each cut, with an additional micro carbon residue (MCR) analysis on the residue. These analyses were repeated in triplicate and averaged for each sample. Further analysis was performed on selected cuts for nitrogen and sulfur types at the University of Alberta.

3.4.1 Distillation

The liquid product was divided into four boiling cuts by two distillation procedures:

1. An atmospheric spinning band distillation of the whole product produced naphtha and middle distillate, with a heavier fraction left in the flask at the final temperature of 350°C.
2. The heavier fraction was then distilled under vacuum to produce the gas oil and residue fractions following the ASTM D1160 procedure.

3.4.2 Carbon and Hydrogen Analysis

The elemental analysis for carbon and hydrogen was done by the Leco analyser.

3.4.3 Sulfur Analysis

The sulfur analysis was done by combustion followed by fluorescence detection at the Syncrude laboratory. Selected samples were verified by analyses performed at the Department of Chemistry in the University of Alberta.

3.4.4 Nitrogen Analysis

The nitrogen analysis was done by combustion followed by chemiluminescent detection.

3.4.5 Metals Analysis

The metals analysis was done using a simultaneous inductively coupled argon plasma system.

3.4.6 Micro Carbon Residue Analysis

The MCR analysis was done using an Alcor system, following the appropriate ASTM method.

3.4.7 Pyrrolic Nitrogen

The procedure used for semi-quantitative measurement of pyrrolic nitrogen was similar to the procedures used by Bungler (1976), Bungler et al. (1979) and McKay et al. (1976), and has been used previously in this department by Jokuty (1992). To analyze for pyrrolic nitrogen, approximately 0.05 g of the sample was dissolved in ACS grade dichloromethane to make 1.0 mL of solution. A Nicolet model 730 infrared spectrometer with a removable cell containing NaCl windows and a 0.5 mm teflon spacer was used to determine the pyrrolic nitrogen content. The actual space between the windows was determined through the interference peaks of the empty cell. When

analysing for pyrrolic nitrogen the absorbance spectrum for pure solvent, ratioed to the background, was used for the reference. The solution containing the sample was placed in the cell and also ratioed to the background, after which the reference was subtracted from this spectrum. Only enough of the reference was subtracted to get rid of negative peaks, 0.7831 of the total. A distinct peak at 3460 cm^{-1} (Bunger et al. (1971)) was obtained and integrated using the Nicolet integration feature with baseline correction. The mass percent pyrrolic nitrogen in the sample was then calculated from Equation 3.1:

$$J = \frac{A}{B \cdot l \cdot w \cdot 10} \quad 3.1$$

- J = concentration of structural group, mol/100 g sample.
 A = peak area, cm^{-1} .
 B = absorbance constant for the group, $\text{mol}^{-1}\text{cm}^{-2}$.
 l = cell thickness, cm.
 w = weight of sample in 1 Ml of solution, g.

For pyrrolic nitrogen, the absorbance constant was 0.7×10^4 (Bunger et al., 1971). The procedure was verified using a mixture containing a known quantity of carbazole in pure solvent. The determination of the pyrrolic nitrogen is not expected to be truly accurate, it is only semi-quantitative due to the differences between pure carbazole in solvent and

actual bitumen. However, it was expected that the results for bitumen would be of the correct order of magnitude, and that the relative error would be the same in all cases. In other words, any trends observed in the data from the bitumen would signify trends in the true pyrrole concentration.

3.4.8 Sulfide Analysis

Aromatic and aliphatic sulfur species could not be readily differentiated using I.R. spectrometry. However, aliphatic sulfur species are much more easily oxidized, changing from sulfides to sulfoxides. These sulfoxides could then be analysed by I.R. spectrometry.

The sulfides in the bitumen and products were mildly oxidized by refluxing for half an hour with tetrabutylammonium periodate, using the method of Green et al. (1993). This mild oxidation converted most of the aliphatic sulfur without appreciably affecting the aromatic sulfur. After removing the solvents, as per the aforementioned method, the remaining sample was dissolved in dichloromethane to form a measured quantity of sample solution. A measured quantity, approximately 0.4 g, of this solution was diluted with dichloromethane to make 1 mL of solution, and the IR procedure described in Section 3.4.7 was used to quantify the sulfur in sulfide form in the prepared sample. The sulfoxide peak was at 1025 cm^{-1} , with an absorption factor of 0.6×10^4 (Bunger et al. (1971)). In this case two 0.5 mm spacers were used between the cell windows, and 100 % of the reference spectrum

was subtracted from the sample spectrum. Knowing the mass percent of this sulfur, as well as the total mass of sample solution, allowed the calculation of the total mass of the sulfur in the sulfide form, which, when divided by the initial mass of sample, allows calculation of the mass % sulfide in the original sample.

This semi-quantitative procedure was verified using 96% dioctyl sulfide in dichloromethane. The five samples were analyzed and showed average error of 4 % and a maximum error of 8 %.

3.5

Catalyst

The catalyst used in these experiments an industrial hydrocracking catalyst. The pellets were 1 mm diameter cylinders, with an average length of 4.5 mm, and had the following composition:

Table 3.1 Catalyst Composition			
Metal	Al ₂ O ₃	MoO ₃	NiO
Percent	84	12.5	3.5

After approximately 2 h in the reactor the catalyst had a surface area of 207 m³/g, measured by BET in the laboratory of Dr. S.E. Wanke, Dept. Chem. Engg., University of Alberta. After approximately 15.5 h the surface area had fallen to 165 m³/g.

Chapter 4
Overall Kinetics

4.1 Introduction

In the hydrocracking of bitumen to form synthetic crude oil, the overall removal of a single component, such as sulfur, from the oil is often of interest. However, both bitumen and the product oil are comprised of a multitude of quite different molecules varying in size, composition and chemical properties. In examining kinetics, the component of interest must therefore be defined in a broader sense than simply denoting a single chemical species. For convenience a single element, such as sulfur or nitrogen, can be selected regardless of the molecule containing the element, or a component can be defined by a property such as a boiling cut or a procedure such as micro carbon residue (MCR). The rate of conversion of such a component can usually be described by the following empirical equation:

$$R_i = k_i \cdot C_i^{n_i} \quad 4.1$$

- R_i = rate of conversion of component i
 k_i = rate constant for conversion of component i
 C_i = concentration of component i
 n_i = reaction order for conversion of component i

The rate can be expressed on a liquid holdup basis, g/(L-

h), as is done for non-catalytic reactions. In catalytic reactions, the rate of conversion is usually expressed on a catalyst mass basis, g/(g catalyst-h). The units for the rate constant will reflect both the reaction type (catalytic or non catalytic) as well as the reaction order. In this power law equation, the reaction order is most commonly in the range $1 \leq n_i \leq 2$.

For a CSTR, the rate can also be calculated from Equation 4.2:

$$R_i = \frac{F_o \cdot C_{i0} - F \cdot C_i}{\beta} \quad 4.2$$

- R_i = rate of conversion of component i
 F_o = inlet liquid flow rate, g/h
 F = outlet liquid flow rate, g/h
 C_{i0} = inlet concentration of component i, mass %
 C_i = concentration of component i in reactor, mass %
 β = liquid holdup volume (L), or catalyst weight (g)

Using equations 4.1 and 4.2, the rate constant and reaction order can be determined from an experimental data set with different concentrations of component i in the reactor.

4.2 Overall Kinetics of Residue Conversion

An important difference between bitumen and conventional crude oil is the amount of high boiling material in the oil.

During hydrocracking a significant portion of this material is transformed to lower boiling material. Although the high boiling point is a reflection of the elemental composition of the molecules and their size, it is easily measured through distillation as described in Chapter 3. Thus, by examining the amount of residue, which is material boiling over 525°C, in the product, the degree of conversion of the bitumen to synthetic crude oil can be determined.

The reactor system described in Chapter 3 was used for a series of catalytic hydrocracking experiments with residence times varying between 0.37 and 1.87 hr. The ratio of hydrogen to liquid feed was 720 (standard L H₂)/(L bitumen), with reactor pressure maintained at 13.65 MPa and temperature at 430°C. In addition one experiment was done at the same conditions with no added catalyst and a residence time of 0.94 hr. As the feed bitumen contains metals such as Fe, V, and Ni which could promote some catalytic effects, this run may not be strictly non-catalytic, but, all considered, the reaction will be mainly thermal.

The residence-time experiments gave a series of products with progressively higher conversions of the residue cut. Equation 4.1, given above, shows the expected relationship between the concentration of residue in the reactor and the rate of its conversion. Based on Equation 4.1, plotting the rate of residue conversion against the concentration of residue for each residence time on a log-log graph should

yield a straight line, with the slope giving the reaction order and the intercept giving the rate constant. Figure 4.1 shows this plot along with a linear regression of the data. The fit of the experimental data to the aforementioned kinetic model was excellent with an r^2 value of 0.98. The slope of the regression line and the 95% confidence interval were 1.09 ± 0.11 , which indicates that the conversion of residue can be considered first order. Indeed, Figure 4.2 shows the same data plotted following equation 4.1 for $n=1.0$ and the r^2 value is still 0.96. The slope in Figure 4.2 gave the first order rate constant for residue conversion, $2.22 \text{ hr}^{-1} \pm 0.08$, on a liquid holdup basis. The first order equation predicted the residue conversion rate within 5 % for all but the shortest residence time.

The 95 % confidence interval of the slope for the first order equation indicates the error from the first order approximation, scatter in the data, and analysis error. An estimate of the reproducibility, that is error caused by scatter and analysis, was obtained by repeating the run with a residence time of 0.87 hr. From this the error in the residue conversion rate was found to be $\pm 2\%$. Examination of Figure 4.2 indicates that this is probably an underestimate of the reproducibility error.

The thermal experiment (no added catalyst) was used to give an estimate of the contribution the added catalyst gave to the conversion of the residue cut. The rates for total and

Figure 4.1
Rate Residue Conversion (g/L-h) vs Residue Concentration (g/L)

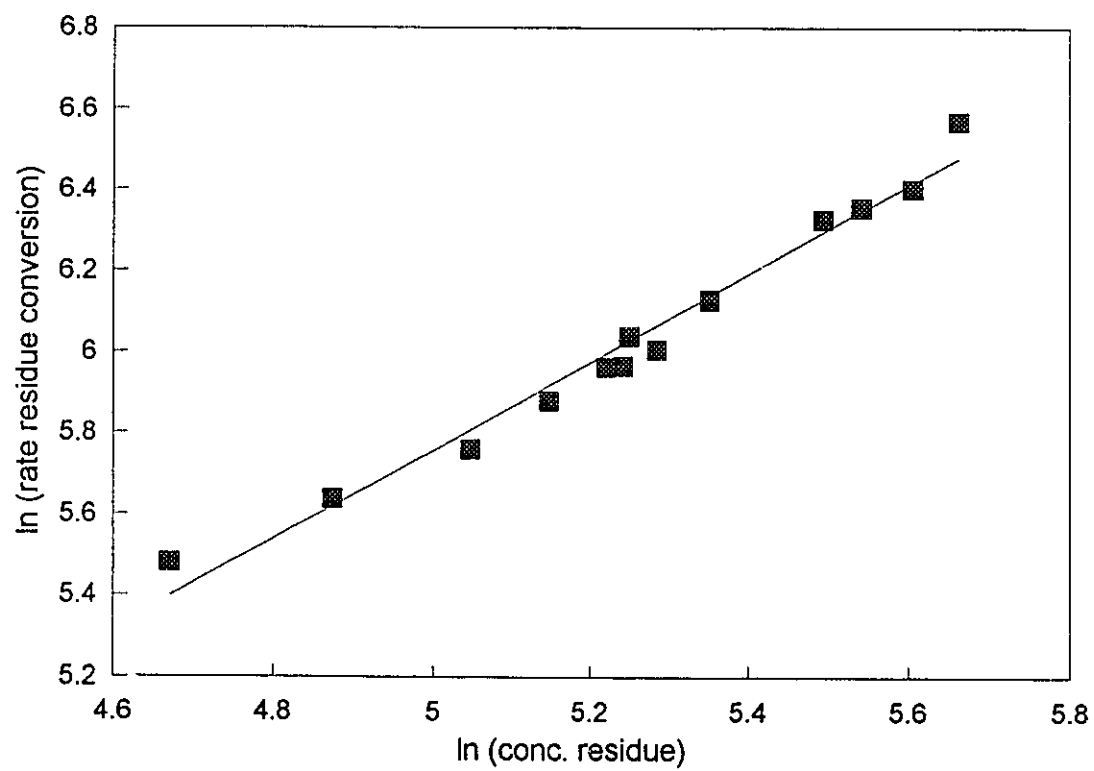
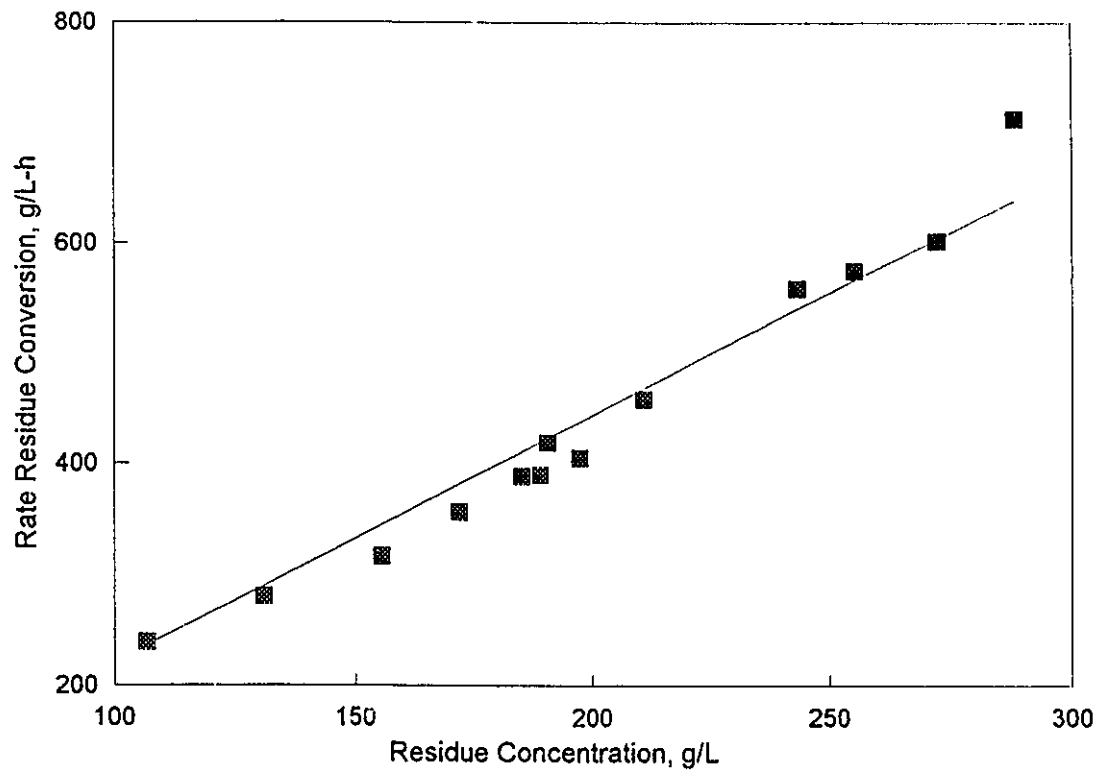


Figure 4.2
Rate of Residue Conversion vs Concentration of Residue

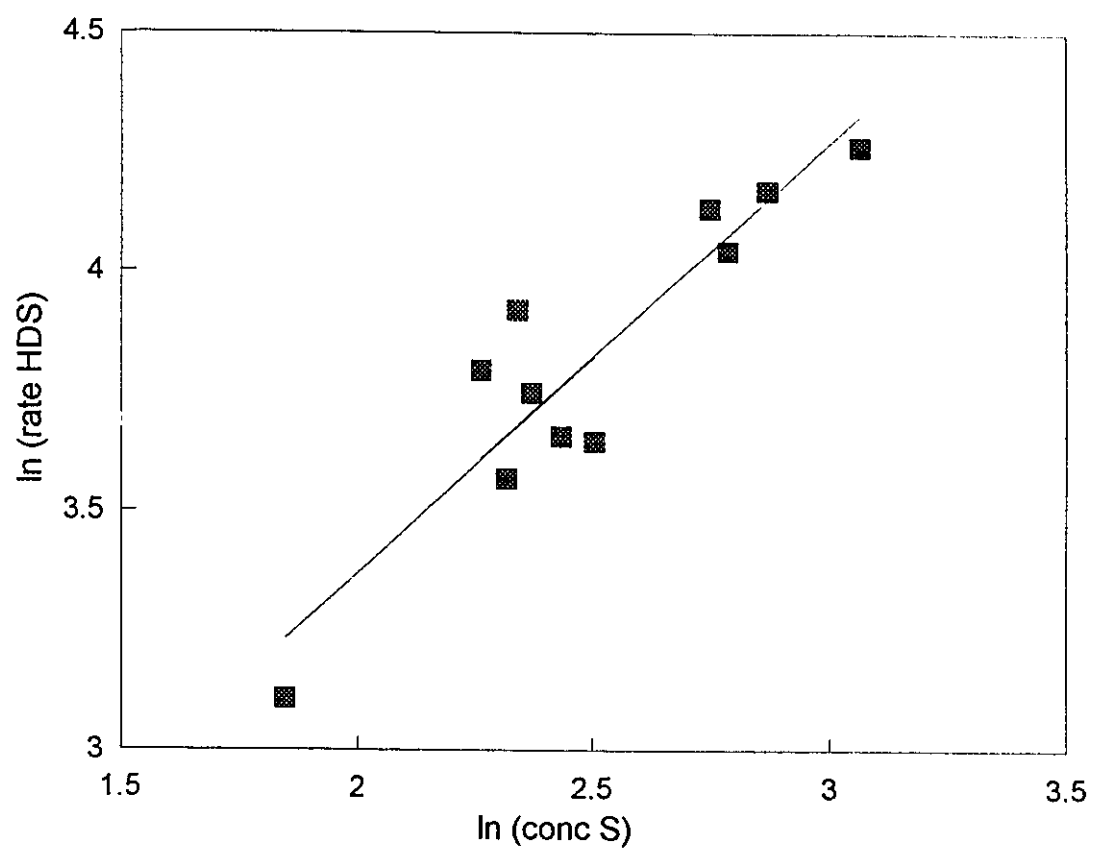


thermal conversion for similar residence times could be directly compared by dividing the former by the latter, but, since reaction rate and residence time are not linearly related, such a comparison cannot be extrapolated to other residence times. Instead, first order was assumed and the rate constant for the thermal residue conversion was calculated to be 1.56 h^{-1} by dividing the rate by the concentration for the single thermal run. Dividing this by the rate constant with added catalyst, reported above, shows approximately 70 % of the residue conversion was thermal. The catalyst to liquid holdup ratio was kept constant at 0.21 g/mL.

4.3 Overall Kinetics of Sulfur Removal

Another important reaction in bitumen upgrading is the removal of sulfur. Although some sulfur is removed without added catalyst, the catalysts used in upgrading are usually picked to promote hydrodesulfurization (HDS) reactions, in which organic sulfur is converted to H_2S . Through the elemental analysis of the bitumen and products as described in Chapter 3, it is possible to examine the kinetics for the overall removal of sulfur in the same fashion as described above for the residue conversion. Using equation 4.1 a logarithmic plot of the rate of HDS against the concentration of sulfur is given in Figure 4.3. The slope of the plot indicated a reaction order of 0.90 ± 0.29 , with an r^2 of 0.84.

Figure 4.3
Rate HDS (g/L-h) vs Conc. Sulfur (g/L)



This result indicated that the kinetics were approximately first order. In this analysis two outlying data points were discarded from Figure 4.3. The reactor runs represented by these two measurements were done on the same day, and both products also gave problems in nitrogen analysis, with negative nitrogen conversions. The cause of this anomaly is not known, but the sulfur analysis was confirmed by the Department of Chemistry at the University of Alberta for both the outliers and two runs bracketing these points, with the results of this analysis given in Table 4.1.

Residence Time, h		0.96	1.25	1.50	1.88
Sulfur Analysis, mass %	SCL	1.26	1.46	1.33	0.72
	U of A	1.24	1.53	1.58	0.82

The possible source of the high sulfur concentrations for the 1.25 and 1.50 h runs is discussed further in Chapter 6.

The sulfur was also analyzed on each of the boiling cuts, which were summed and compared to the overall analysis for each run. Performing a linear regression on the summed vs overall data gives a slope of 1.05 ± 0.03 and an r^2 of 0.97, indicating the summed values tend to be 5 % higher than the overall values. The discrepancy between the summed and overall sulfur concentration was as high as 19 %, which lead to errors in the HDS rate as high as 14 %. Although the

single repeated run described in Section 4.2 indicates a reproducibility error for the HDS rate of only 2 %, the summed vs totalled error alone indicates that this is not a realistic number. Although the sulfur measurements were done in triplicate such that the three results were within 1 % of each other, if the maximum error between the summed and overall sulfur content is a more realistic estimate of the error in the sulfur analysis then this would help explain the scatter in Figure 4.3. Removing the single point with the lowest concentration gives a reaction order of 0.77 ± 0.38 .

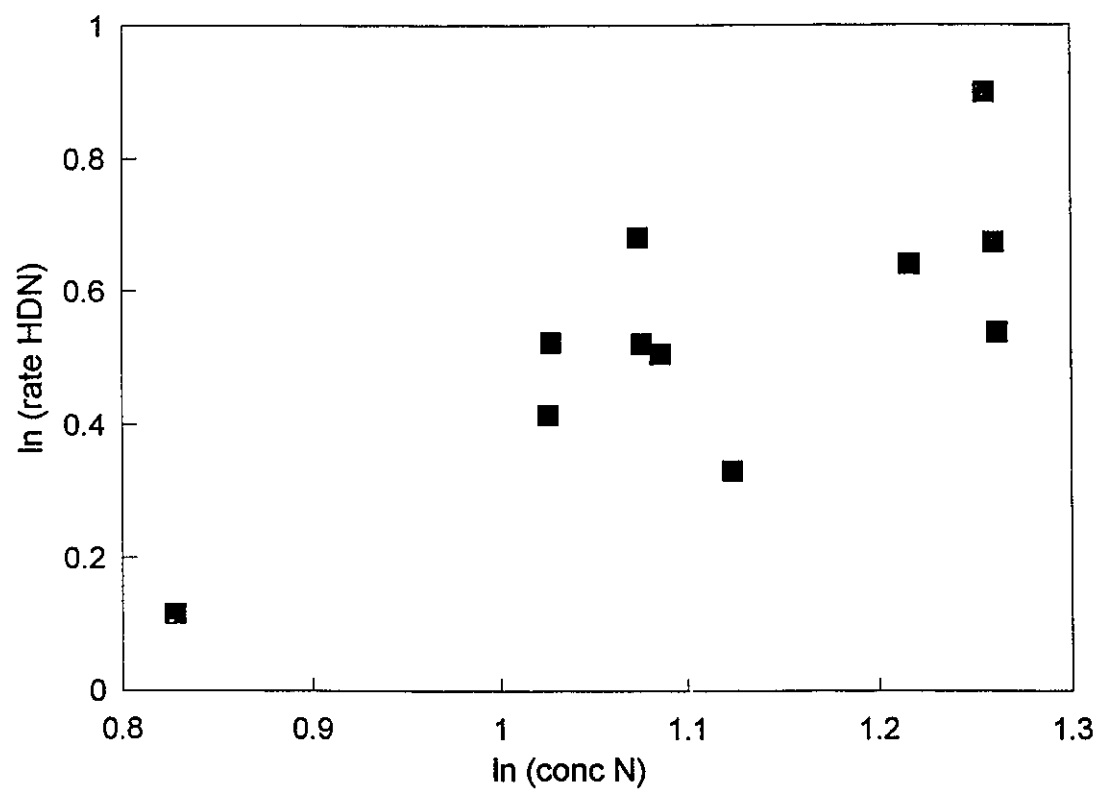
The first order rate constant for the HDS reaction was found to be $3.66 \pm 0.31 \text{ h}^{-1}$, which indicated that the sulphur reaction was approximately 10 % thermal.

4.4 Overall Kinetics of Nitrogen Removal

The removal of nitrogen from bitumen during upgrading was studied in a similar fashion. In general, nitrogen compounds were present in lower concentrations than sulfur and were also harder to remove. Figure 4.4 shows the relationship between the rate of hydrodenitrogenation (HDN) and the nitrogen concentration for the residence time data described above. A linear regression gave a reaction order of 1.19 ± 0.74 , close to the first order kinetics as reported in the literature. The regression r^2 value is 0.59.

Following the same procedure outlined for the sulfur conversion, the error in the nitrogen conversion from the

Figure 4.4
Rate HDN (g/L-h) vs Conc. Nitrogen (g/L)

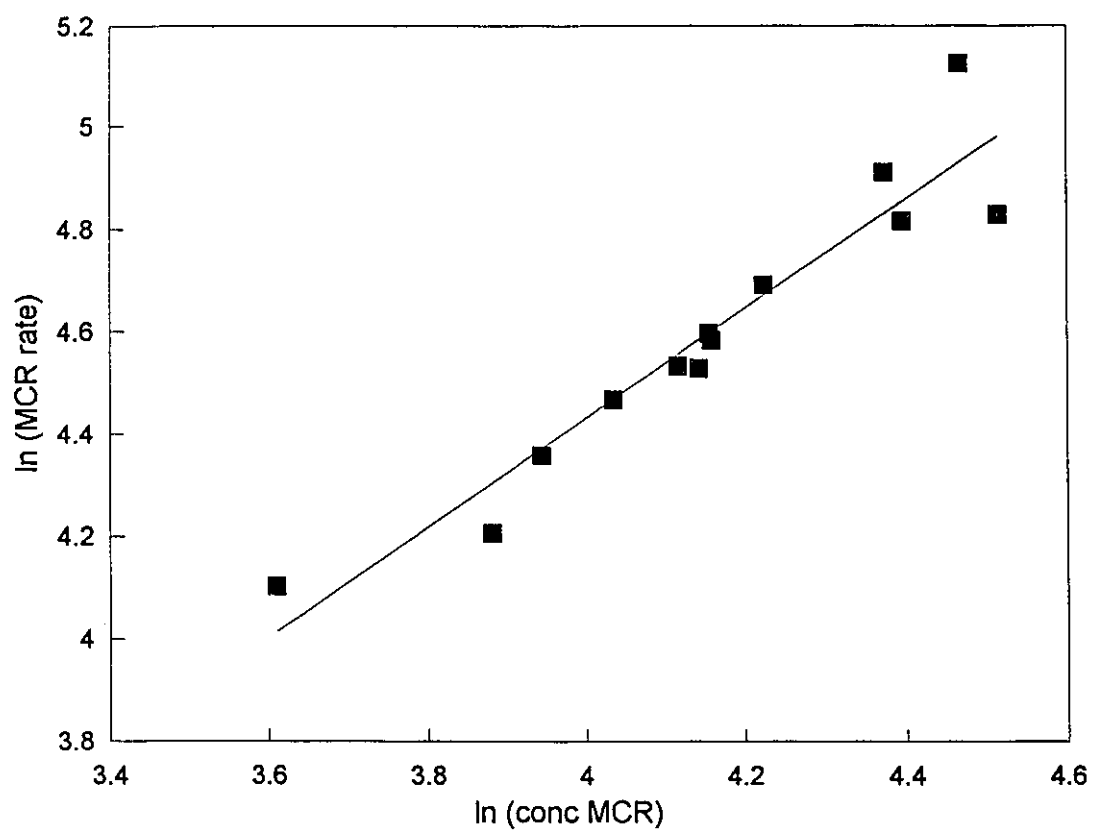


repeated run was found to be $\pm 1\%$. Performing a linear regression on the totalled vs overall nitrogen gives a slope of 0.93 ± 0.06 , with an r^2 of 0.74. Although the triplicate nitrogen measurements done by the Syncrude laboratory were within 1 relative percent, the low r^2 value between the summed cuts and the overall measurement indicates some unaccountable analysis error could exist, especially in the preparation of the cuts by distillation. Although this error does not have a large impact on the concentrations, it could significantly affect the relatively small rates, contributing to the scatter in Figure 4.4. Removal of the lone point at the lowest concentration gives a reaction order of 0.93 ± 1.11 . The HDN reaction was found to be approximately 0 % thermal, i.e. no measurable change in nitrogen was observed in the absence of catalyst.

4.5 Removal of Micro Carbon Residue

MCR was the solid material left over after pyrolyzing the residue boiling cut under an inert gas, and was measured as described in Chapter 3. The kinetics for MCR conversion were determined in the same way as for residue conversion. The logarithmic plot of the rate of MCR conversion against the concentration of MCR for the residence time data is given in Figure 4.5. A linear regression gave a reaction order of 1.07 ± 0.23 with an r^2 of 0.91. Once again the same procedure was followed as for the residue conversion, giving a MCR

Figure 4.5
Ln MCR Conversion Rate vs Ln Conc. MCR



conversion error of $\pm 1\%$ from the repeated run. The first order rate constant was $1.58 \pm 0.11 \text{ hr}^{-1}$ and the estimated thermal contribution for MCR conversion was 30 %.

Stoichiometric Plots

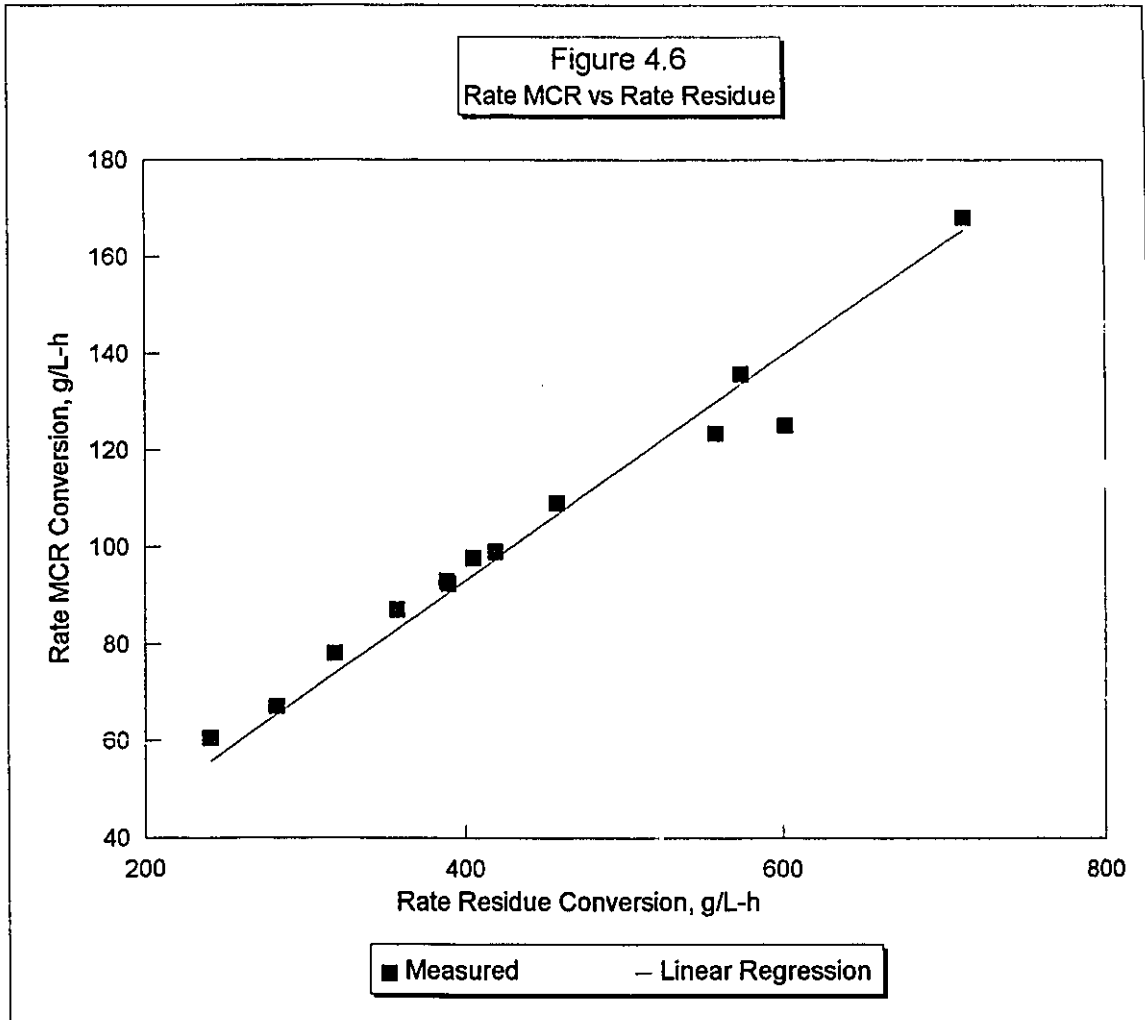
If a reaction is linearly dependent on the same variable as another reaction, then plotting the rates against each other will give a straight line. For instance, if appearance of naphtha and middle distillate are both proportional to residue conversion, then plotting the rates against each other will give a straight line with the slope being equal to the ratio of the rate constants. This ratio indicates the stoichiometry of the residue conversion in so far as the naphtha and middle distillate are concerned. By plotting one reaction against another, an indication of the relationship between the reactions can therefore be found. Ideally the rates should be calculated on a molar basis, however, for bitumen, where the molecular weights vary widely and a good average molecular weight is hard to obtain, a mass basis was used instead. Equations 4.3 and 4.4 illustrate this example, where the cross plot would give the ratio of the stoichiometric coefficients:

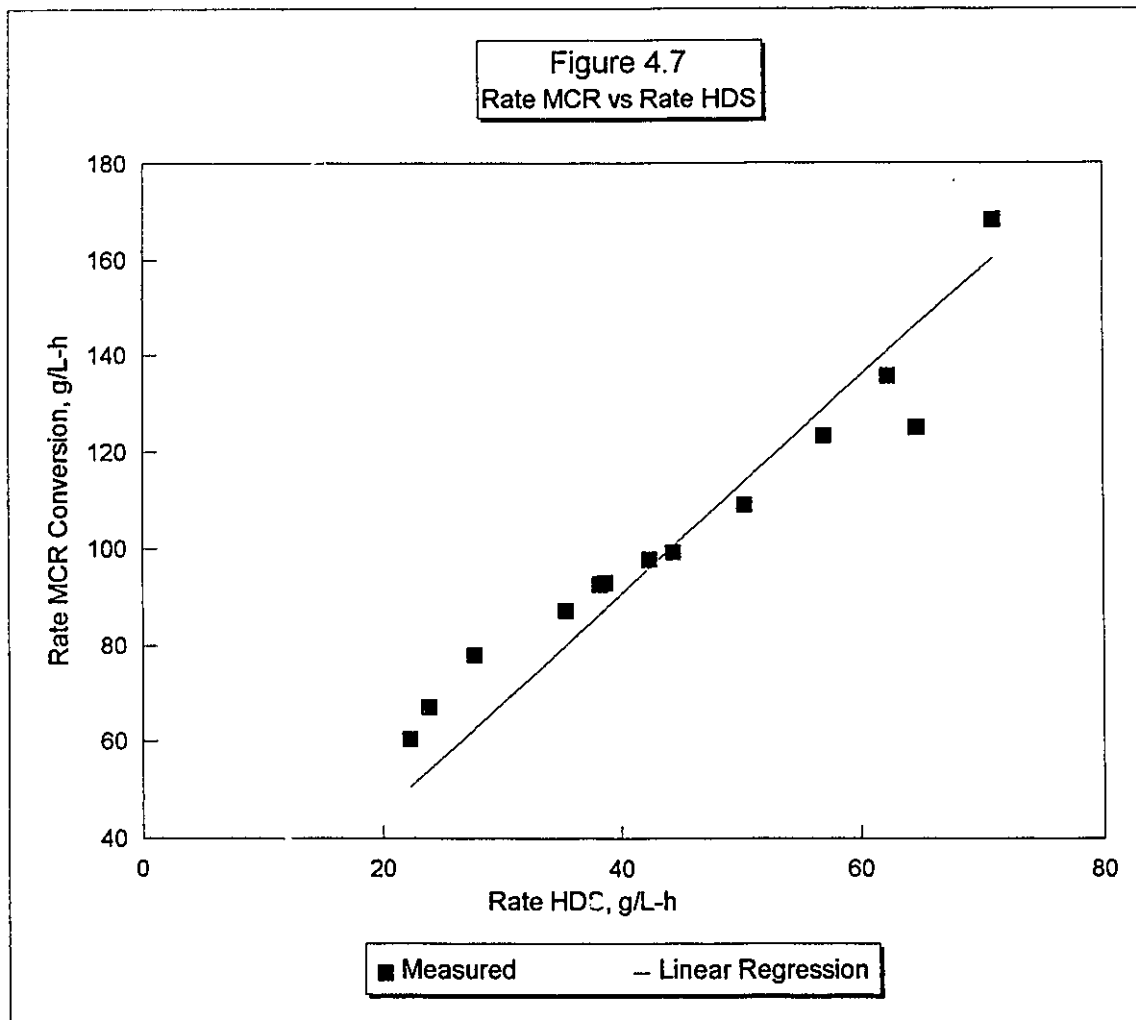
$$R_{nap} = S_{nap} \cdot k_{resid} \cdot C_{resid} \quad 4.3$$

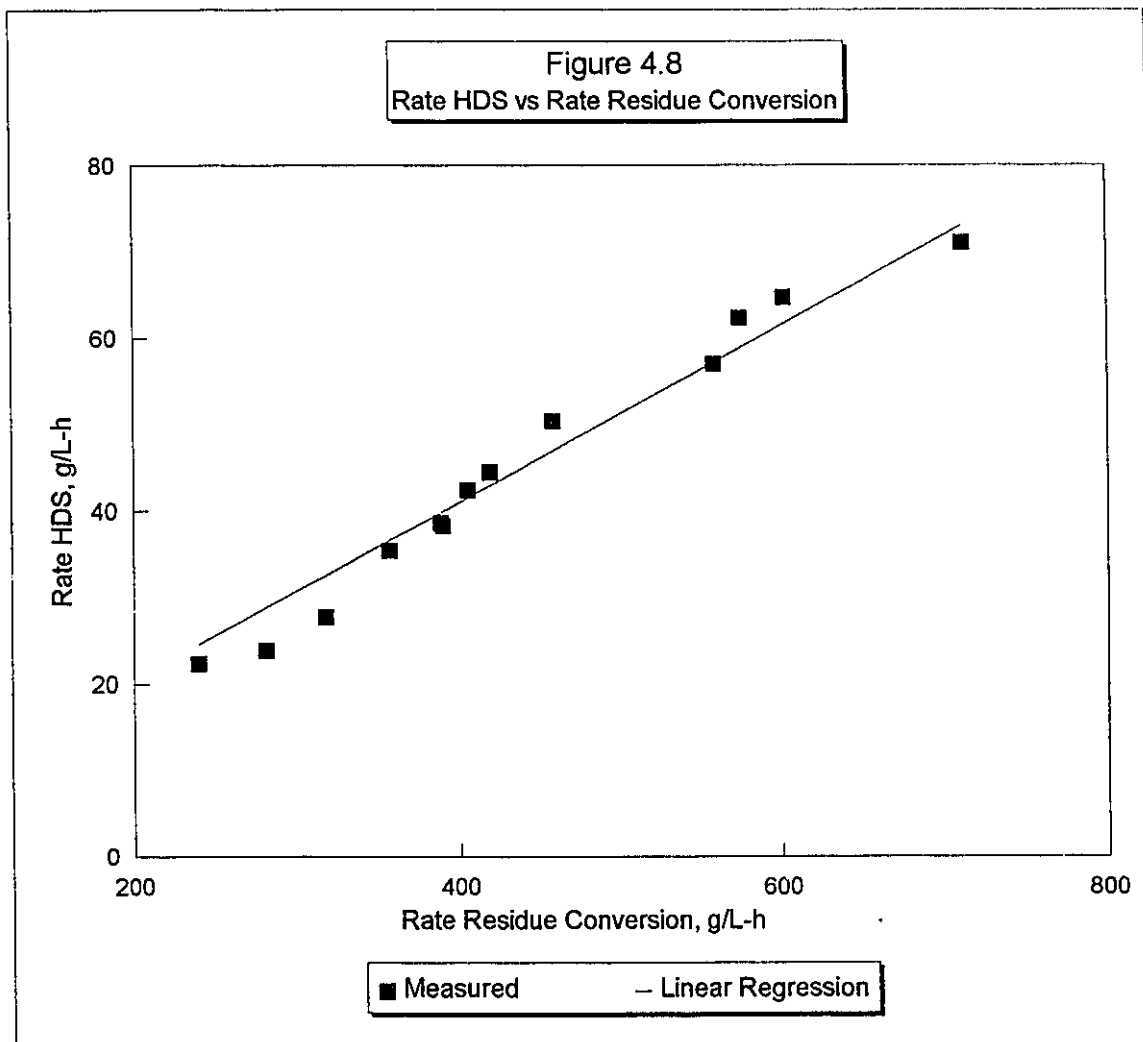
$$R_{mid} = S_{mid} \cdot k_{resid} \cdot C_{resid} \quad 4.4$$

R_{nap}	=	rate of naphtha appearance
R_{mid}	=	rate of middle distillate appearance
s_{nap}	=	stoichiometric coefficient for proportion of residue going to naphtha
s_{mid}	=	stoichiometric coefficient for proportion of residue going to middle distillate
k_{resid}	=	first order rate constant for residue conversion
C_{resid}	=	residue concentration in reactor

Figure 4.6 shows the MCR conversion rate vs the residue conversion rate for the residence time data described above. As can be seen from the figure there is an excellent correlation between the two rates, where the linear regression is forced through zero. Figure 4.7 shows a similar plot for MCR vs HDS, and Figure 4.8 shows the plot for HDS vs residue conversion. Figure 4.7 does not show a good correlation, indicating that MCR conversion is not stoichiometrically related to HDS. Figure 4.8 indicates a better correlation between HDS and residue but this is somewhat ambiguous. A good correlation is not expected here due to the results illustrated in Figures 4.6 and 4.7.







It is important to note that if, for instance, one looks at two independent first order reactions taking place in the same reactor, then the following relationship will be true:

$$\frac{R_1}{\frac{m_{1,in}}{V} - R_1} = \frac{k_1}{k_2} \cdot \frac{R_2}{\frac{m_{2,in}}{V} - R_2} \quad 4.5$$

- R_1 = rate of reaction 1, g/L-h.
 R_2 = rate of reaction 2, g/L-h.
 k_1 = first order rate constant for reaction 1, h^{-1} .
 k_2 = first order rate constant for reaction 2, h^{-1} .
 $m_{1,in}$ = inlet mass rate of 1, g/h.
 $m_{2,in}$ = inlet mass rate of 2, g/h.
 V = reactor volume, L

Rearranging this equation gives:

$$R_1 = R_2 \cdot \frac{m_{1,in} \cdot k_1}{m_{2,in} \cdot k_2} + \left(1 - \frac{k_1}{k_2}\right) \cdot \frac{R_1 \cdot R_2 \cdot V}{m_{2,in}} \quad 4.6$$

If k_1 is approximately the same as k_2 , then the rates will appear to be linearly dependent although they are unrelated. As the first order rate constants were 2.22, 3.66 and 1.58 for residue conversion, HDS and MCR conversion respectively, this may apply to Figures 4.6 through 4.3. The fact that the cross plot of MCR and HDS give the worst fit and

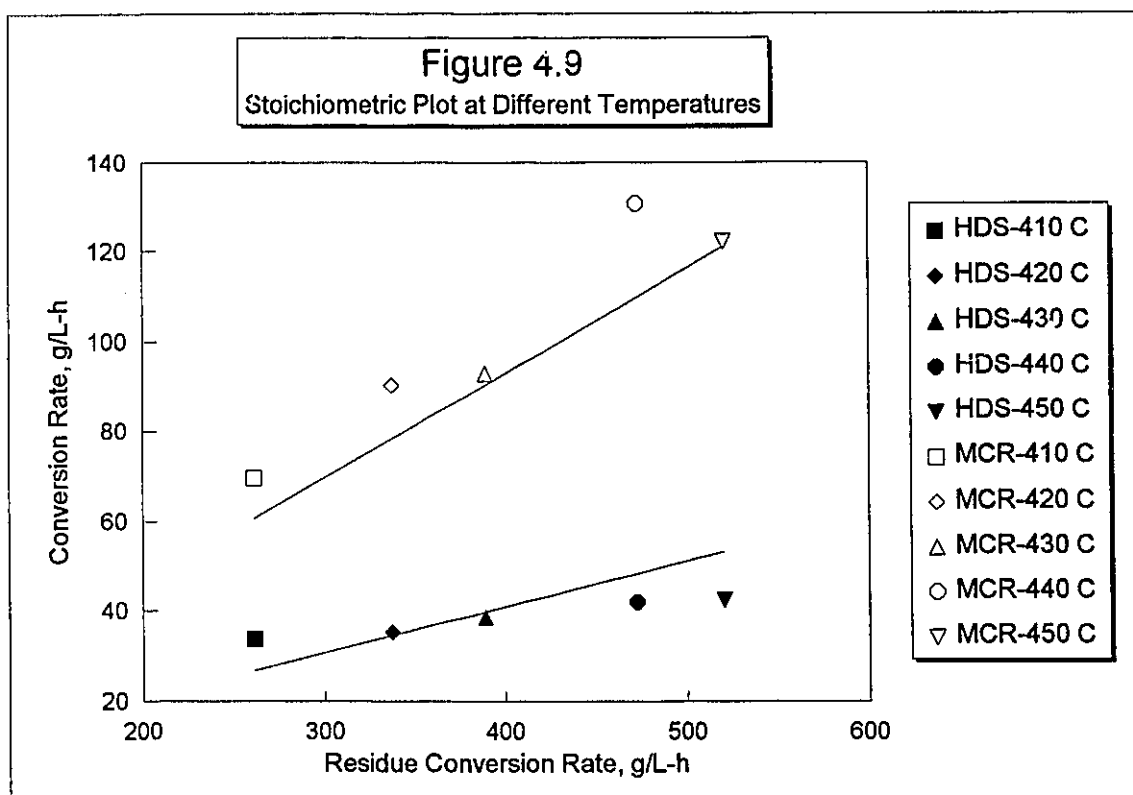
have the greatest difference between rate constants is consistent with this phenomena. The better correlation between HDS and residue conversion may result from the rate constants being closer together. A further check can be done by cross plotting the data at other temperatures, which, for a stoichiometric relationship, should follow the same slopes as those calculated above. This is demonstrated in Figure 4.9, where this does not appear to be the case.

4.7 Conclusions

The kinetic data obtained for the catalytic hydrocracking of Athabasca bitumen are summarized in Table 4.2.

Reaction	Residue Conversion	HDS	HDN	MCR Conversion
Order	1.09 ± 0.11	0.90 ± 0.29	1.19 ± 0.74	1.07 ± 0.23
First Order Rate Constant h ⁻¹	2.22 ± 0.08	3.66 ± 0.31	0.57 ± 0.05	1.58 ± 0.11
Estimated Thermal Contribution %	70	10	0	30

Estimating the error by comparing two runs done at the same conditions showed little difference in concentrations, with errors on the order of 2 %. The error of analysis in the



sulfur and nitrogen data was also estimated by summing the element from each cut and comparing this to the overall measurement. The sulfur data did not show significant variation when compared in this way, therefore, the scatter in the kinetic sulfur plot was attributed to differences other than error in the sulfur analysis. The nitrogen data did show significant variation when compared with the summed cuts and this, compounded with the problems noted for sulfur, resulted in the low r^2 value of 0.59 for the kinetic fit of the nitrogen data.

Comparing the residue conversion, HDS and MCR conversion reactions using stoichiometric plots suggests that these reactions are not stoichiometrically related.

Chapter 5
Kinetic Model for Hydrocracking of Residue

5.1 Introduction

The primary reaction in hydrocracking is the breaking of large molecules into smaller ones. The kinetics of other reactions such as heteroatom removal are affected by the cracking of the carbon-carbon bonds in their parent molecules, as the structure containing the heteroatom affects its kinetic behavior. Species like sulfur and nitrogen will be carried from heavier to lighter cuts as the heavier molecules are cracked. This cracking will influence their removal in several ways, such as changing the apparent kinetics through changes in diffusivity or steric hindering of reactions on the catalyst surface. For these reasons a lumped model for heteroatom removal that incorporates the effect of molecular size will require an overall hydrocracking model as a starting point. Furthermore, any attempts to predict hydrocracking based on the reactions of model compounds will need, as a check, an overall model which predicts the product distribution. This hydrocracking model should ideally be able to take any feed, defined by easily measured boiling cuts, and predict the distribution of boiling cuts in the product. Although this degree of generality is not attainable for a simple model, it should be possible to model a specific feed type, for example Athabasca bitumen, regardless of the boiling distribution in the feed.

5.2 Kinetic Model of Mosby et al. (1986)

Models for residue conversion based on boiling cuts are almost absent from the literature. A model was developed by Mosby et al. (1986) for describing the performance of a residue hydrotreater using lumped first order kinetics. Although the Mosby paper was very brief, with few details given, they considered the cracking reactions to be strictly thermal and heteroatom removal to be strictly catalytic. No information about activation energies was provided. Figure 5.1 shows the Mosby model, which divided the residue into easy and hard lumps and the gas oil into feed and product lumps; all the first order rate constants were relative to the conversion of hard residue to product gas oil, for which the rate constant was set to one. A scaling factor must then be used to adjust the entire network for the specific reaction conditions. Dividing the residue and gas oil each into two lumps was apparently done on a purely empirical basis to give the best fit possible to their data.

In order to fit the Mosby model to the results from the hydrocracking runs reported here, two parameters can be adjusted: the proportion of the residue classified as easy or hard, and a single scaling factor for all the rate constants. The first step in using this model was to guess a scaling factor and scale all the rate constants (k_i). A good first guess for the scaling factor is the value such that the

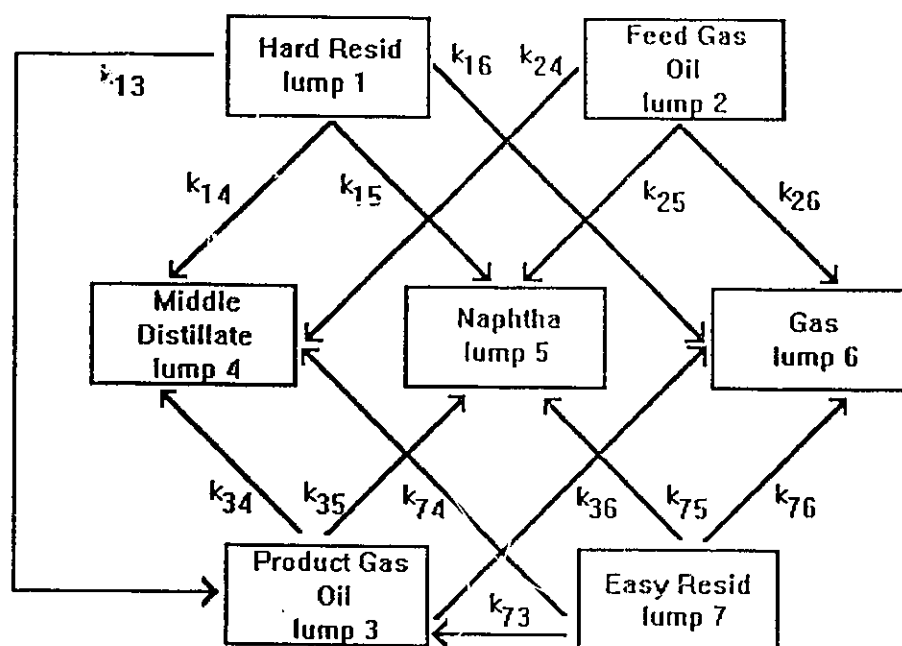


Figure 5.1
Kinetic Model for Hydrocracking of Residue
[Mosby et al., 1986]

predicted residue conversion is the same as the measured conversion. For an irreversible first order reaction in a CSTR the conversion of species i can then be calculated from the following equation:

$$X_i = \frac{\alpha \cdot k_i \cdot \tau}{1 + \alpha \cdot k_i \cdot \tau} \quad 5.1$$

- X_i = fractional conversion of species i .
 k_i = first order rate constant for conversion of species i , h^{-1} .
 τ = residence time based on liquid holdup at 20 °C, h.
 α = scaling factor

This equation allows the conversion of both easy and hard residue to be calculated. By setting the proportion of hard versus easy residue, the inlet concentrations of these residues were calculated, from which, together with the conversions, the concentration of each residue type in the reactor was calculated. For example:

$$C_1 = \frac{F_{1,0} \cdot (1 - X_1)}{F} \cdot \rho \quad 5.2$$

- C_1 = concentration of hard residue in reactor, g/L.
 $F_{1,0}$ = mass inlet rate of hard residue, g/h.

- F = total mass outlet rate, g/h.
 X₁ = conversion of hard residue.
 ρ = density of reactor liquid, g/L.

Knowing the concentrations of the two residue types permits the calculation of the rate of product gas oil formation:

$$R_{3,formation} = \alpha \cdot k_{13} \cdot C_1 + \alpha \cdot k_{73} \cdot C_7 \quad 5.3$$

R_{3,formation} = rate of product gas oil formation, g/(L-h).

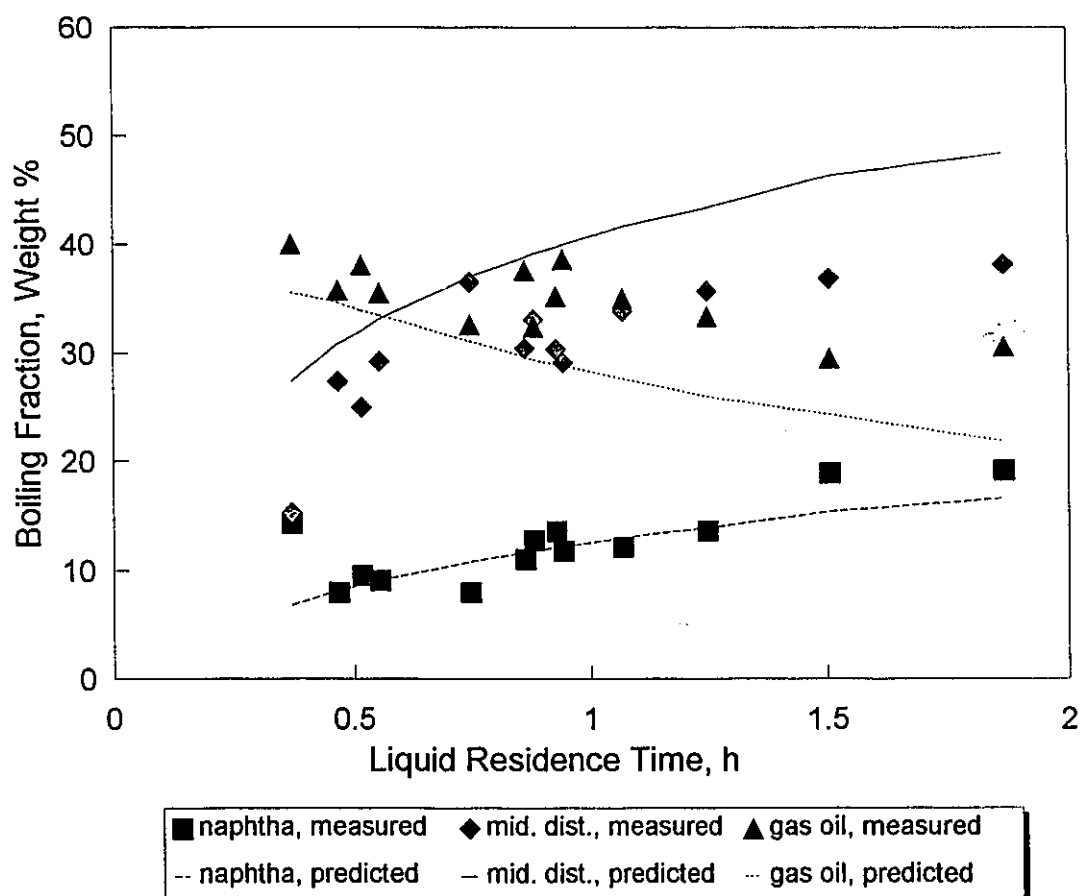
- C₁ = concentration of hard residue in the reactor, g/L.
 C₇ = concentration of easy residue in the reactor, g/L.
 k₁₃ = first order rate constant for the conversion of hard residue to product gas oil, h⁻¹.
 k₇₃ = first order rate constant for the conversion of easy residue to product gas oil, h⁻¹.
 α = scaling factor

The conversion of both feed and product gas oil were calculated in the same way that the residue conversions were calculated. The rate of formation of the middle distillate, naphtha and gases were determined from the known concentrations of the residues and gas oils. After the k_i's were scaled and the fraction of hard residue was specified then, for a given residence time, the product distribution was

predicted from the Mosby model. The best fit to the data required adjusting both the fraction of hard residue and the value of α .

The data collected included a series of catalytic runs with different residence times, at 430 °C and 13.7 MPa. These reactor runs are described in Chapter 4. By changing both the proportion of each residue type and the scaling factor, an attempt was made to fit the Mosby model to these data. The sum of squared residuals (SSR) indicated how well each set of parameters fit the data. The best fit was given by 94 % hard residue in the feed and a scaling factor of 0.95. As can be seen in Figure 5.2, these parameters gave a poor fit to the data. The model consistently underpredicted the amount of gas oil and overpredicted the amount of middle distillate.

Figure 5.2
Fit of Mosby Model to Data for Hydrocracking of Athabasca Bitumen



5.3 Modified Model for Hydrocracking

Due to the problem encountered in fitting the Mosby model to the hydrocracking data, modification of the model was necessary. Changing the different relative k 's results in 16 potential adjustable parameters, which would make modeling a pointless exercise. Since most of the Athabasca residue was "hard", the "easy" residue lump was removed from the model. In addition, to simplify the analysis, the model was recast in terms of a first order rate of disappearance of a lump and a set of stoichiometric coefficients. For example, in the original model the rate of naphtha formation from the hard residue was calculated as follows:

$$R_{15} = \alpha \cdot k_{15} \cdot C_1 \quad 5.4$$

R_{15} = rate of conversion of hard residue to naphtha,
g/(L-h).

α = scaling factor.

k_{15} = first order rate constant for the conversion of hard
residue to naphtha, h^{-1} .

C_1 = hard residue concentration in reactor, g/L.

In terms of stoichiometric coefficients the rate would be calculated from:

$$R_{15} = S_{15} \cdot R_{1, total} \quad 5.5$$

R_{15} = rate of conversion of hard residue to naphtha,
g/(L-h).

S_{15} = stoichiometric coefficient for the conversion of
hard residue to naphtha.

$R_{1, total}$ = total rate of hard residue conversion,
g/(L-h).

Figure 5.3 shows the modified model, with first order rate constants replaced by stoichiometric coefficients. This formulation of the model indicates that there are three independent reactions and thirteen stoichiometric coefficients for a total of sixteen parameters (Table 5.1).

Lump	1	2	3
Conversion Rate	R_1	R_2	R_3
Stoichiometric Coefficients	S_{13}	-	-
	S_{14}	S_{24}	S_{34}
	S_{15}	S_{25}	S_{35}
	S_{16}	S_{26}	S_{36}

By definition, for each lump in the table the stoichiometric coefficients must sum to 1, which removes one adjustable coefficient from each lump, reducing the total adjustable parameters to 10.

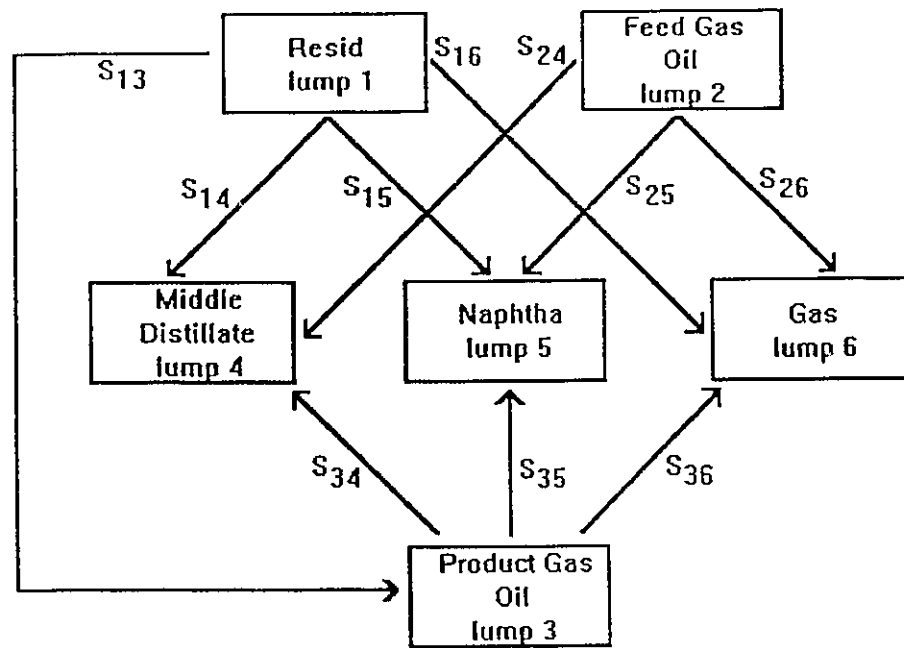


Figure 5.3
Modified Hydrocracking Model

5.3.1 Parameter Estimation

To further reduce the number of adjustable parameters it is desirable to get direct measurements of the kinetics for catalytic hydrocracking of the feed gas oil. Data of this nature were available for virgin Athabasca gas oil in the thesis of Chung (1982), at temperatures of 420 and 440 °C. Using these data to calculate the first order rate constants for the transformation of this gas oil to middle distillate, naphtha and gas at the two temperatures allowed calculation of the pre-exponential factors and activation energies for these reactions. This in turn made it possible to predict the first order rate constants for these reactions at 430 °C. As the liquid holdups from Chung's work were questionable and the runs had no added catalyst, the actual rates cannot be used. However, by using the ratio of the individual k_i to the overall k for the cracking of this gas oil, the stoichiometric coefficients for this reaction can be determined. For example:

$$S_{25} = \frac{k_{25}}{k_{2, total}} \quad 5.6$$

S_{25} = stoichiometric coefficient for the conversion of feed gas oil to naphtha.

k_{25} = first order rate constant for the conversion of feed gas oil to naphtha, h^{-1} .

$k_{2,\text{total}}$ = first order rate constant for the total conversion of feed gas oil, h^{-1} .

The rate of conversion of feed gas oil to naphtha can then be calculated by multiplying the total rate of feed gas oil conversion by this stoichiometric coefficient.

The kinetics for the hydrocracking of the product gas oil were also estimated, this time using data from the thesis of Man (1981). The feed used in this study was CANMET hydrocracked heavy gas oil, which was reacted at 425 °C and 17.2 MPa. Although a pressure of 13.9 MPa was used in the present study, comparing other runs done by Man at 13.8 MPa and 17.2 MPa showed little change in the product distribution with pressure. Once again, uncertainty in the liquid holdup and use of the slightly lower temperature made direct rate calculations questionable, therefore stoichiometric coefficients were calculated from Man's data. Table 5.2 shows the proportion of the gas oils going to the various product fractions.

Gas Oil Type	Stoichiometric Coefficient to Mid. Dist.	Stoichiometric Coefficient to Naphtha	Stoichiometric Coefficient to Gas
Product	0.20	0.60	0.20
Feed	0.45	0.41	0.14

The rate of residue conversion was established by fitting the residence time data to first order kinetics, as described in Chapter 4, thereby determining this rate directly from the experimental data. This approach resulted in a total of five adjustable parameters in the modified Mosby model: three of the residue conversion coefficients, the rate of product gas oil (PGO) conversion and the rate of feed gas oil (FGO) conversion.

As noted above, to fit the modified model to the reactor data the measured residue conversion was fit with first order kinetics, giving a rate constant of 2.217 hr^{-1} at 430°C and 13.7 MPa with an r^2 of 0.96. The details of this regression were given in Chapter 4. The expected residue conversion for each residence time was calculated from equation 5.1, which smooths the data and prevents the propagation of any error in the individual residue concentrations. The rate was then calculated from the conversion:

$$R_i = \frac{F_{i0} \cdot X_i}{v} \quad 5.7$$

- R_i = rate of conversion of lump i, g/(L-h).
 F_{i0} = inlet mass flow rate of lump i, g/h.
 X_i = conversion of lump i.
 v = liquid holdup in reactor, L.

Setting the stoichiometric coefficients for the residue reactions then gave the rate of formation of PGO and products from the residue. Finally, setting the first order rate constants for the overall conversion of PGO and FGO to products allowed the calculation of their conversion rates through equations 5.1 and 5.6. Once all the rates were determined, a mass balance could be performed on each lump. From this balance the outlet flow of each fraction could be calculated for a given residence time, and expressed as a mass % by dividing the fraction's predicted outlet mass flow rate by the measured total outlet mass flow rate. To force the predicted outlet mass flow rate to be the same as the measured rate, the predicted residue outlet rate was determined by difference between the predicted sum of the other fractions and the total measured rate. The five adjustable parameters were used to give the best fit of the reactor data, with a minimal sum of squared residual.

Changing the stoichiometric coefficient for the rate of residue going to naphtha between 0 and 9 % only changed the total sum of squared residuals (SSR) by 4 %. Due to the insensitivity of the model it is important to examine other data sets for the hydrocracking of Athabasca bitumen to define the best values for the adjustable parameters in this model. Two catalytic hydrocracker runs were done by Gray et al. (1992) for a report to CANMET using a more severely topped Athabasca bitumen, giving a feed with 70 % residue content, as

opposed to 55 % in the residence time series reported here. These data were obtained with a slightly different ratio of catalyst weight to liquid holdup than that used in this experiment, 152 g/l as opposed to 208 g/l. By separately calculating the thermal and catalytic contributions from the residence time series data, the CANMET data can be scaled to correct for the amount of catalyst. The thermal first order rate constant for residue conversion was measured in this study at 430°C and 13.7 MPa, with a residence time of 0.94 hr. This thermal rate constant was 1.556 hr^{-1} . Subtracting this value from the rate constant with catalyst, 2.22 hr^{-1} , and dividing by the catalyst to holdup ratio, 208 g/l, gave a purely catalytic rate constant of $0.00319 \text{ l}/(\text{hr-gcat})$. For the CANMET data the expected first order rate constant for residue conversion was found by multiplying the catalytic contribution by the catalyst to holdup ratio, 152 g/l, and adding this to the thermal constant, 1.556 hr^{-1} . This resulted in an expected residue conversion rate constant of 2.04 hr^{-1} , which was 92 % of the constant for the residence time data calculated in Chapter 4.

In addition to the effect of a different amount of catalyst, the liquid holdup for this case may not be accurate, but can be scaled to the residence time series data by forcing it with the first order rate constant. For the CSTR the following relationship holds:

$$\frac{F_{1,o} - F_1}{v} = k_{1,total} \cdot C_1 \quad 5.8$$

$F_{1,o}$ = mass inlet rate of residue, g/hr.

F_1 = mass outlet rate of residue, g/hr.

v = liquid holdup in reactor, l.

$k_{1,total}$ = first order rate constant for residue conversion, hr^{-1} .

C_1 = residue concentration in the reactor, g/l.

Since the rate constant was calculated above, and the flow rates and residue concentration were measured, the liquid holdup can be treated as an unknown and calculated from equation 5.8. This results in a corrected residence time of 0.60 hr. Essentially this procedure involved predicting the expected residue conversion for the CANMET data based on the residence time data, with adjustment for the amount of catalyst; the residence time was then adjusted so that the CANMET data fit this predicted conversion. It was assumed that the effect of the smaller quantity of catalyst would affect the gas oil to the same degree as the residue, so the rate constants for the conversion of the gas oils were also multiplied by 0.92. The modified model was then fit to the average of the two CANMET runs.

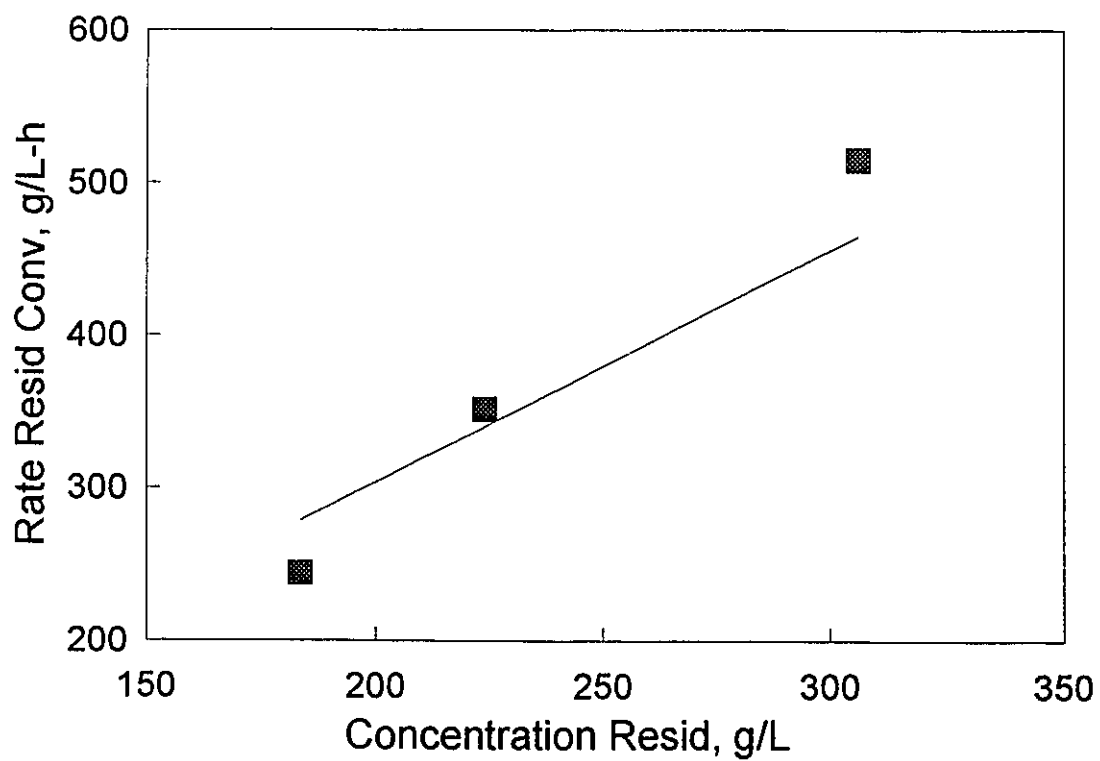
Another data set was available for an experiment with only thermal conversion, that is with no added catalyst. One

thermal run that was carried out in this study, with a residence time of 0.94 hr, was described above. Other data were also available at the same conditions from work done by Dr. Farhad Koresheh, with residence times of 0.47 and 1.88 hr, using the reactor system and procedure described in Chapter 3. Fitting these residue conversions to first order kinetics gave an estimate of the rate constant of 1.519 hr^{-1} , 0.685 times the catalytic constant. This fit is illustrated in Figure 5.4. Multiplying the rate constants for the conversion of feed and product gas oils by 0.685 would therefore scale the modified model for use with thermal data.

To find the best set of parameters the SSR was minimized using the catalytic residence time data, with the residue to naphtha stoichiometric coefficient (s_{15}) varied between 0 and 0.11. Values higher than 0.11 gave a negative conversion of product gas oil. Table 5.3 shows that, as mentioned above, the best set of parameters for the catalytic residence time data was the set with the residue to naphtha coefficient of 0. The set which best fit the CANMET data had a residue to naphtha coefficient (s_{15}) of 0.05, and the set which best fits the thermal data has a naphtha coefficient of 0.13. An intermediate value of $s_{15} = 0.06$ was selected based on these three results. As Figure 5.5 indicates, the chosen parameters gave a satisfactory fit to the measured values for the residence time data.

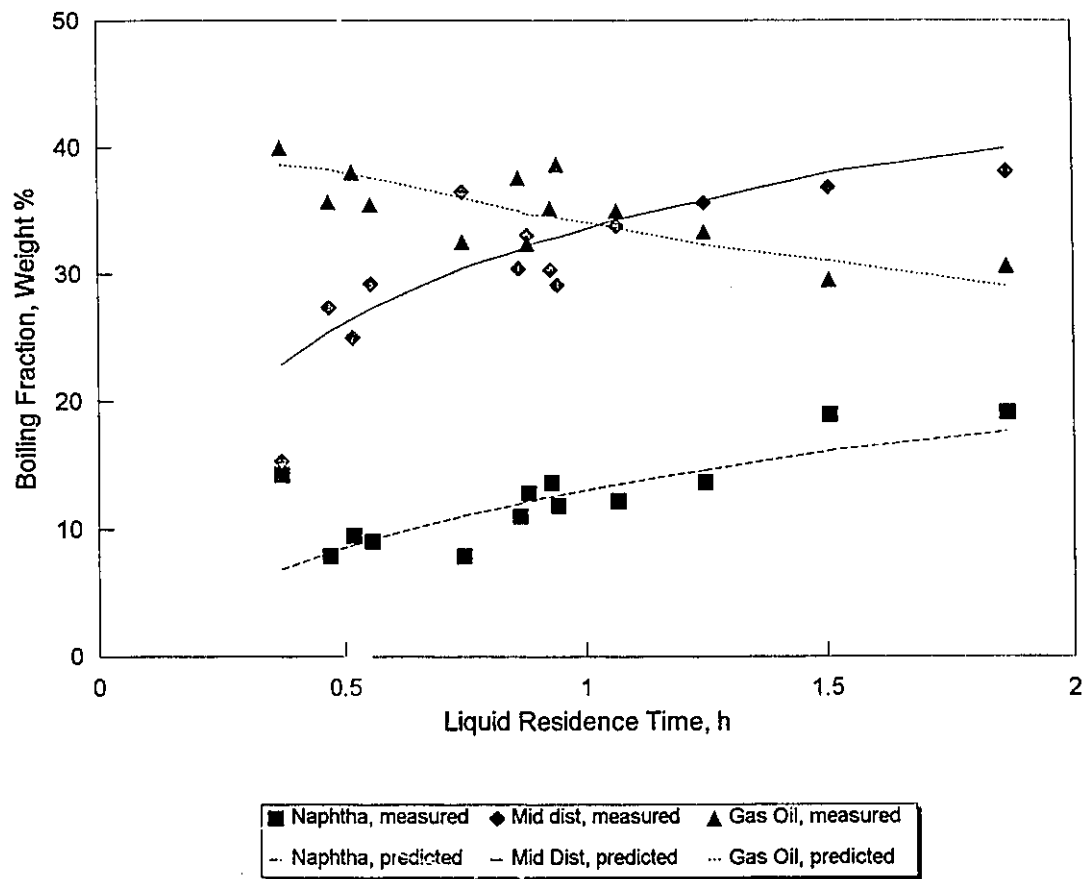
When minimizing the SSR, cases where there were specific

Figure 5.4
First Order Fit for Residue Conversion, Thermal Data



■ Measured Data – Fit, forced through 0

Figure 5.5
Fit of Modified Mosby Model to Residence Time Data



biases for a certain cut were avoided; for example, if the model always over predicted the amount of naphtha, then this was considered an unsatisfactory solution and was discarded.

Table 5.3 Best Fit Parameters					
Best Fit For:		R.Time Data	CANMET	Thermal	Overall
Stoichiometric Coefficient, Residue to:	PGO (s_{13})	0.56	0.46	0.28	0.43
	Mid (s_{14})	0.34	0.38	0.44	0.39
	Nap (s_{15})	0.00	0.05	0.13	0.06
	Gas (s_{16})	0.10	0.12	0.15	0.12
First Order Rate Constant	PGO (k_2)	0.24	0.2	0.07	0.17
	FGO k_3	1.59	1.18	0.76	1.13
Sum of Squared Residuals	R.Time Data	3036	3111	3258	3132
	CANMET	215.5	161.0	401.3	169.0
	Thermal	1712	1766	1523	1678

Figure 5.6 demonstrates that there are no strong biases in the error between the predicted and measured product composition at each residence time for this set of parameters.

Figure 5.6
Residuals for the Residence Time Data

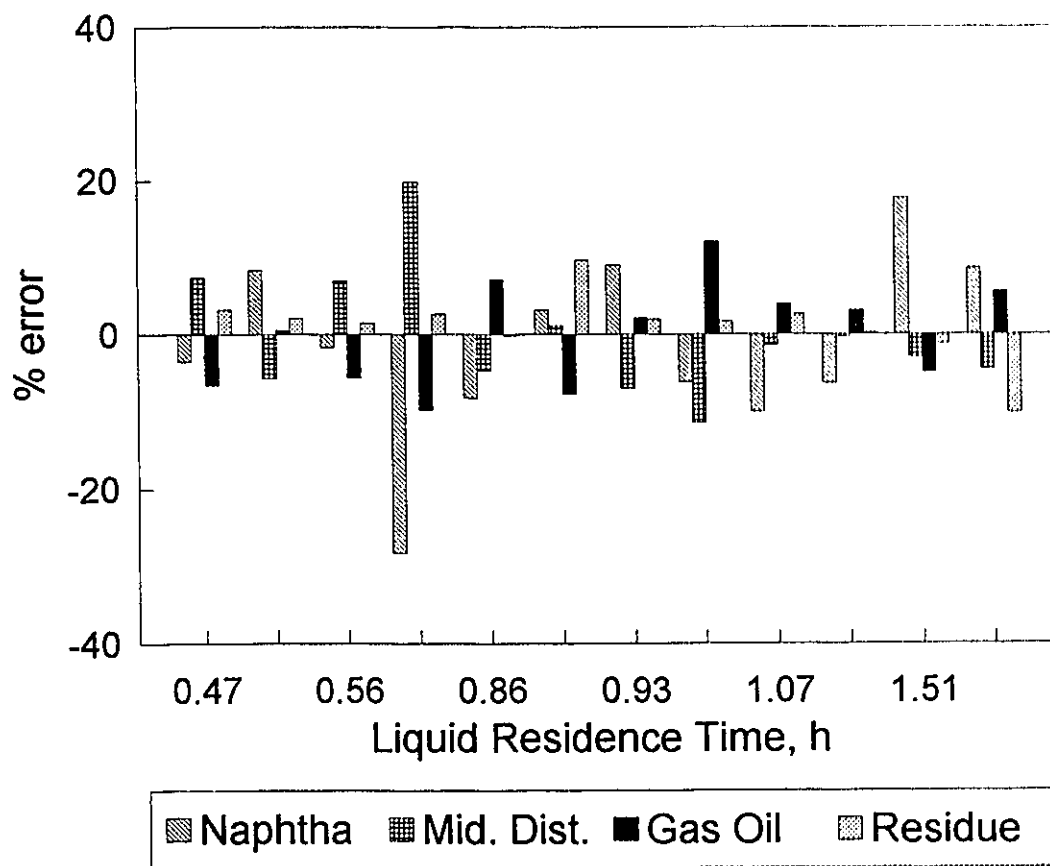
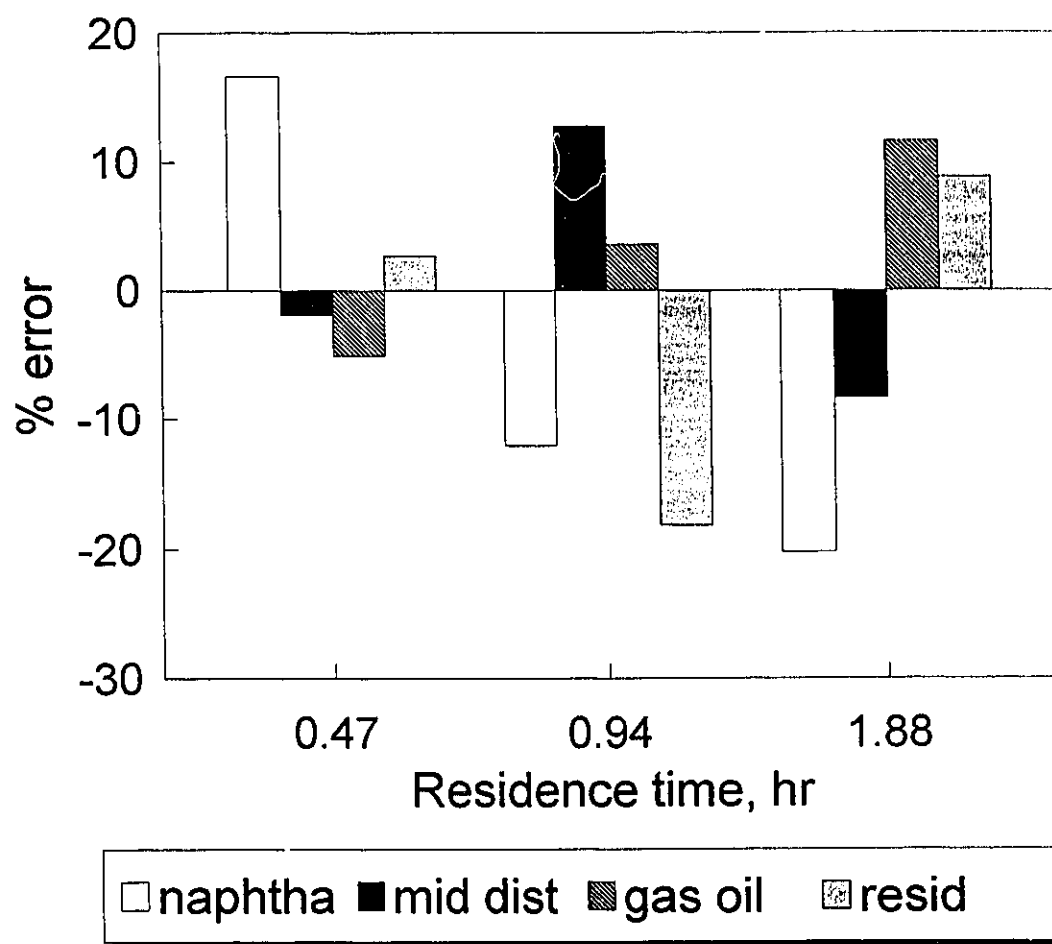


Figure 5.7 shows a similar plot for the thermal data, where the large error for a few of the values, such as the lowest residence time naphtha, contribute to the large residual seen for the thermal data in Table 5.3. Table 5.4 gives the fit for the CANMET data.

Table 5.4 Modified model, best fit to CANMET data		
Cut	Predicted Mass %	Measured Mass %
Naphtha	8.4	8.7
Middle Distillate	21.5	19.6
Gas Oil	35.4	38.1
Residue	34.8	33.6

The total outlet liquid mass flow rate for the reactor was inaccurate due to problems with the electronic scale (described in Chapter 3), so it was calculated by difference through a carbon balance on the total inlet liquid and outlet gas flow rates. As noted above, this 'measured' outlet liquid flow rate was used in the modified model as the sum of the outlet rates for all the liquid fractions. Because the same outlet liquid flow rates are used in both cases, the predicted outlet gas flow rate, although not directly used in setting the parameters, should be consistent with the measured values of gas rate when a good fit of the liquid product distribution is obtained. However, the initial mass balance on the feeds and products from the reactor had a small bias of more feed

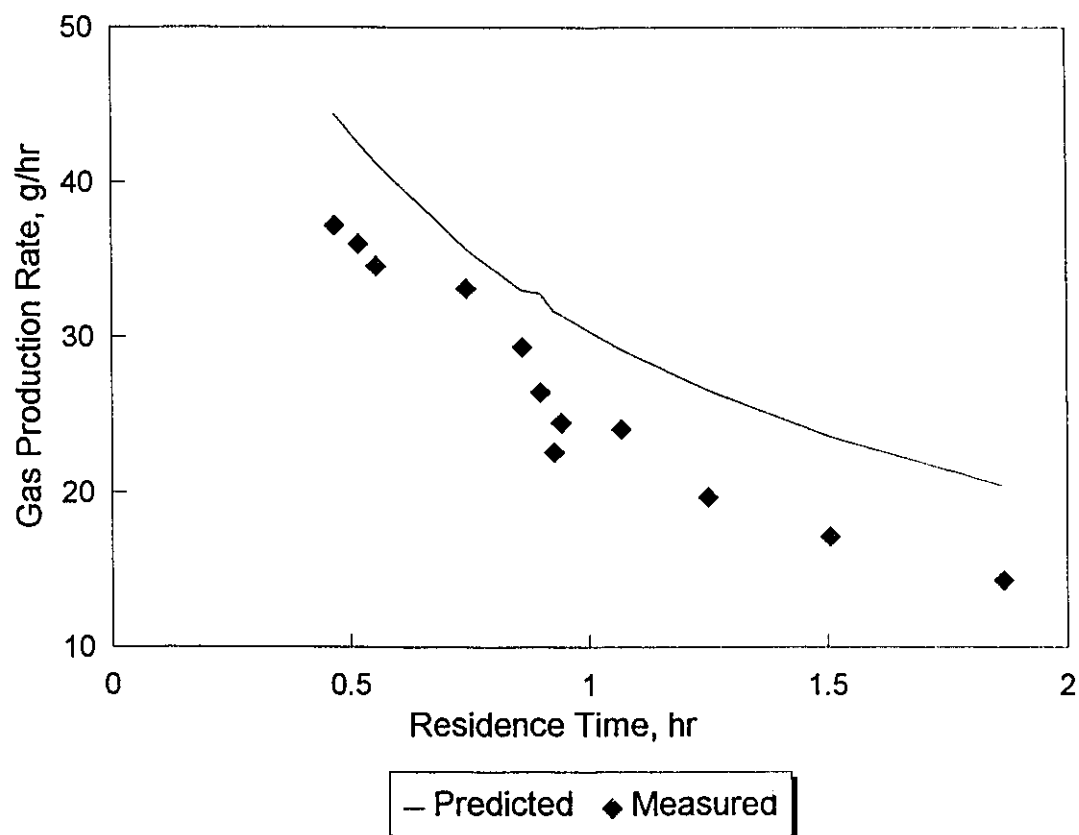
Figure 5.7
Residuals for the Thermal Data



than product. This is because a carbon balance was used to estimate the outlet rate, which ignores some minor components such as H_2O , which leave with the gas. In the modified model all of this error appears in the gas production rate, which is only about 7 % of the liquid rates, giving a consistent offset of approximately 20 %. This fit is demonstrated in Figure 5.8 for the modified model using the overall parameters.

One last approach was undertaken to try to reduce the number of adjustable parameters. The data for the feed gas oil taken from Chung (1982) was used as reported, including the total rate constant. Observing the data reported in Table 5.3, it was noted that the product gas oil appears to have a much lower rate constant than the feed gas oil. Evidence for this was seen in work done by Man (1981), where, above, it was assumed that the feed used represented product gas oil. He actually used the gas oil cut from the CANMET hydrocracker, which may be a combination of uncracked feed and product gas oil. The data presented for the gas oil conversion did show a change in kinetics at long residence times, which was consistent with these two lumps. Estimating the product distribution from cracking at long residence times gave slightly different stoichiometric coefficients than those used for the data presented in Table 5.3. This is demonstrated in Table 5.5. The SSR was 2873 for the residence time data, 415 for the CANMET data and 1585 for the thermal data. This was a better fit than that given in Table 5.3 for both the

Figure 5.8
Gas Production Rate for Residence Time Data



residence time and thermal data, except here there are four adjustable parameters instead of five as the total rate constant for the conversion of PGO is taken directly from Chung.

Table 5.5 Stoichiometric Coefficients for Modified Model			
Product	Reactant		
	Residue	PGO	FGO
PGO	0.53	-	-
Mid. Dist.	0.35	0.00	0.45
Naphtha	0.00	0.95	0.41
Gas	0.12	0.05	0.14
First Order Rate Constant, h^{-1}	2.22	0.13	1.71

5.4

Conclusions

By modifying the hydrocracking model proposed by Mosby et al. (1986), the product distribution for the catalytic hydrocracking of Athabasca bitumen can be predicted. However, unique values for the adjustable parameters for this modified model do not appear to be definable unless other data are considered. Modifying the feed to contain a higher percentage of residue cut or not adding catalyst resulted in different best fit values for the adjustable parameters. Nonetheless, a single set of stoichiometric parameters did give a reasonable fit to all the data sets. To verify the values for these adjustable parameters, it would be necessary to measure directly the first order rate constant for feed gas oil conversion using this reactor apparatus.

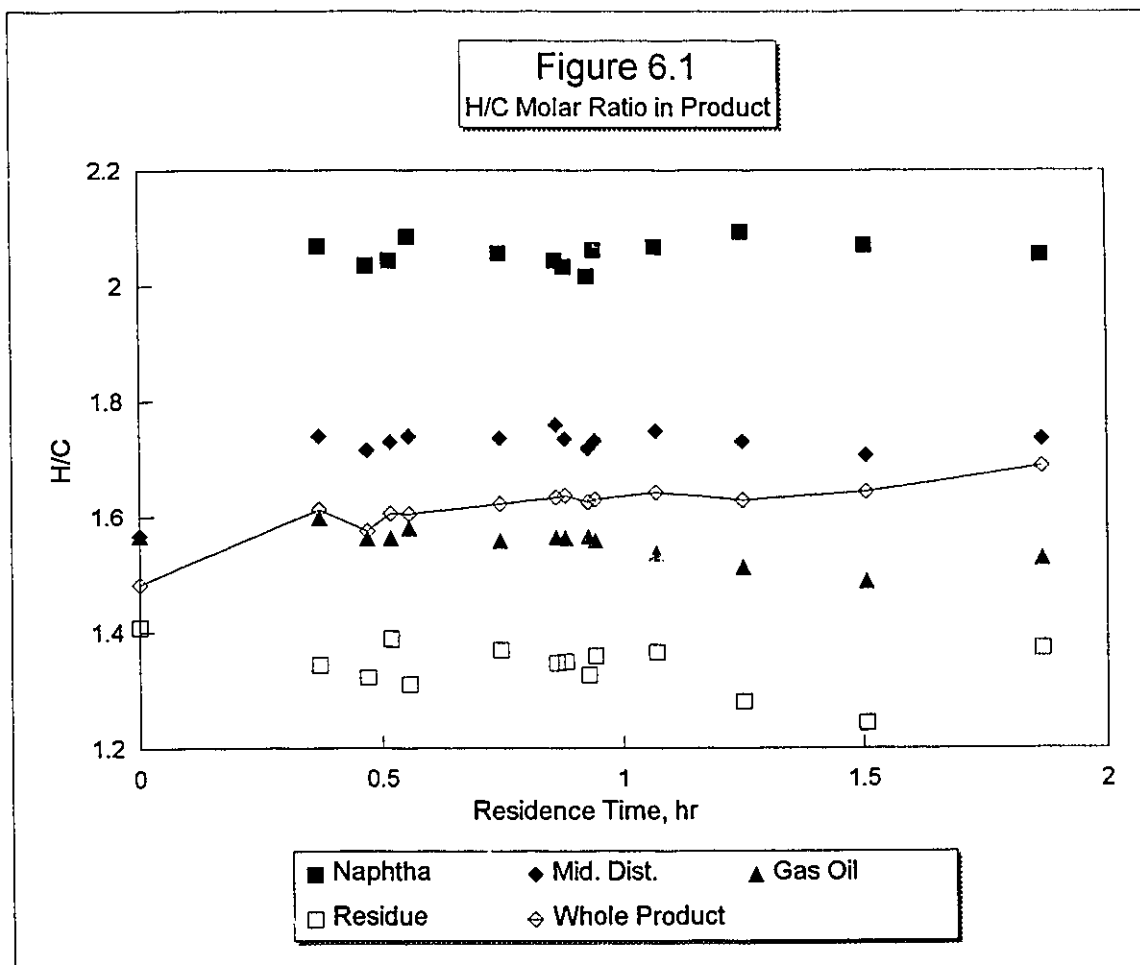
Chapter 6
Sulfide and Pyrrole Analysis

6.1 Introduction

The kinetics for the overall removal of sulfur and nitrogen from bitumen during hydrocracking were discussed in Chapter 4. For this overall removal, the sulfur and nitrogen were treated as pure reactants; the various sulfur and nitrogen compounds with differing molecular weights, as well as the types of molecules containing the heteroatom were not differentiated. However, the type of molecule containing the heteroatom may have a significant influence on its removal; additionally, as sulfur and nitrogen removal are mostly catalytic, the molecular size will also have some impact. To study these phenomena, the residence time and thermal data described in Chapter 4 were used to examine the sulfur and nitrogen removal within each boiling cut, with an additional attempt made to differentiate the pyrrolic nitrogen from the total nitrogen removal, as well as the thiophenic from the aliphatic sulfur removal.

6.2 Hydrogenation

Bitumen contains aromatic structures which can be hydrogenated to facilitate conversion. As discussed in Chapter 2, the hydrogenation reactions in the lighter cuts may be limited by thermodynamics at the conditions used in this study. However, heavy cuts such as the residue should not show these effects. Figure 6.1 shows the ratio of hydrogen to carbon in the various boiling cuts for the catalytic residence



time experiments; the H/C ratio is related to the aromaticity of the cut, but only in a qualitative way due to the influence of complications such as naphthenic (non-aromatic) rings. The rough correlation between the H/C ratio and aromaticity is discussed in Chapter 2; as described earlier the H/C ratio is higher for the lighter fractions which have smaller average molecular weights. Due to the relative strengths of the carbon-carbon bonds in different structures, it is expected that most aromatic rings will remain intact during cracking, with most of the bond breakage taking place in paraffinic and naphthenic structures. This cracking will tend to break up the large paraffinic structures and cleave the side chains. As a result most the long chain would be broken up and should end up in the lighter cuts, resulting in a high H/C ratio for these cuts. This high H/C ratio is not a catalytic phenomena but could be a thermal cracking process based on the similar H/C ratio in the products from the thermal runs.

Girgis and Gates (1991) noted that, in general, it becomes increasingly difficult to hydrogenate larger fused ring aromatics fully. The initial hydrogenation to form a dihydro structure is relatively easy, with further hydrogenation becoming progressively harder. This hydrogenation process explains why the residue cut does not show a decline in the H/C ratio with residence time as more conversion to lighter fractions with higher H/C ratios takes place. The partial hydrogenation of the large saturated ring

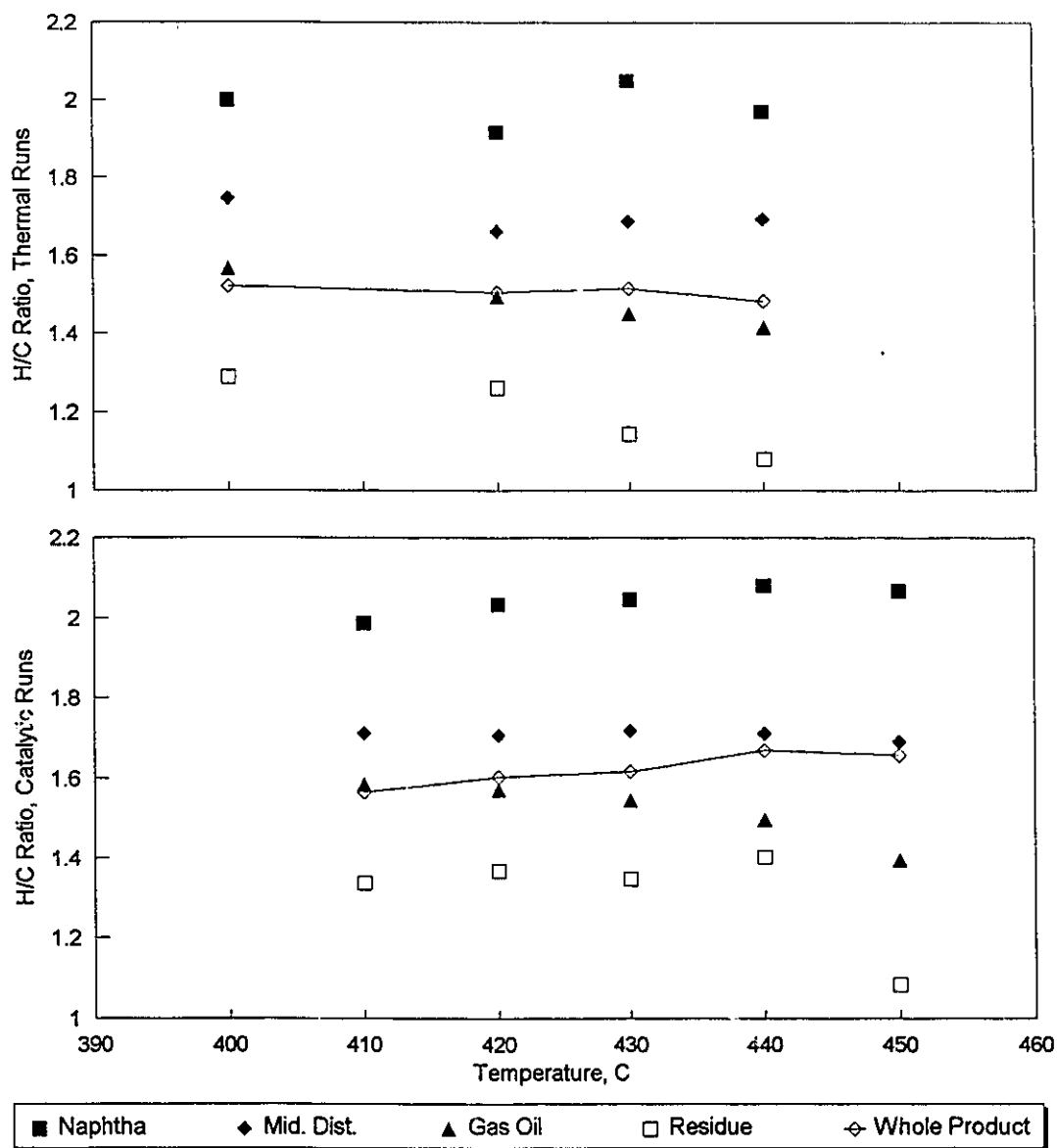
structures in the residue would compensate for the preferential loss of the paraffins. Still, over longer reaction time the residue would be expected to contain fewer paraffinic side chains and bridges (paraffinic chains linking two aromatic ring structures) of significant size, so the products going to the lightest cuts should be more aromatic. This change in the residue was seen by Gray et al. (1992) during the hydrocracking of several types of bitumen, including Athabasca bitumen. As it is much more difficult to hydrogenate small aromatic rings, due to resonance stability considerations, a net decrease in the H/C ratio for the lighter cuts with residence time would then be expected. Although this change was not seen, it may have been masked due to the small incremental change in the amount of the lighter cuts with the additional residence time. Examination of Figure 5.5 shows that increasing the residence time from 1 h to 2 h only increased the amount of naphtha and middle distillate by about 30 %. This result, combined with the qualitative nature of the H/C ratio, may hide small increases in the aromaticity of the lighter cuts. NMR analysis of these samples would provide a more direct answer.

The gas oil cut was somewhat different than the other cuts as it was both a reactant in cracking reactions and a product. From the modelling discussed in Chapter 5 it appears that this cut may represent two distinct lumps, the feed gas oil, and the product gas oil from the residue conversion. The

feed gas oil would be expected to have a higher proportion of paraffinic side chains and bridges than the residue cut. The product gas oil, on the other hand, may have a higher proportion of condensed ring structures as the side chains have already been removed. This trend is consistent with the slight decrease in the H/C ratio with residence time observed in Figure 6.1 since, from the modelling done in Chapter 5, the gas oil is made up of a higher and higher proportion of product gas oil as the residence time is increased.

It was noted in Chapter 4 that the runs with residence times of 1.25 and 1.5 h showed no nitrogen and very little sulfur removal. This did not fit in with the rest of the data, so these runs were not used in the calculations of the overall nitrogen and sulfur kinetics. The residue conversion, however, was normal for both these runs. Careful examination of the data log for the single day when both of these runs were carried out did not show any abnormalities. Examination of Figure 6.1 shows the H/C ratio for these two runs was also anomalous, but only for the heavy fractions. A comparison of catalytic vs thermal runs for several temperatures is given in Figure 6.2, and from this it can be seen that the catalyst makes little difference to the H/C ratio for the naphtha and middle distillate cuts, but does maintain a higher ratio for the gas oil and residue cuts. Considering all of the above observations, it appears that the catalyst was somehow inactivated for the run in question, resulting in normal

Figure 6.2
H/C Molar Ratio vs Temperature



thermal reactions, such as residue conversion, but reducing the catalytic reactions, such as sulfur and nitrogen removal and hydrogenation of the heavy fractions.

The effect of temperature on the H/C ratio will depend on the controlling mechanism. From Girgis and Gates (1991) it is expected that hydrogenation reactions reach equilibrium quickly for small model compounds and that the equilibrium constant for the hydrogenation of aromatic rings will get smaller with increasing temperature, reducing the amount of hydrogenation taking place. Conversely, increasing the temperature may increase the rate of hydrogenation, and thus the H/C ratio, if the reaction is kinetically controlled. Both phenomena were observed for distillate fractions of Alberta synthetic crudes by Wilson et al. (1985). In Figure 6.2, dehydrogenation is clearly seen for the thermal runs for all the cuts except the naphtha and middle distillate. The hydrogen to carbon ratio was constant for the whole product, and the same as the feed ratio within the estimated error of $\pm 2 \%$, which implies there is little hydrogenation activity without a catalyst. It therefore seems likely that the dehydrogenation of the heavier cuts is caused by increased cracking with temperature of the paraffinic components in these cuts, resulting in a depletion of the H/C ratio for the heavy cuts but not for the whole product. Since the hydrogen to carbon ratio in coke is much lower than in the product, the formation of coke might affect the H/C ratio in the residue.

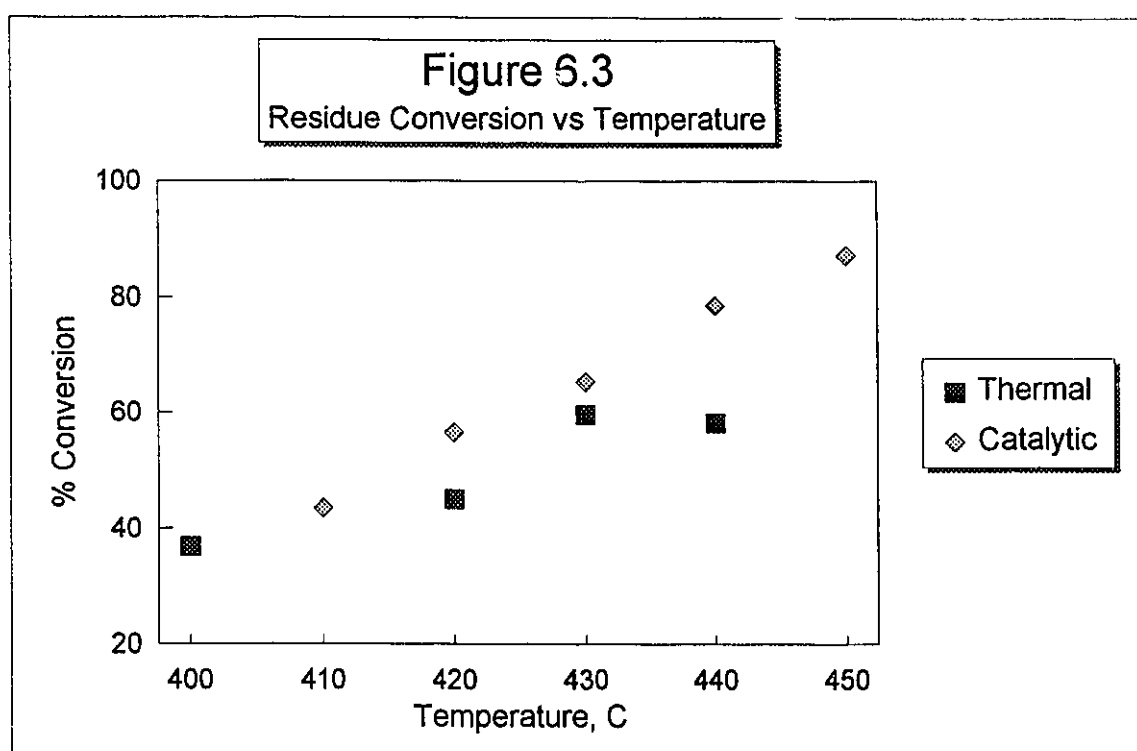
However, although the coke formation was not quantified in this study, it was noted that it did not change substantially between runs and formed at less than 5 g/h in the bottom of the reactor. Doubling this rate of coke formation would change the H/C ratio by less than 1 %, so it is inconsequential to these results.

The whole product for the catalytic case shows an increase in the H/C ratio with temperature. Summing the hydrogen and carbon contents in the boiling cuts and comparing this to the overall measurements gives an average error of less than ± 1 %. This result indicates that the increase in the hydrogen to carbon ratio with temperature is real. Examination of Figure 6.2 indicates that the catalyst has little effect on the light cuts which maintain their H/C ratio with an increase in temperature. For the heavier cuts the H/C ratio for the thermal runs may decrease with increased temperature due to preferential cracking of paraffinic material as discussed above. The catalyst in this case seems able to counter this tendency, possibly by increasing the rates of hydrogenation reactions with temperature, preventing the dehydrogenation of the residue and middle distillate cuts up to 440 °C.

The naphtha actually shows a slight increase in the H/C ratio with temperature, although it is not clear whether this is due to an increased hydrogenation of the benzene type structures in the naphtha, or because hydrogenation of the

residue and gas oil cuts results in the production of more paraffins. The gas oil still shows a decrease in the H/C ratio with temperature, likely due to the influence to the two gas oil types, as discussed above. The H/C ratio for the gas oil is higher for the catalytic than the thermal case for each temperature.

The most striking difference between the H/C profile for the catalytic runs and the thermal runs demonstrated in Figure 6.2 is the maintenance of the H/C ratio for the residue at close to the feed level for the catalytic case up to 440 °C. In fact, Girgis and Gates (1991) note that increasing the temperature results in lower equilibrium conversions in aromatic hydrogenations which would lead to lower actual conversions if equilibrium was attained. However, Figure 6.3 shows that for both the thermal and catalytic cases the residue conversion actually goes up with temperature. The simplest reason for this phenomenon is that the large ring structures in the residue cut reach equilibrium slowly, so that up to about 440 °C the hydrogenation of this cut is kinetically, rather than thermodynamically, limited. Some evidence for this observation in the literature was discussed in Chapter 2; larger ring structures reach equilibrium more slowly, as do actual distillate cuts as opposed to model compounds. Thus the residue cut would not be expected to attain equilibrium under the conditions used in this study.



6.3 Nitrogen Types

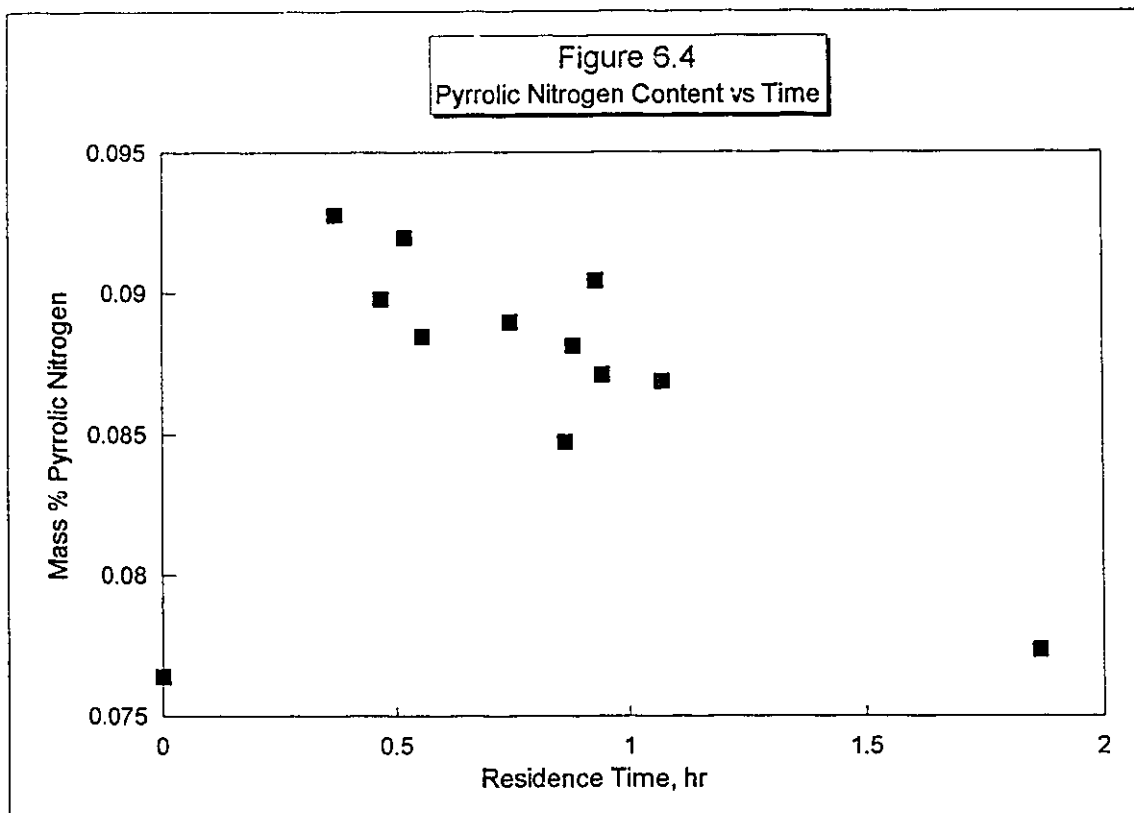
As indicated in Chapter 2, bitumen contains two main types of nitrogen compounds, both of which are aromatic: the basic pyridine benzologues and the neutral pyrrole benzologues. As described in Chapter 3, pyrrolic nitrogen can be approximately quantified using IR spectroscopy, whereas the total nitrogen can be quantified through combustion followed by chemiluminescent detection. Although the pyrrolic nitrogen analysis is only semi-quantitative, it is expected to be proportional to the true value. This means the relative concentrations of the pyrrolic and total nitrogen can be compared at different residence times; such a comparison indicates the relative ease of conversion of each nitrogen type. The order for the overall conversion of pyrrolic nitrogen can be calculated in the same manner as described for the total nitrogen in Chapter 4, but the rate constant does not reflect the true value due to the semi-quantitative nature of the analysis. This can be seen in Equation 6.1, where the semi-quantitative measurements are corrected to give the true kinetics:

$$\alpha \cdot R_p = k \cdot (\alpha \cdot C_p)^n \quad 6.1$$

- α = correction factor.
- R_p = rate of pyrrolic nitrogen removal, g/l-h.
- k = rate constant, (g/l)¹⁻ⁿ/h.
- C_p = concentration of pyrrolic nitrogen, g/l.
- n = reaction order.

Although the correction factor is not known, plotting this equation on logarithmic coordinates would give a straight line, with the slope giving the reaction order and the intercept giving the rate constant multiplied by the correction factor to the power $n-1$.

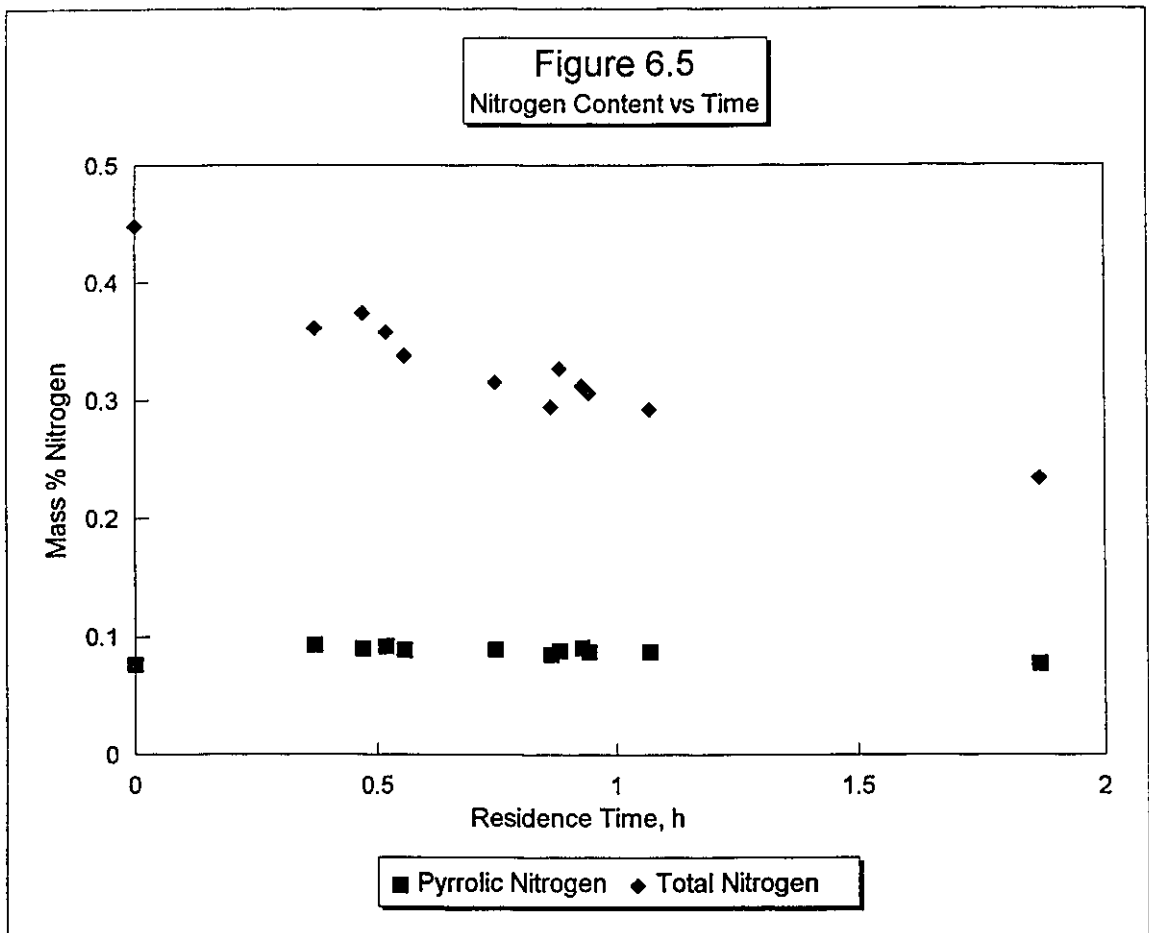
The change with residence time of the pyrrolic nitrogen content is demonstrated in Figure 6.4. The mass percent pyrrolic nitrogen on the y-axis is calculated by dividing the outlet liquid mass rate of pyrrolic nitrogen by the inlet bitumen feed rate, which corrects for the mass lost as gas. Plotting the data in this fashion indicates the conversion of nitrogen in the reactor, which may not be apparent if only the mass % nitrogen in the outlet liquid product is examined; the ratio of liquid product to liquid feed decreased with residence time, so if no nitrogen is converted there is an apparent increase in the nitrogen content with residence time if the mass % nitrogen in the liquid product is used directly. The conversion can be calculated from Equation 6.2, where the mass % pyrrole in the feed is not known:



$$X = 1 - \frac{1}{\omega_{in}} \cdot \frac{\dot{m}_{out}}{\dot{m}_{in}} \cdot \omega_{out} \quad 6.2$$

- X = conversion.
 ω_{in} = mass % pyrrole in feed bitumen.
 ω_{out} = mass % pyrrole in total liquid product.
 \dot{m}_{in} = bitumen feed mass flow rate.
 \dot{m}_{out} = liquid product mass flow rate.

As can be seen in the Figure 6.4, there is an initial rise in the pyrrolic nitrogen content which makes the kinetic analysis difficult, as all the rates are then calculated to be negative. An explanation for this phenomenon is that some of the pyrrolic nitrogen does not appear in the analysis of the bitumen, but shows up after light conversion. Figure 6.5 shows the changes in both the total and pyrrolic nitrogen content with residence time. As can be seen from the figure, the total nitrogen content shows a decrease rather than an increase with residence time. This initial rise in the concentration of pyrrolic, but not total, nitrogen may arise from nitrogen in aromatic structures which have a side chain rather than a hydrogen atom attached to the nitrogen atom. As the IR analysis is based on the nitrogen-hydrogen bond, this structure would not appear as pyrrolic nitrogen. However, it is relatively easy to break off such a side chain and replace



it with a hydrogen atom, resulting in the apparent formation of pyrrolic nitrogen with light conversion, but not affecting the total nitrogen content. These nitrogen structures were proposed by Jacobson and Gray (1987) to explain difficulties in closing the nitrogen balance during the detailed analysis of nitrogen species in Peace River bitumen. The apparent formation of pyrrole, based on IR analysis, could also be due to intermediates in the hydrogenation of basic nitrogen structures such as acridine. Primary and secondary amines would give an N-H stretch band in IR analysis, and such species have been proposed as intermediates in conversion of acridine (Zaqadshi et al., 1982) and benzoquinoline (Shabtai et al., 1989). Analysis of actual oils, however, has never given evidence for sufficient free amines to account for the measured IR absorbances (Choi and Gray, 1988; Jokuty and Gray, 1992). Furthermore, comparing the increase in pyrrolic nitrogen for catalytic and thermal runs with a residence time on 0.94 h, given in Table 6.1, it can be seen that the increase in pyrrolic nitrogen content, on a feed basis, is similar for the catalytic and thermal cases. The thermal run shows essentially no nitrogen removal but an appearance of significantly more pyrrolic nitrogen than any of the catalytic cases demonstrated in Figure 6.4; the catalytic run shows conversion of total nitrogen and a smaller jump in the pyrrole content.

Table 6.1 Nitrogen Compounds in Hydrocracker Product		
Reactor Conditions	Total Nitrogen Mass %	Pyrrolic Nitrogen Mass %
Feed Bitumen	0.444	0.069
430°C No Added Catalyst	0.437	0.096
430°C Added Catalyst	0.306	0.086

As noted in Chapter 4, almost all the nitrogen removal comes from the added catalyst, so the total nitrogen results are as expected. As well, cracking is essentially a thermal reaction, so the jump in the pyrrolic nitrogen content for both cases is consistent if the hypothesis of a N-substituted pyrrole structure is correct. If hydrogenation of basic nitrogen were the source of the increase, then the thermal case, which shows essentially no hydrogenation in Figure 6.2, should not indicate significant hydrogenation of the basic nitrogen either, and therefore no increase in the pyrrolic nitrogen content.

The larger increase in pyrrolic nitrogen content for the thermal 430°C product over the catalytic product is consistent with catalytic hydrogenation of the carbon rings. Catalytic hydrogenation of nitrogen containing rings has been proposed for Athabasca bitumen during hydrodenitrogenation at commercial reactor conditions by Jokuty and Gray (1992). In fact, in their review article, Girgis and Gates (1991) found that hydrogenation of the nitrogen containing ring often

accompanied HDN for several model compounds. Taking the hydrogenation into account would imply the pyrrolic nitrogen content for the thermal case reflects the cracking of the N-substituted chain from aromatic structures, while the catalytic case also reflects hydrogenation of these structures, resulting in less pyrrolic nitrogen for the catalytic case on a net basis.

An attempt was made to estimate the rate, and thus the reaction order, of the pyrrole conversion. A linear regression was performed on the data demonstrated in Figure 6.1 to give the following relationship between pyrrole content and residence time (R.T.) with an r^2 value of 0.82:

$$\text{Mass \% Pyrrole} = 0.0956 - 0.00928 \cdot R.T. \quad 6.3$$

By using the intercept as the true pyrrole content of the feed bitumen and calculating the rates and concentrations at different residence times, a log-log plot can be done for the pyrrole. These data are presented in Figure 6.6 but, as in the total nitrogen case discussed in Chapter 4, the scatter in the data is of the same magnitude as the conversion, so an estimation of the reaction order is not possible.

Figure 6.7 shows the total and pyrrolic nitrogen contents for the four boiling cuts at the various residence times. The nitrogen is expressed as a straight mass % rather than on a feed basis, so this figure demonstrates the relative removal of the nitrogen types. It can be misleading to only look at

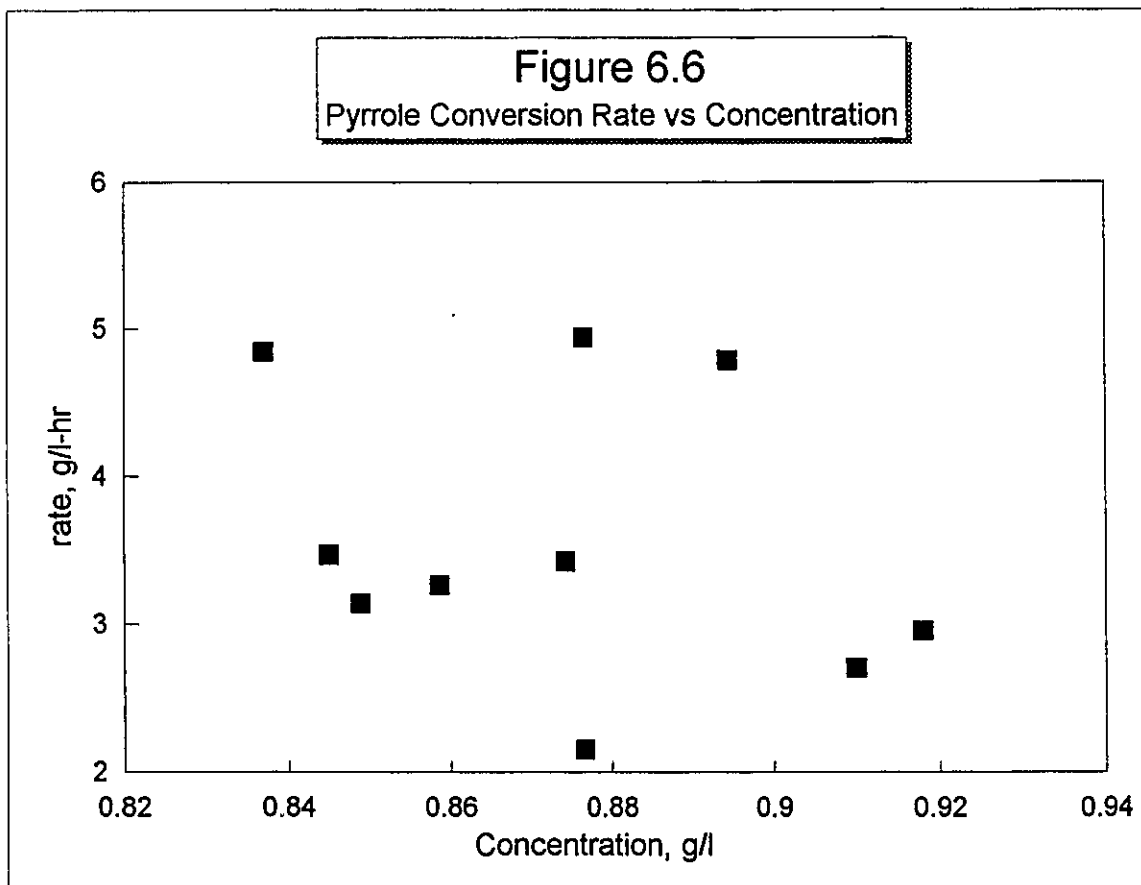
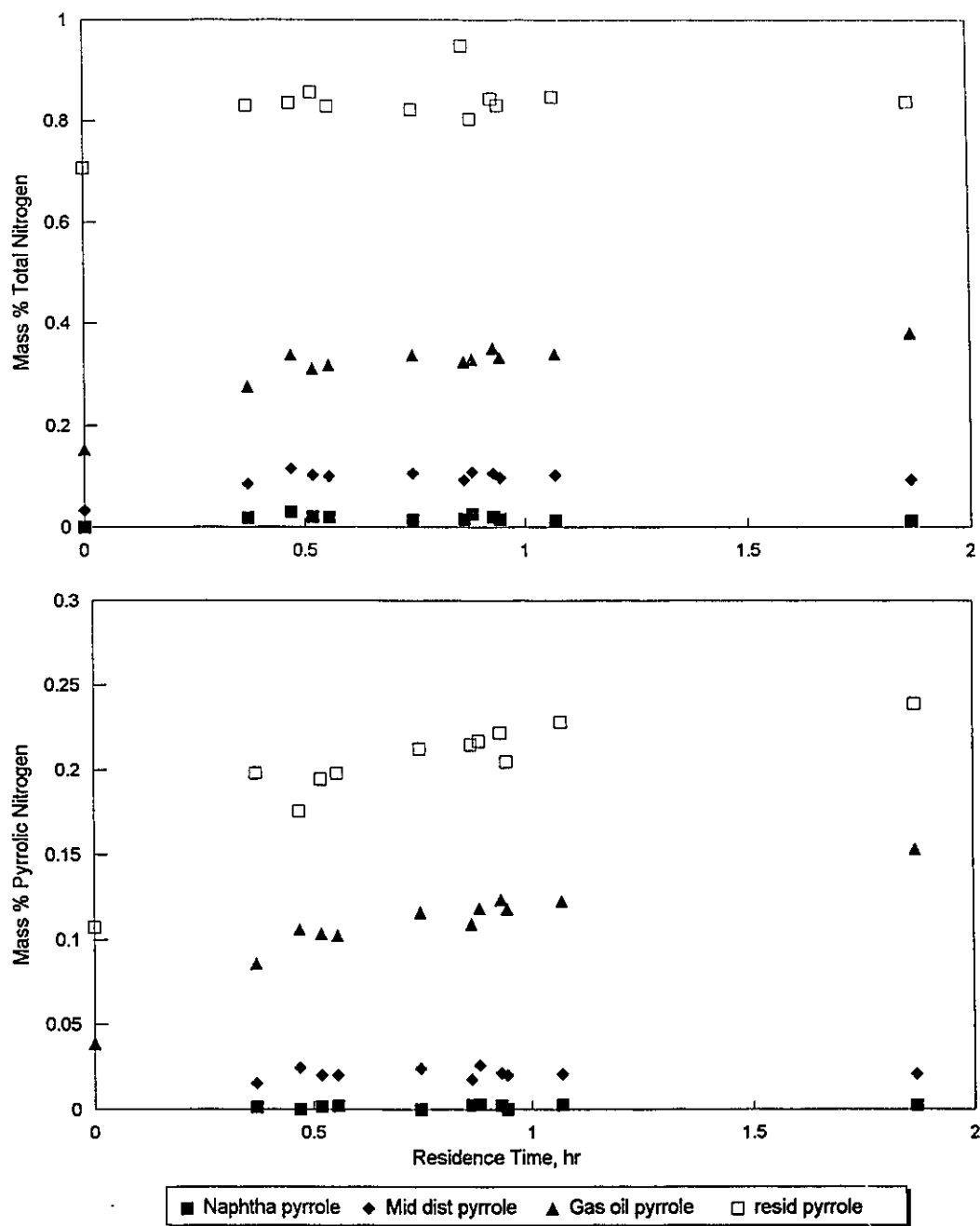


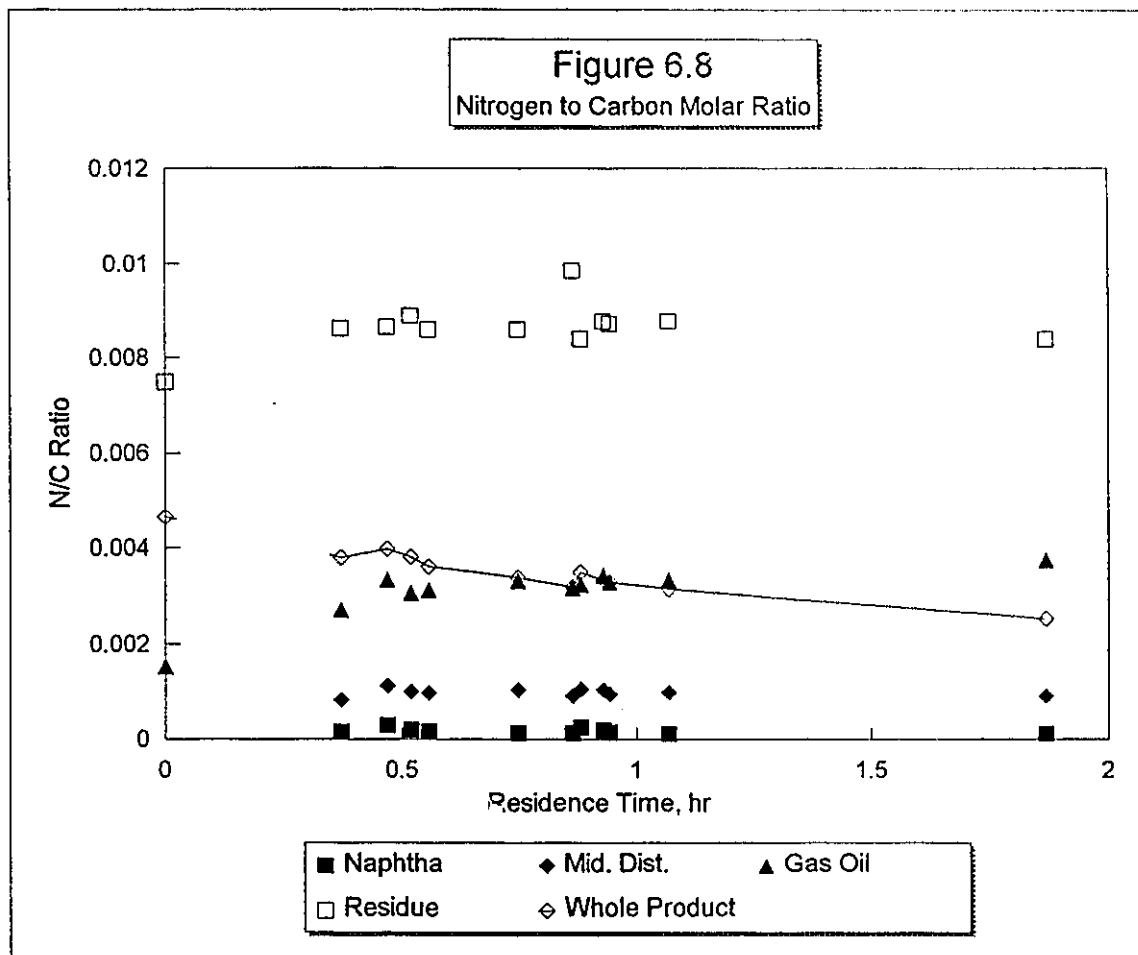
Figure 6.7
Nitrogen Content in Boiling Cuts vs Residence Time



changes in the mass % nitrogen in a cut on an absolute basis, as preferential removal of heavier molecules, such as sulfur, from the cut would result in an increase in the mass % nitrogen; comparing the nitrogen types within a cut does, however, avoid this problem. Comparing the mass % of total and pyrrolic nitrogen in Figure 6.7, there is an increase in the relative amount of pyrrolic to total nitrogen in the residue and gas oil fractions with residence time.

Figure 6.8 gives the change in the ratio of the mol % total nitrogen to the mol % carbon in the fractions vs residence time. The N/C ratio in the residue cut is steady with time, indicating that the nitrogen is not preferentially removed. There are three ways that nitrogen can be removed from the residue cut: as a gas through HDN reactions, as a liquid from residue conversion and as a solid from coking. Although the coke probably has more nitrogen than the residue, it is a relatively small component of the product.

The HDN and hydrocarbon conversion reactions are somewhat related as the removal of the nitrogen atom results in a break in the carbon network at that point. However, this would not necessarily result in the conversion of the molecule to lighter fractions, so the residue nitrogen to carbon ratio should go down if there is some direct nitrogen removal and unbiased movement of the remaining nitrogen to the lighter cuts due to cracking. This prediction is not in agreement with Figure 6.8, which shows a steady N/C ratio with time.



If, on the other hand, most of the residue conversion is through the breaking of carbon-carbon bonds, then the same N/C ratio would remain in the residue, which is in agreement with Figure 6.8. Thus the steady N/C ratio in the residue could be caused by no direct nitrogen conversion in the residue cut, with all the nitrogen leaving as part of the lighter cuts, some of which is then converted to give the lower N/C ratio of these cuts. However, Girgis and Gates (1991), in their review article, do not give any indication of such a scenario. In fact, they give data by Mathur et al. (1982) which indicates the opposite trend for selected basic nitrogen heterocyclic compounds: the rate constant for HDN goes up with increasing number of rings in the structure.

The steady ratio could also be the result of some direct nitrogen conversion in the residue cut, along with preferential removal of low nitrogen structures to the lighter cuts. In section 6.2 it was noted that the lighter cuts received a proportionally greater amount of paraffinic material; additionally, Jacobson and Gray (1987), in an analysis of Peace River Bitumen, did not see any amines or amides. The paraffinic material going to the lighter cuts should therefore be relatively nitrogen poor, resulting in less nitrogen in the lighter cuts. In addition, structures containing nitrogen atoms usually have higher boiling points than those without. This argument provides some good reasons to expect a bias in the nitrogen content of the material going

to the lighter cuts through cracking, along with an expectation from Girgis and Gates (1991) of significant nitrogen removal from the heavy cuts, which implies that the steady nitrogen to carbon ratio in the residue is due to a balance between direct removal of nitrogen by catalyst, and preferential removal of carbon by cracking.

As noted in Chapter 4, the nitrogen conversion is almost completely a catalytic phenomena. If there is an intrinsic diffusion limitation for the larger molecules one would expect better conversion for the lighter cuts. However, in section 6.2, the hydrogenation of the naphtha and middle distillate were found to be unaffected by the presence of a catalyst, whereas the residue cut was affected. Comparing the total nitrogen removal in the same fashion also indicates that the catalyst has little affect on the naphtha and middle distillate cuts. The steady N/C ratio entering the cut from the residue will be reduced by the conversion of the nitrogen at any residence time. Assuming first order kinetics and performing a nitrogen balance on a cut, with the concentration of nitrogen approximated by the N/C ratio, the following relationship will hold:

$$N/C_{cut} = \frac{N/C_{in}}{1 + k \cdot \tau} \quad 6.4$$

N/C_{in} = Nitrogen to carbon ratio entering the cut.

N/C_{cut} = Nitrogen to carbon ratio in the cut.

k = First order rate constant for nitrogen conversion in cut.

τ = Residence time.

For the gas oil cut, the inlet N/C ratio is contributed to by both the feed gas oil N/C ratio and the product gas oil through the residue N/C ratio. It goes up with residence time as there is more residue conversion, which then makes up a higher percentage of the total ratio, which outweighs the increased nitrogen conversion with residence time. For the light cuts the inlet N/C ratio is made up of contributions from the cracking of both the residue and the gas oil fractions.

The initial jump in the nitrogen concentration in the residue fraction reflects a preferential removal of carbon in the first stages of residue conversion. Jacobson and Gray (1987), in an analysis of Peace River Bitumen, did not find amines or amides attached to aliphatic structures. Aliphatic side chains should therefore not contain nitrogen, so removing these structures may account for the initial preferential carbon removal.

Table 6.2 shows the pyrrolic and total nitrogen content for thermal runs done at increasing temperatures. Looking at the mass % nitrogen in the product and comparing this between runs can be somewhat misleading, as more feed is converted to gas at higher temperatures. This means that for the same feed rate the product rate will be lower, and if there is the same

amount of nitrogen in the product this will result in an increase in the mass %. Simply expressing the nitrogen as g/h avoids this problem but can give misleading results if the feed rate is not quite the same, so all the nitrogen contents

Temperature °C	400	420	430	440
Total Nitrogen Mass % (Feed Basis)	0.42	0.45	0.41	0.39
Pyrrolic Nitrogen Mass % (Feed Basis)	0.076	0.092	0.096	0.081
Ratio Pyrrolic/ Total	0.18	0.20	0.23	0.21
H/C Ratio	0.128	0.126	0.127	0.125

have been expressed as mass % on a feed basis, as discussed above for the residence time data. The feed was 0.44 % total nitrogen, which, when the error in the nitrogen analysis of ± 5 % discussed in Chapter 4 is included, is consistent with no nitrogen having been converted and having left with the gas for all but the 440 °C case. Figure 6.4, discussed above, indicates a scatter of approximately ± 5 % in the data for pyrrolic nitrogen concentration. The data in Table 6.2

indicates a definite increase in the pyrrolic nitrogen content beyond this error bound when the temperature is increased from 400 to 420 °C. This result is consistent with the proposed N-substituted pyrrole structure because all the nitrogen substituted groups may not have been removed in the milder conditions. This result would also be consistent with dehydrogenation as seen by the decreasing H/C ratio, except amines are not present in the feed ready to be dehydrogenated. The decrease in both nitrogen types when the temperature is increased from 430 to 440 °C indicates that some nitrogen conversion has taken place. The decrease in the ratio of the pyrrolic to total nitrogen by 10 % is consistent with equal or greater conversion of pyrrolic than total nitrogen, but not with greater conversion of total than pyrrolic nitrogen when the 5 % error in both nitrogen types is taken into account.

Table 6.3 gives the nitrogen contents and hydrogen to carbon ratio for catalytic conversion at temperatures varying between 410 and 450 °C, with a residence time of 0.94 h. The pyrrolic nitrogen does not vary from the average of 0.083 mass % by more than the error of $\pm 5\%$, and the variation does not show a distinct trend. Although the catalyst does show hydrogenation activity, these structures seem to be unaffected by this activity in the whole product. As expected, the total nitrogen removal does increase with temperature, whereas little evidence for this was seen in the thermal case.

Table 6.3 Catalytic Changes in Nitrogen Compounds with Temperature					
Temperature °C	410	420	430	440	450
Total Nitrogen Mass % (Feed Basis)	0.368	0.308	0.306	0.243	0.264
Pyrrolic Nitrogen Mass % (Feed Basis)	0.083	0.079	0.086	0.081	0.087
Ratio Pyrrolic/ Total	0.23	0.26	0.28	0.33	0.33
H/C Ratio	0.132	0.135	0.136	0.138	0.139
Liquid Ratio: Product/Feed	0.94	0.93	0.93	0.92	0.90

The H/C ratio, as well as the total and pyrrolic nitrogen contents for each cut for the catalytic runs between 410 and 450 °C are illustrated in Figure 6.9. These data are presented on a straight mass percent basis by dividing the mass of the nitrogen by the mass of the cut. Note that an increase in the nitrogen content for the residue cut does not imply formation of nitrogen, but rather preferential removal of low nitrogen content structures with increased conversion.

The gas oil fraction, being harder to partially hydrogenate, shows the opposite trend with temperature. The thermal temperature data in Figure 6.10 show a decrease in the

Figure 6.9
Boiling Cut Composition, Catalytic Runs

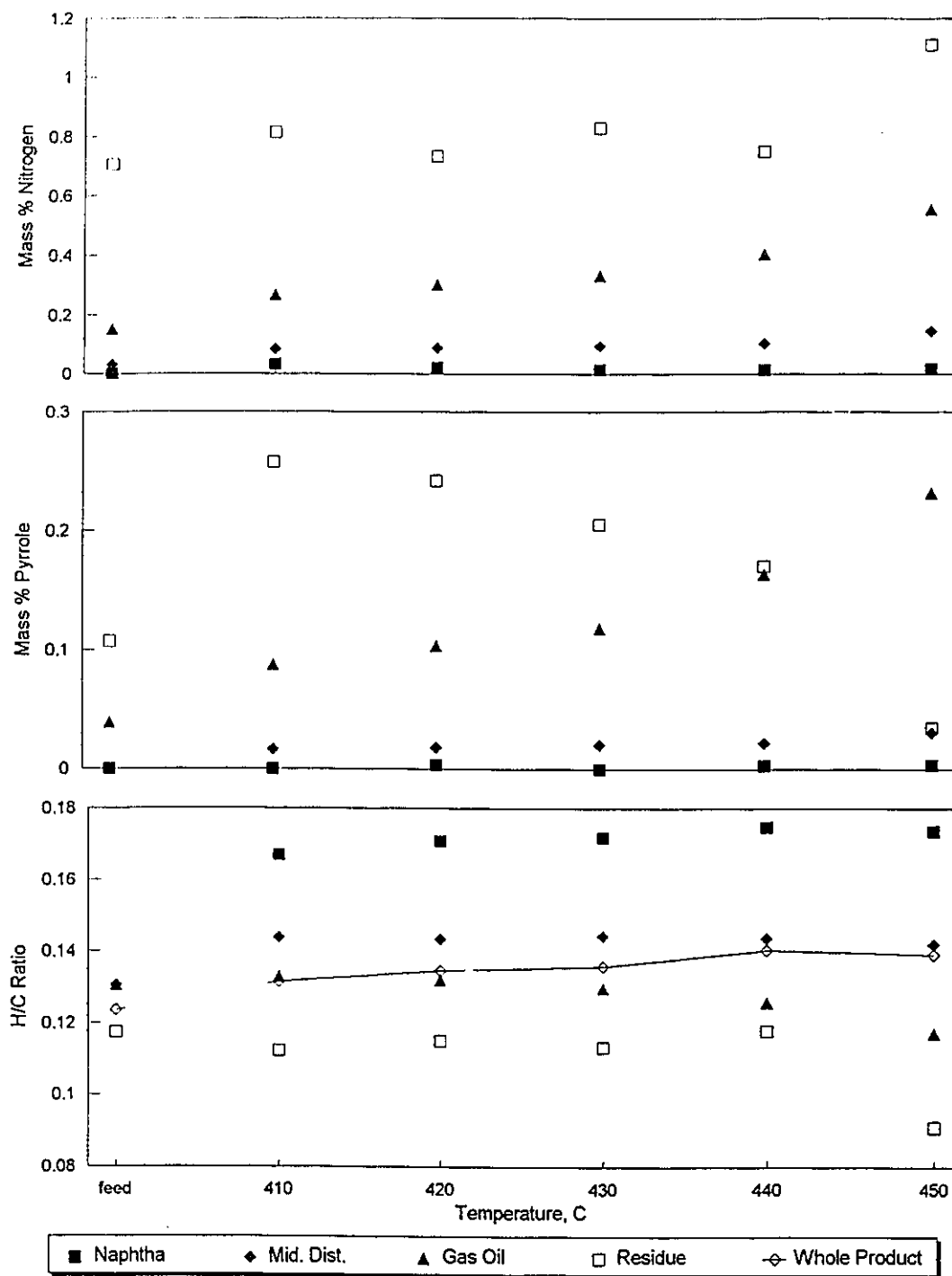
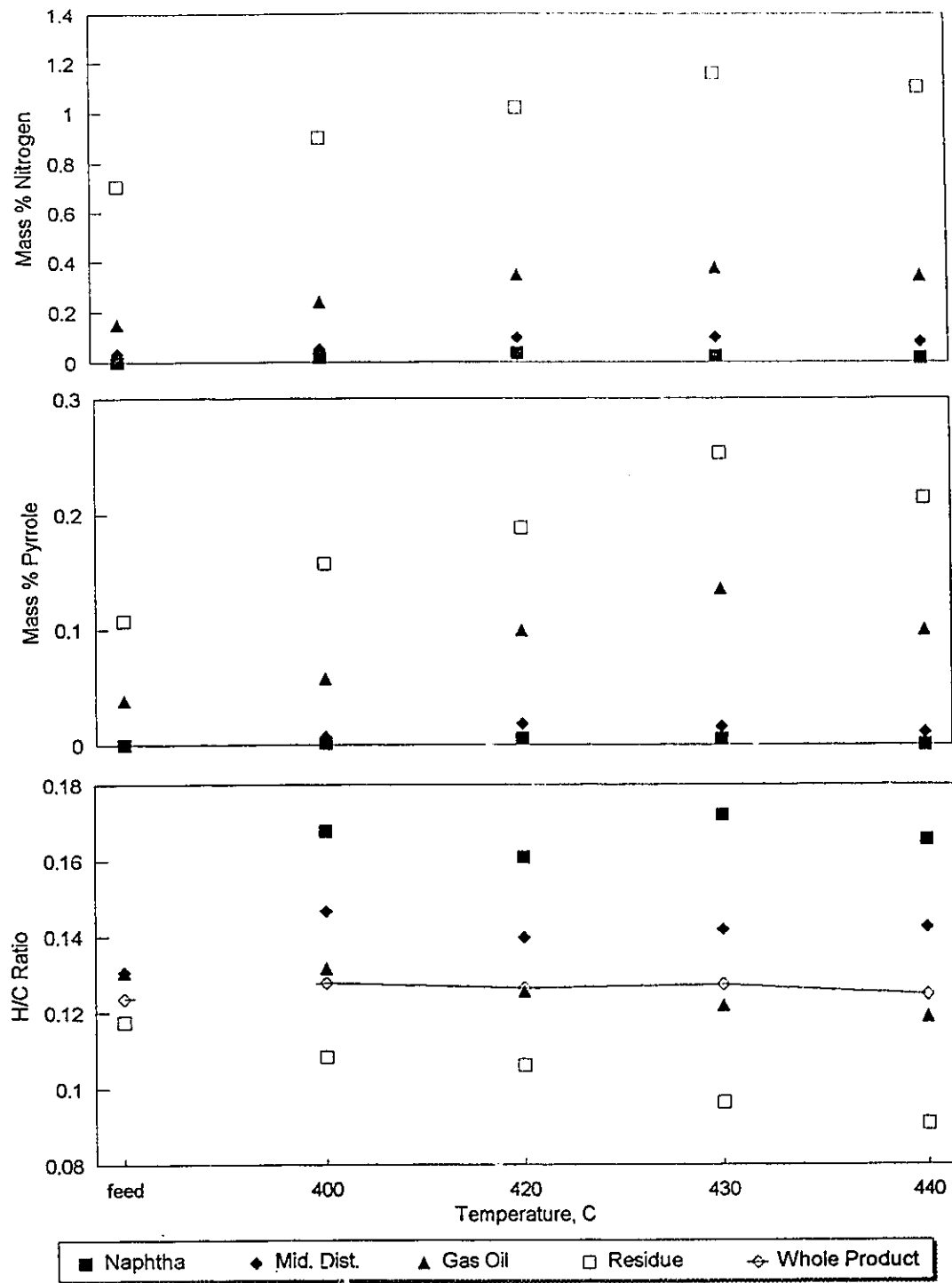


Figure 6.10
Boiling Cut Composition, Thermal Runs



H/C ratio with temperature in the residue cut, as well as a relative increase in the pyrrolic to total nitrogen content. This indicates the expected dehydrogenation with increasing temperature in the residue cut, but the whole product shows a flat H/C profile.

Another explanation for the preferential removal of pyrrolic nitrogen may be through condensation reactions that would eventually lead to coke formation. Mochida et al. (1977) found that acidic catalysts such as aluminum chloride can cause a variety of aromatic structures to form coke. In this study the presence of heteroatoms did not have a significant influence on the coking rate. In a further study, Mochida et al. (1978) specifically investigated carbazole as the coke forming structure. In these investigations the process for coke formation was by oligomerization through the aromatic carbon-carbon bonds. Although breakage of the N-H bond was not specifically discussed, if this did happen then a bond may form between the nitrogen and a carbon atom in another aromatic group, causing a decrease in the IR signal for the N-H bond, which would then result in an apparent decrease in the pyrrole content. As long as this process did not continue to the point of condensation to form coke, the total nitrogen content would not be affected. Mochida et al. (1978) saw an increase in the amount of carbonization with temperature, which is consistent with the decrease in the pyrrole content for the residue fraction with temperature.

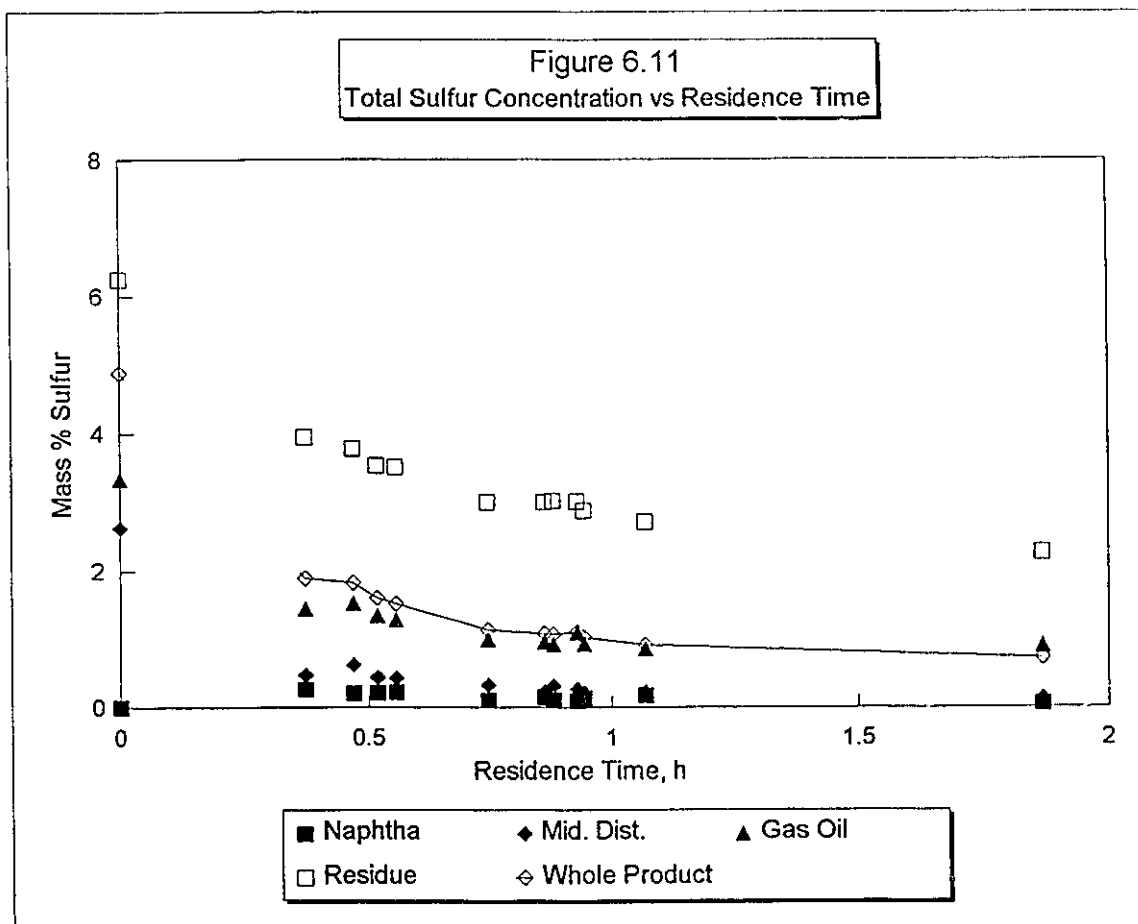
The fact that this decrease with temperature is not seen for the thermal case is also consistent with this explanation, as the oligomerization reactions are a catalytic phenomenon. Furthermore, the carbonization scheme proposed by Mochida et al. (1978) involves partial hydrogenation of the aromatic rings, which, as discussed in Chapter 2, may be facilitated by larger ring structures through resonance stabilization; this is consistent with the phenomenon being apparent in the residue cut.

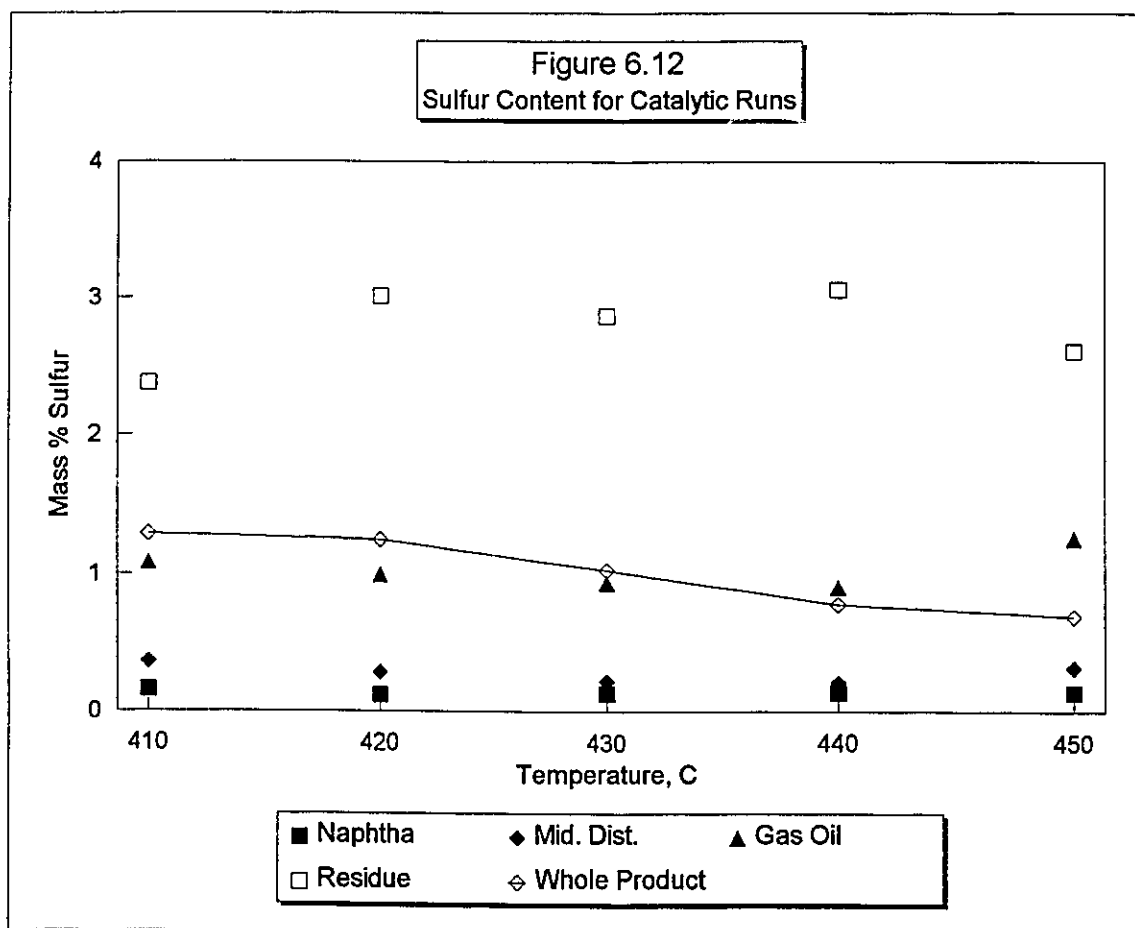
Combining the cracking model presented in Chapter 5 with the nitrogen data discussed in this chapter could give a general model for nitrogen removal. Equation 6.4 gives the nitrogen balance on any cut, where the nitrogen conversion for the cut can be found from the difference between the rate at which nitrogen enters the cut, either as inlet flow or from conversion of heavier cuts, and the rate at which it leaves the reactor with the cut. The inlet and outlet rates and compositions are known, and, using the model from Chapter 5, the rate at which material enters from other cuts is known. If the nitrogen content of this entering material is the same as that of the rest of the cut from which it is cracked, then the rate of nitrogen removal for each cut can be determined. However, previous sections have given reasons to cast doubt on the validity of this assumption. There may be a different nitrogen content in the hydrocracking product material than in

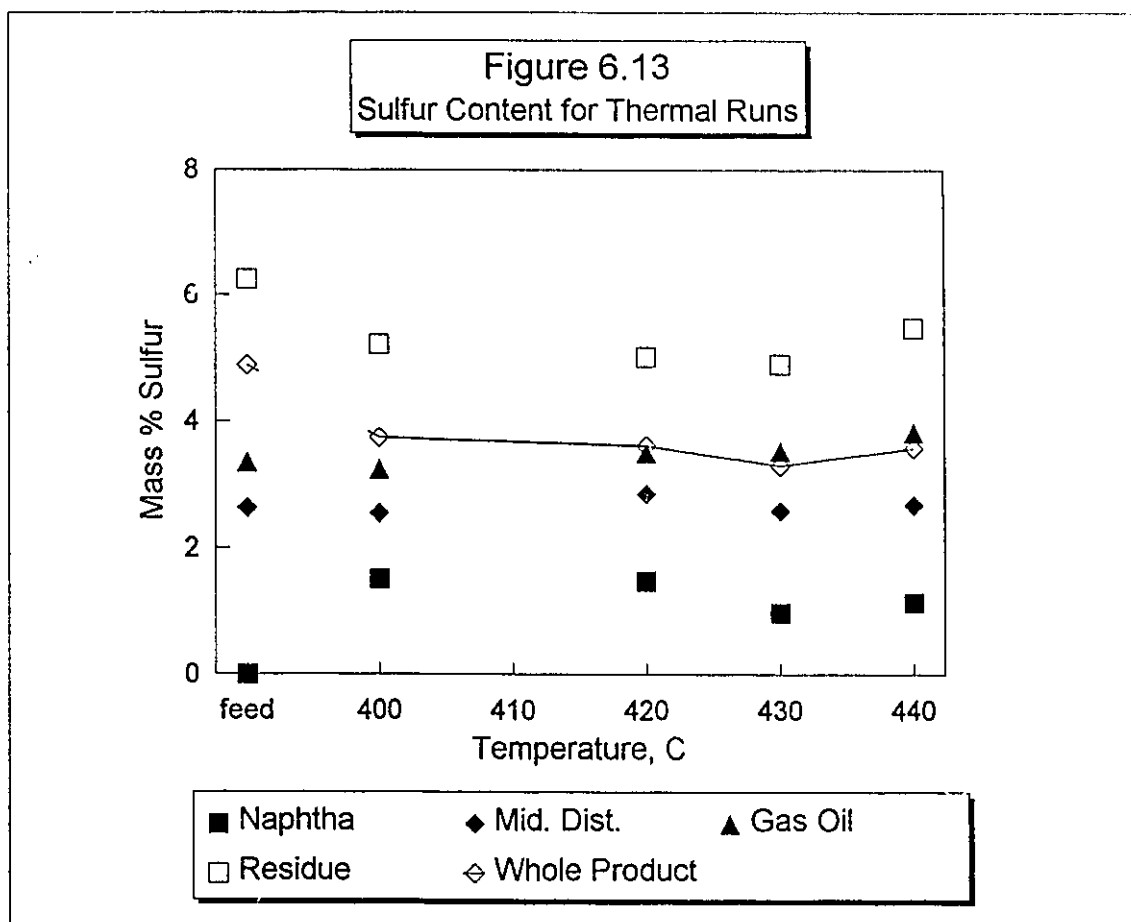
the material which is cracking. This should be taken into account when nitrogen removal is modelled.

6.4 Sulfur

The conversion of sulfur is similar in many ways to the conversion of nitrogen, except, as explained in Chapter 2, the sulfur atom can be directly removed from aromatic structures by hydrogenolysis. Figure 6.11 shows the data as a function of residence time for the sulfur content of the boiling cuts. As discussed in Chapter 4, the overall sulfur conversion is approximately first order. Unlike the nitrogen case, the sulfur content of the lighter cuts does show a decrease with residence time. Between residence times of 0.37 and 1.87 h, the relative drop in the sulfur content of the lighter cuts is double that of the heavier cuts, which is one indication that sulfur conversion is taking place in the light cuts. Figure 6.12 indicates the change in sulfur content with temperature for catalytic runs. As can be seen in the figure, the sulfur content in each cut does not change substantially with temperature, although the overall sulfur content does drop due to the increased cracking of the heavier cuts with temperature. Figure 6.13 gives the change in sulfur content with temperature for thermal runs. Once again the concentration profiles for the various cuts are flat, even for the overall sulfur content, with the exception of a slight decrease for the naphtha. Comparison of the catalytic and







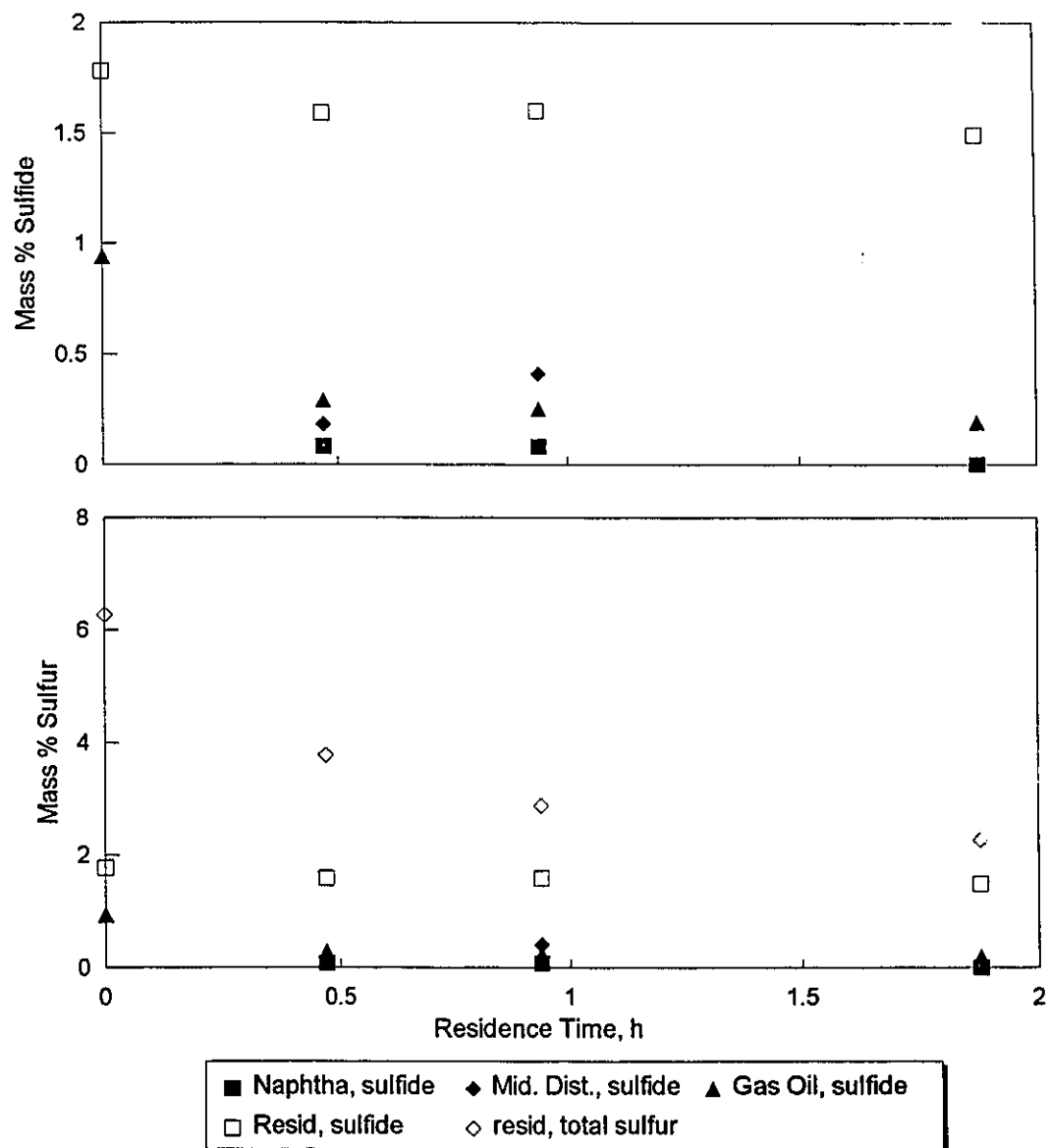
thermal cases indicates the large influence the catalyst has on sulfur removal, with the ratio of catalytic sulfur content to the thermal sulfur contents decreasing with boiling point as indicated in Table 6.4 for runs done at 420 °C.

Table 6.4 Catalytic to Thermal Sulfur Ratio at 420°C				
Cut	Naphtha	Mid. Dist.	Gas Oil	Residue
$\frac{S_{cat}}{S_{therm}}$	0.083	0.099	0.285	0.600

This result may be an effect of different intrinsic rate constants for the larger molecules due to problems such as steric hindrance or aromaticity. Trytten (1989), using narrow boiling gas oil fractions, found that the intrinsic rate constants for HDS decreased with increased feed average molecular weight. Girgis and Gates (1991), in their review article on catalytic HDS of heavy fossil fuels, noted that generally the fewer the number of aromatic rings in the structure incorporating the sulfur atom the easier it is to convert the sulfur. Structures having three or more rings had similar reactivities. Although these data were gathered for aromatic structures at lower temperatures and pressures than those used in this study, the general trend is in agreement with the observations in Table 6.4 where the catalytic conversion increased for smaller molecular sizes.

Figure 6.14 shows the non-aromatic sulfur, or sulfide, content for the feed and reaction products for selected

Figure 6.14
Sulfur Content vs Residence Time



residence times. Although sulfides are quite reactive, the net conversion shown in the figure is quite low, even though the total sulfur conversion demonstrated in Figure 6.11 is significant. This discrepancy is especially apparent for the residue cut in the lower part of Figure 6.14, where almost all the sulfur conversion appears to be coming from the thiophenic component, which is assumed to be the difference between the total and sulfide sulfur.

In Chapter 2, two mechanisms for sulfur removal were discussed: direct hydrogenolysis and hydrogenation followed by HDS. This reaction network is illustrated in Figure 2.2. The general trend was increasing importance of the hydrogenation pathway with ring size. Additionally, most studies were done with cobalt rather than nickel catalysts, which is used in this study; the use of nickel catalyst should increase the hydrogenation reactions. If thiophenes are being converted to sulfides, then these sulfides would be subject to thermal cracking and catalytic hydrodesulfurization to give hydrogen sulfide. The reactions of thiophene would be strictly catalytic; therefore, any reduction in the catalytic function would reduce the conversion of thiophene to sulfides. Since sulfides could still react thermally to form hydrogen sulfide, a reduction in catalyst activity would reduce the sulfide concentration.

This hypothesis was tested by reacting bitumen without Ni-Mo catalyst, so that thermal reactions would predominate,

and at lower hydrogen pressure so that the hydrogenation reactions would occur at a lower rate. The sulfide concentrations and ratio of sulfide to total sulfur in the boiling fractions of the products are listed in Tables 6.5 and 6.6 respectively. The sulfide concentrations in the residue fractions from thermal and low-pressure processing were lower than in the residue from catalytic processing at any residence time, consistent with the qualitative prediction Figure 2.2. Concentration differences between the distillate fractions from the three experiments were much less significant. The ratio of sulfide to total sulfur in the residue fraction was also two-fold lower, due to reduced desulfurization overall in the absence of catalyst and at reduced pressure. The same trend in the ratio of sulfide to total sulfur was also observed in the distillate fractions. The consistency between the behaviour of the sulfides in the residue and the simple reaction model in Figure 2.2 suggested that the experimental results were representative of the actual distribution of sulfur species in the residue product.

Table 6.5			
Mass % Sulfide in Cuts			
Cut	Catalytic	Thermal	Low Pressure
Naphtha	0.08	0	0
Mid. Dist.	0.41	0.34	0.17
Gas Oil	0.25	0.48	0.23
Residue	1.60	0.98	0.71
Whole	0.51	0.51	0.15

Table 6.6 Sulfide to Sulfur Ratio in Cuts			
Cut	Catalytic	Thermal	Low Pressure
Naphtha	0.611	0	0
Mid. Dist.	1.87	0.132	0.360
Gas Oil	0.268	0.136	0.159
Residue	0.557	0.200	0.180
Whole	0.497	0.240	0.119

6.4.1 Kinetics of removal of sulfur types

The rate expressions for reaction of the two types of sulfur species in a continuous-flow catalytic reactor can be written as follows, assuming first-order kinetics and negligible change in liquid volume between inlet and outlet:

$$\frac{(\omega_{thio,i} - \omega_{thio})}{\tau} = (\kappa_1 + \kappa_2) \omega_{thio} \quad 6.5$$

$\omega_{thio,i}$ = inlet weight fraction of thiophenic sulfur in residue.

ω_{thio} = outlet weight fraction of thiophenic sulfur in residue.

τ = mean residence time, h.

κ_1 = rate constant for thiophene hydrogenation, h^{-1} .

κ_2 = rate constant for thiophene hydrogenolysis, h^{-1} .

The corresponding equation for the sulfide sulfur is given by:

$$\frac{(\omega_{sulf,i} - \omega_{sulf})}{\tau} = -\kappa_1 \omega_{thio} + \kappa_3 \omega_{sulf} \quad 6.6$$

$\omega_{sulf,i}$ = inlet weight fraction of sulfide sulfur in residue.

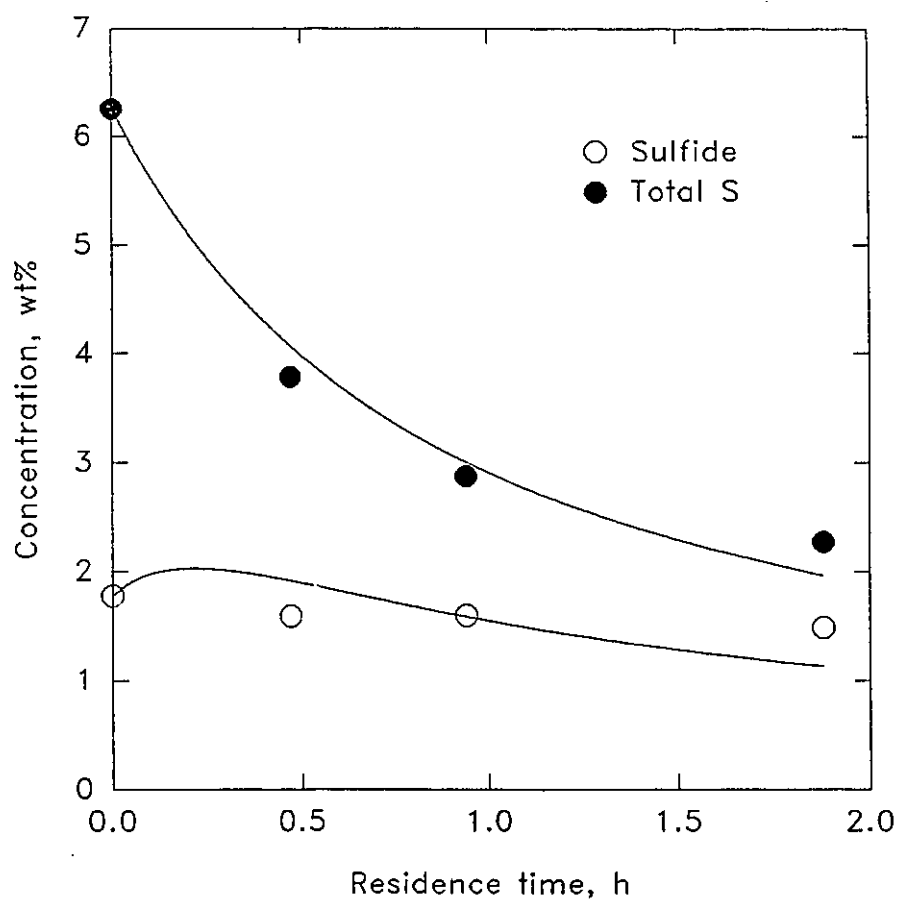
ω_{sulf} = outlet weight fraction of sulfide sulfur in residue.

κ_3 = rate constant for sulfide conversion, h^{-1} .

Equations 6.5 and 6.6 are easily solved to give the outlet concentrations of thiophenic and sulfide sulfur in terms of the mean residence time, τ , $w_{\text{thio},i}$ and $w_{\text{sulf},i}$, and the three rate constants. The concentration of thiophenic sulfur was approximated as $w_{\text{total}} - w_{\text{sulf}}$. Although the residue was undergoing cracking reactions, with concomitant removal of sulfur to the distillate products, it can be easily shown that the above rate expressions are appropriate for sulfur removal from the residue by desulfurization, as opposed to migration of sulfur with the cracked products.

The curves in Figure 6.15 show the best fit of the kinetic model to the experimental data for total sulfur and sulfide sulfur, using values of the rate constants $k_1 = 1.2 \text{ h}^{-1}$, $k_2 = 1.1 \text{ h}^{-1}$ and $k_3 = 1.2 \text{ h}^{-1}$. Although the concentration of sulfide sulfur in the residue did not change significantly as residence time was increased, this behaviour was consistent with the reaction scheme from Figure 2.2, and the corresponding kinetic model when the rate constants for thiophene and sulfide reactions were all of similar magnitude. These kinetic parameters, and the sustained concentration of sulfides as an intermediate, showed that the catalyst was less selective toward sulfur heterocycles in the residue than in

Figure 6.15
Theoretical Fit to Sulfur Data



the distillates. As a result, more hydrogenation of carbon rings would occur and less selective hydrogenolysis.

A number of reaction networks for thiophenic compounds have been presented in the literature, based on model studies. The data of Table 6.7 summarize these results in terms of the ratio of the rate of hydrogenation of the thiophenic ring to form the non-aromatic cyclic sulfide, to the rate of hydrogenolysis which is the direct catalytic removal of sulfur from the thiophene.

Table 6.7 Ratio of Sulfide Formation to Hydrogenolysis in Hydrotreating of Thiophenic Model Compounds over Co-Mo on γ -Alumina Catalyst				
Model Compound	T, °C	P, MPa	Ratio of Sulfide Formation to Hydrogenolysis	Reference
Thiophene	300	3	0	Van Parijs and Froment, 1986
Benzothiophene	300	3-10	0.7-2.2*	Van Parijs et al., 1986
Dibenzothiophene	300	10	0.0015	Hoalla et al., 1980
Benzo[b]naphtho[2,3-d]thiophene	300	7	0.32	Sapre et al., 1980
Benzo[b]naphtho[1,2-d]thiophene	250	3	0.51	Vrinat, 1983

* Depending on pressure

Clearly, the series of compounds from thiophene to benzonaphthothiophene did not exhibit consistent behaviour, although differences in catalyst formulation and reactor conditions could contribute to the disparate results. The actual compounds in a residue fraction would be substituted with various groups, but data on the reaction networks for substituted thiophenes are not available. Benzothiophene had the highest initial rate of sulfide formation, mainly because Van Parijs et al. (1986) observed that the sulfide formation reaction was so fast that a hydrogenation equilibrium was established between benzothiophene and 1,2-dihydrobenzothiophene (the sulfide). No sulfide was detectable in the studies by Van Parijs and Froment (1986) of hydrotreatment of thiophene, although the sulfide (tetrahydrothiophene in this case) has been suggested as a short-lived intermediate (Girgis and Gates, 1991). The tendency of the thiophenes in the residue fraction to form sulfides as intermediates suggests that the thiophenic compounds behave more like benzothiophene and benzonaphthothiophene than dibenzothiophene.

6.5 Effectiveness Factor

Data were gathered using crushed catalyst to study the effect of catalyst size on the various reactions taking place during hydrocracking. Assuming first order kinetics, the relationship between the Thiele modulus and the effectiveness factor is given by Equation 6.7:

$$\eta = \frac{3\Phi \cdot \coth(3\Phi) - 1}{3\Phi^2} \quad 6.7$$

Where

$$\Phi = \frac{V}{S} \cdot \sqrt{\frac{k \cdot \rho_s}{D_{eA}}}$$

- η = effectiveness factor
- Φ = Thiele Modulus
- V = catalyst pellet volume
- S = catalyst pellet surface area
- k = intrinsic rate constant
- ρ_s = catalyst density
- D_{eA} = diffusivity of reacting compound in catalyst

In this study the intrinsic rate constant and diffusivity are not known. By using pellets crushed to 925 and 600 μm spheres, as well as the uncrushed 1000 μm cylinders, a unique intrinsic rate constant and ratio of density to diffusivity

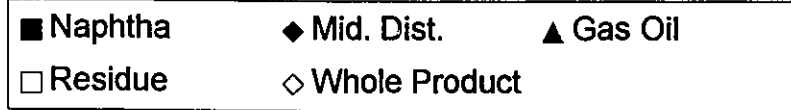
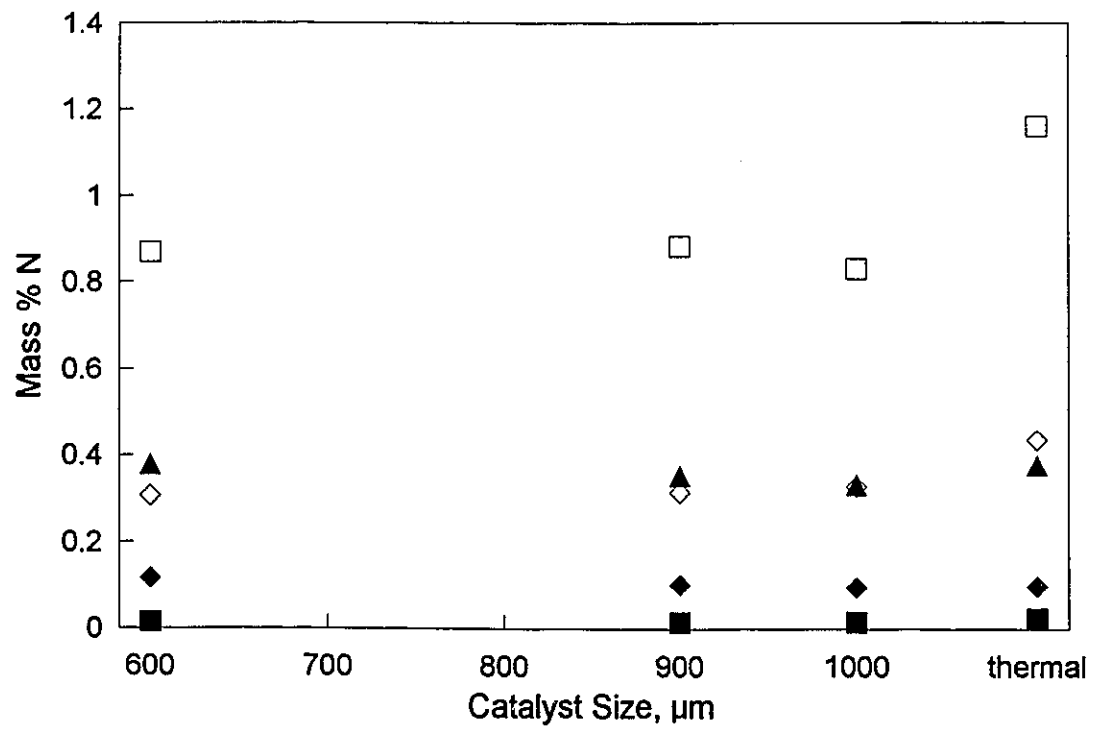
(Equation 6.7) were found by minimizing the total squared residual for all three cases. This was done for the residue conversion to give an intrinsic catalytic rate constant of 1.81 h^{-1} , with the uncrushed pellet having an effectiveness factor of 0.28; the fit using these parameters is demonstrated in Table 6.8.

Catalyst Radius, mm	V/S mm	Estimated η	Calculated η
0.50	0.225	0.28	0.27
0.46	0.077	0.51	0.62
0.30	0.050	0.82	0.77

Observations on these catalyst pellets by Ghorpadkar (1993) indicated that there is a coating of coke on the pellet surface. This may add a further barrier to diffusion and shift the relationship between the effectiveness factor and the Thiele modulus, resulting in the discrepancies indicated in Table 6.8.

The effect of catalyst size on other kinetics, such as nitrogen and sulfur removal, tends to be related to the residue conversion, since the diffusivity of the residue in the catalyst is an important factor in both cases. Figure 6.16 shows the nitrogen content for the cuts at the various catalyst sizes. The slight differences in the nitrogen contents for the various cuts is well within the expected

Figure 6.16
Total N Concentration vs Catalyst Size



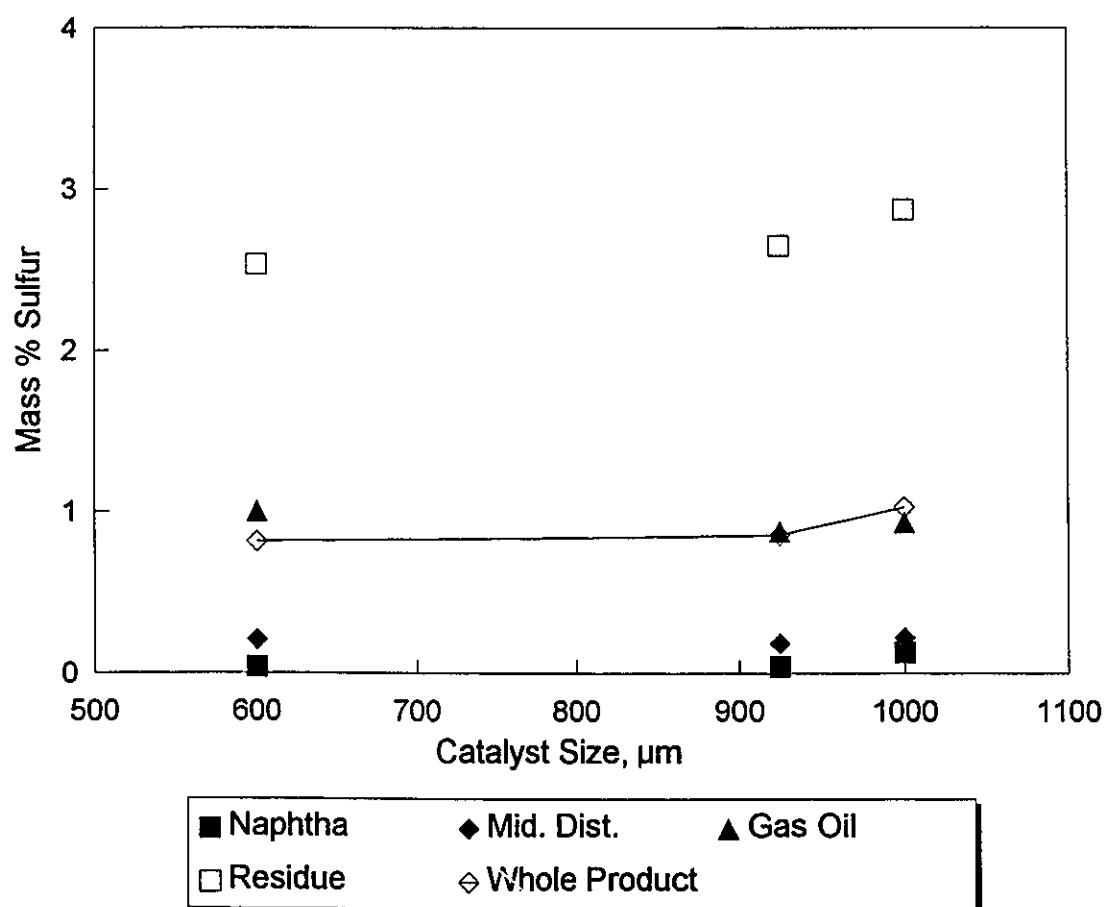
scatter for the nitrogen data. Equation 6.8 indicates that for first order reactions the conversion is related to the product of the rate constant and residence time.

$$\frac{X_R}{1 - X_R} = \eta_{R,a} \cdot k_R \cdot \tau \quad 6.8$$

- X_R = residue conversion
- $\eta_{R,a}$ = effectiveness factor for residue conversion with catalyst size a
- k_R = residue conversion intrinsic rate constant
- τ = residence time

Since changing the residence time has the same effect as changing the effectiveness factor, the profile for Figure 6.16 should show the same trend as seen in the nitrogen vs residence time graph, which it does. Figure 6.17 gives the sulfur profile for the various catalyst sizes. Once again the trends are the same as seen in the residence time graph, with less sulfur present for smaller catalyst sizes. Comparing the sulfur content of the various cuts with the estimated content for the residence time data with the same residue conversion shows good agreement except for the naphtha cut, as demonstrated in Table 6.9. This implies that for the larger molecules the change in the effectiveness factor for sulfur conversion is similar to the change for residue conversion with the change in catalyst size. This in turn implies a

Figure 6.17
Total Sulfur Concentration vs Catalyst



similar ratio of intrinsic rate constant to diffusivity for these reactions. In the case of nitrogen little change is seen compared to the error, so not much can be said about the intrinsic rate constant for HDN.

Residue Conv. %	65.3	69.0		73.1		
Residence Time h	0.94	1.14	0.94	1.42	0.94	
Catalyst Size μm	1000	1000	925	1000	600	
Mass % Sulfur	Naphtha	0.13	0.16	0.04	0.12	0.04
	M. Dist.	0.22	0.21	0.19	0.18	0.21
	Gas Oil	0.93	0.86	0.88	0.88	1.00
	Residue	2.87	2.67	2.65	2.52	2.53
	Whole	1.03	0.90	0.86	0.83	0.82

In summary the effectiveness factor for the residue conversion is a good indication of the general effect of the catalyst size on hydrocracking reactions, when the residence time profile is taken into account. Since these processes are all related to hydrogenation reactions, this relationship does make sense. However, due to the small range and scatter in the data, a fundamental relationship is not proposed here.

Trytten (1989) found that for the hydrocracking of gas oil derived from Athabasca bitumen, the effectiveness factor for HDS was smallest for the cuts in the naphtha range. This

was due to the fact that the intrinsic rate constant fell faster than the diffusivity with molecular weight, resulting in larger Thiele moduli for the lightest cuts. This effect was not as prevalent for the HDN reaction. Since hydrogenation of ring structures is slower for structures with fewer rings, this may be an indication that the hydrogenolysis pathway is more important for the lighter cuts. The literature discussed in Chapter 2 also supports this hypothesis.

6.6

Conclusions

- With addition of catalyst the dehydrogenation of the residue and middle distillate cuts is prevented up to 440 °C.
- The pyrrolic nitrogen content of the residue products for the thermal case was consistent with the cracking of N-substituted chains from pyrrolic structures. The significant reduction of pyrroles in the presence of catalyst at high severity was consistent with the occurrence of bridge formation at the nitrogen atom.
- Evidence was seen for significant hydrogenation of thiophenes to give sulfides, resulting in flat sulfide

profiles in all the cuts while total sulfur content dropped significantly.

- The intrinsic rate constant for residue conversion was found to be 1.81 h^{-1} and the effectiveness factor for residue conversion for the whole catalyst pellet was approximately 0.3.

- With the exception of naphtha, the sulfur contents of the product fractions were the same at a given level of residue conversion, regardless of whether that conversion was achieved by longer residence time or smaller catalyst pellets.

Chapter 7
List of References

- Ammus, J.M.; Androutsopoulos, G.P. "HDS Kinetic Studies on Greek Oil Residue in a Spinning Basket Reactor". *Ind. Eng. Chem. Res.* 1987, 26, 494.
- Beret, S.; Reynolds, J.G. "Effect of Prehydrogenation on Hydroconversion of Maya Residuum, Part II: Hydrogen Incorporation". *Fuel Sci. and Tech. Int.* 1990, 3, 191-219.
- Beret, S.; Reynolds, J.G. "Hydrogen Incorporation in Residuum Conversion". Symposium on New Chemistry of Heavy Ends Presented Before the Division of Petroleum Chemistry, Inc. American Chemical Society Chicago Meeting, Sept. 1985, 664-671.
- Bhinde, M.V. "Quinoline Hydrodenitrogenation Kinetics and Reaction Inhibition". Ph.D. Dissertation, U. of Delaware, Newark 1979.
- Broderick, D.H.; Gates, B.C. "Hydrogenolysis and Hydrogenation of dibenzothiophene Catalyzed by Sulfided $\text{CoO-MoO}_3/\gamma\text{-Al}_2\text{O}_3$: The Reaction Kinetics". *AIChE Journal* 1981, 4, 663-673.
- Bunger, J.W. *Am. Chem. Soc. Adv. Chem. Ser.* 1976, 151, 121.
- Bunger, J.W.; Thomas, K.P.; Dorrence, S.M. *Fuel* 1979, 58, 183.
- Chung, S.Y.K. "Thermal Processing of Heavy Gas Oils". M.Sc. Thesis, Department of Chemical Engineering, University of Alberta, 1982.
- DeWind, M.; Plantenga, F.L.; Heinerman, J.J.L. "Upflow vs Downflow Testing of Hydrotreating Catalysts". *Appl. Catal.* 1988, 43, 239.
- Egiebor, N.O.; Gray, M.R.; Cyr, N. " ^{13}C -NMR characterization of organic residues on spent hydroprocessing, hydrocracking, and demetallization catalysts". *Appl. Catal.* 1989, 55, 81-91.
- Fogler, H.S. *Elements of Chemical Reactor Design*, Prentice-Hall, Englewood Cliffs, NJ, 1986.
- Girgis, M.J.; Gates, B.C. "Reactivities, Reaction Networks, and Kinetics in High-Pressure Catalytic Hydroprocessing". *Ind. Eng. Chem. Res.* 1991, 30, 2021-2058.
- Gray, M.R.; Choi, J.H.K.; Egiebor, N.O.; Kirchen, R.P.; Sanford, E.C. "Structural group analysis of residues from Athabasca bitumen". *Fuel Sci. Technol. Int.* 1989, 7, 599-610.
- Gray, M.R. "Lumped Kinetics of Structural Groups: Hydrotreating of Heavy Distillate". *Ind. Eng. Chem. Res.*, 1990, 29, 505-512.

Gray, M.R.; Jokuty, P.; Yeniova, H.; Nazarewycz, L.; Wanke, S.E.; Achia, U.; Krzywicki, A.; Sanford, E.C.; Sy, O.K.Y. "The relationship between chemical structure and reactivity of Alberta bitumens", *Can J. Chem. Eng.* 1991, 69, 833-843.

Gray, M.R.; Khorasheh, F.; Wanke, S.E.; Achia, U.; Krzywicki, A.; Sanford, E.C.; Sy, O.K.Y., Ternan, M. "The role of catalyst in hydrocracking residues from Alberta bitumens", *Can J. Chem. Eng.* 1991, 69, 833-843.

Gray, M.R.; Krzywicki, A.Z.; Wanke, S.E. "Chemical Transformation During Resid Upgrading: Catalytic and Thermal". Report for CANMET, 1992. SSC File No.: 06SQ.23440-7-9011.

Green, J.B.; Yu, S.K.-T.; Pearson, C.D.; Reynolds, J.W. "Analysis of sulfur compound types in asphalt", *Energy Fuels* 1993, 7, 119-126.

Ho, T.C. "Hydrodenitrogenation catalysts", *Catal. Rev. -Sci. Engin.* 1988, 30, 117-160.

Houalla, M.; Nag, N.K.; Sapre, A.V.; Broderick, D.H.; Gates, B.C. "Hydrodesulfurization of Dibenzothiophene Catalyzed by Sulfided $\text{CoO-MoO}_3\gamma\text{-Al}_2\text{O}_3$: The Reaction Network". *AIChE Journal* 1978, 6, 1015-1021.

Houalla, M.; Broderick, D.H.; Sapre, A.V.; Nag, N.K.; deBeer, V.H.J.; Gates, B.C.; Kwart, H. "Hydrodesulfurization of Methyl-Substituted Dibenzothiophenes Catalyzed by Sulfided $\text{CoO-MoO}_3\gamma\text{-Al}_2\text{O}_3$ ". *J. Catal.* 1980, 61, 523-527.

Jacobson, J.M.; Gray, M.R. The use of infrared spectroscopy and nitrogen titration in structural group analysis of bitumen. *Fuel* 66, 749-752 (1987).

Jokuty, P.L.; Gray, M.R. "Resistant Nitrogen Compounds in Hydrotreated Gas Oil from Athabasca Bitumen". *Energy and Fuels* 1991, 6, 791-795.

Jokuty, P.L. "Nitrogen Compounds in Hydrotreated Gas Oil". MSc Thesis, Dept. Chem., University of Alberta, 1992.

Khorasheh, F.; Rangwala, H.; Gray, M.R.; Dalla Lana, I.G. "Interactions between thermal and catalytic reactions in mild hydrocracking of gas oil". *Energy Fuels* 1989, 3, 716-722.

Koseoglu, R.O.; Phillips, C.R. "Kinetic models for the non-catalytic hydrocracking of Athabasca bitumen". *Fuel* 1988, 67, 906-915.

Lee, H.H. *Heterogeneous Reactor Design*. 1985.

- Lemberton, J.-L.; Guisnet, M. "Phenathrene Hydroconversion as a Potential Test Reaction for the Hydrogenation and Cracking Properties of Coal Hydroliquefaction Catalysts". *Appl. Catal.* 1984, 13, 181-192.
- Man, G.P. "Hydroprocessing of Heavy Gas Oil in a Continuous Stirred Tank Reactor". MSc Thesis, Dept. Chem. Engg, University of Alberta, 1981.
- McKay, J.F.; Weber, J.M.; Latham, D.R., *Anal. Chem.* 1976, 48, 891-898.
- Miki, Y.; Yamadaya, S.; Oba, M.; Sugimoto, Y. "Role of catalyst in hydrocracking of heavy oil", *J. Catal.* 1983, 83, 371-383.
- Mochida, I.; Shin-ichi, I.; Maeda, K.; Takeshita, K. "Carbonization of Aromatic Hydrocarbons-VI". *Carbon* 1977, 15, 9-16.
- Mochida, I.; Ando, T.; Maeda, K.; Takeshita, K. "Carbonization of Aromatic Hydrocarbons-VII". *Carbon* 1978, 16, 453-458.
- Mosby, J.F.; Buttke, R.D.; Cox, J.A.; Nikolaidis, C. "Process Characterization of Expanded-Bed Reactor in Series", *Chem. Eng. Sci.* 1986, 4, 989-995.
- Payzant, J.D.; Mojelsky, T.W.; Strausz, O.P. "Improved methods for the selective isolation of the sulfide and thiophenic classes of compounds from petroleum". *Energy Fuels* 1989, 3, 449-454.
- Reynolds, J.C.; Beret, S. "Effect of Prehydrogenation on Hydroconversion of Maya Residuum, Part I: Process Characterization". *Fuel Sci. and Tech. Int.* 1989, 2, 165-186.
- Sapre, A.V.; Broderick, D.H.; Frankael, D.; Gates, B.C. Nag, N.K. "Hydrodesulfurization of benzo[b]naphtho[2,3-d]thiophene catalyzed by sulfided CoMo-MoO₃/γ-Al₂O₃; The reaction network". *AIChE J.* 1980, 26, 690-694.
- Sapre, A.V.; Gates, B.C. "Hydrogenation of Aromatic Hydrocarbons Catalyzed by Sulfided CoO-MoO₃/γ-Al₂O₃. Reactivities and Reaction Networks". *Ind. Eng. Chem. Process Des. Dev.* 1981, 20, 68-73.
- Steer, J.G.; Muehlenbachs, K.; Gray, M.R. "Stable isotope analysis of hydrogen transfer during catalytic hydrocracking of residues". *Energy Fuels* 1992, 6, 540-544.

- Sundaram, K.M.; Katzer, J.R.; Bischoff, K.B. "Modeling of hydroprocessing reactions". *Chem. Eng. Comm.* 1988, 71, 53-71.
- Shuit, G.C.A.; Gates, B.C. *AICHE Journal* 1973, 19, 3, 434.
- Van Parijs, I.A.; Froment, G.F. "Kinetics of Hydrodesulfurization on a Co-Mo/ γ -Al₂O₃ Catalyst. 1. Kinetics of Hydrogenolysis of Thiophene". *Ind. Eng. Chem. Prod. Res. Dev.* 1986, 25, 431-436.
- Van Parijs, I.A.; Hosten, L.H.; Froment, G.F. "Kinetics of Hydrodesulfurization on a Co-Mo/ γ -Al₂O₃ Catalyst. 2. Kinetics of Hydrogenolysis of Benzothiophene". *Ind. Eng. Chem. Prod. Res. Dev.* 1986, 25, 437-443.
- Vrinat, M.L. "The Kinetics of the Hydrodesulfurization Process-A Review". *Applied Catalysis* 1983, 137-158.
- Weekman, V.W. *AICHE Journal* 1974, 20, 833.
- Whitaker, S.; Cassano, A.E. (eds) *Concepts and Design of Chemical Reactors* 1986, Gordon and Breach, Switzerland.
- Wilson, M.F.; Fisher, I.P.; Kriz, J.F. "Hydrogenation of Aromatic Compounds in Synthetic Crude Distillates Catalyzed by Sulfided Ni-W/ γ -Al₂O₃". *J. Catal.* 1985, 95, 155-166.
- Wu, W.L.; Haynes, H.W. "Hydrocracking Condensed-Ring Aromatics Over Nonacidic Catalysts". *ACS Symposium Series* 1975, 20, 65-81.

Appendix A
Reactor Data

Summary of Reactor Runs

<u>SCL #</u>	<u>Run Description</u>	<u>Page</u>
3HPP0006/7	Feed Bitumen	146
3HPP0005	1000 mL/h run	147
3HPP0003	800 mL/h run	149
3HPP0012	730 mL/h run	151
3HPP0004	675 mL/h run	153
3HPP0008	500 mL/h run	155
3HPP0009	430 mL/h run	157
3HPP0010	430 mL/h repeat run	159
3HPP0013	400 mL/h low hydrogen rate run	161
3HPP0014	400 mL/h run	163
3HPP0011	350 mL/h run	165
3HPP0017	300 mL/h run	167
3HPP0016	250 mL/h run	169
3HPP0015	200 mL/h run	171
3HPP0018	410 °C catalytic run	173
3HPP0019	420 °C catalytic run	175
3HPP0020	440 °C catalytic run	177
3HPP0021	450 °C catalytic run	179
3HPP0002	400 °C thermal run	181
3HPP0027	420 °C thermal run	183
3HPP0026	430 °C thermal run	185
3HPP0001	440 °C thermal run	187
3HPP0025	low pressure run	189
3HPP0022	925 μ m ground catalyst run	191

<u>SCL #</u>	<u>Run Description</u>	<u>Page</u>
3HPP0023	600 μm ground catalyst run	193

Feed Bitumen

Feed Boiling Cuts			MCR		
naptha	mass %	0.000	residue	mass %	27.120
mid dist	mass %	7.020	whole prod.	mass %	14.905
gas oil	mass %	38.019			
vac resid	mass %	54.961			

Feed Composition

	sulfur	sulfur	nitrogen	nitrogen
	m% of cut	% of whole	m% of cut	m% of whole
naptha	0.000	0.000	0.000	0.000
mid dist	2.615	0.184	0.032	0.002
gas oil	3.333	1.267	0.152	0.058
vac resid	6.256	3.438	0.706	0.388
	mass % S:	4.889	mass % N:	0.448
	mass % S:		mass % N:	
	(from tot)	4.735	(from tot)	0.444
	error %	-3.256	error %	-1.000
	N as	N as carb	S as	S as Sulfide
	carbazol,m%	m% of whole	Sulfide, m%	m% of whole
naptha	0.000	0.000	0.000	0.000
mid dist	0.000	0.000	0.940	0.066
gas oil	0.039	0.015	0.940	0.357
vac resid	0.107	0.059	1.780	0.978
	mass % N:	0.074	mass % S:	1.402
	mass % N:		mass % S:	
	(from tot)	0.069	(from tot)	1.250
	error %	-6.132	error %	-12.134
	Hydrogen	Hydrogen	Carbon	Carbon
	m% of cut	% of whole	m% of cut	m% of whole
naptha	0.000	0.000	0.000	0.000
mid dist	11.080	0.778	84.860	5.957
gas oil	11.080	4.213	84.860	32.263
vac resid	9.500	5.221	80.870	44.447
	mass % H:	10.212	mass % C:	82.667
	mass % H:		mass % C:	
	(from tot)	10.070	(from tot)	82.300
	error %	-1.406	error %	-0.446

OCT 1 1992 430C 1000 mL/hr 13.7 MPa
78 g cat

Liquid			Gas		
	feed			Feed	
vlt esso	mL/hr	1012.000	H2 init	meter read	310.500
temp correct	mL/hr	1119.272	H2 final	meter read	317.500
bitumen rate	g/hr	1033.088	time	min	5.069
residence t	hr	0.371	H2	slm	6.849
			H	mol/hr	34.676

Product			Product		
init mass	g	6905.100	o.g. init	meter read	0.000
final mass	g	7250.900	o.g. final	meter read	7.154
time	hr	0.351	time	min	5.348
rate	g/hr	985.185	o.g.	slm	5.311
sulfur	mass %	2.270	o.g.	mol/hr	13.443
nitrogen	mass %	0.372	H2S+NH4+H2	mol/hr	13.034
carbon	mass %	85.180			
hydrogen	mass %	11.140			

Product by mass balance

duct Boiling Cuts					
naptha	mass %	14.250	H2S	mol/hr	0.830
mid dist	mass %	15.272	NH4	mol/hr	0.066
gas oil	mass %	39.958	H2	mol/hr	12.275
vac resid	mass %	30.521	H2S+NH4+H2	mol/hr	13.170
			error	%	-1.047
	MCR				
residue	mass %	33.540	carbon bal		
whole prod.	mass %	9.738	error	%	0.060

Product Composition

	sulfur	sulfur	nitrogen	nitrogen
	m% of cut	m% of whole	m% of cut	m% of whole
naptha	0.2586	0.037	0.0170	0.0024
mid dist	0.4727	0.072	0.0839	0.0128
gas oil	1.4474	0.578	0.2753	0.1100
vac resid	3.9524	1.206	0.8298	0.2533
	mass % S:	1.894	mass % N:	0.3785
	mass % S:		mass % N:	
	(from tot)	2.270	(from tot)	0.3718
	error %	16.577	error %	-1.8023

Sulfide data collected by :
Colin Winklmeier

	N as carbazol,m%	N as carb m% of whole	S as Sulfide,m%	S as Sulfide m% of whole
naptha	0.0013	0.0002		
mid dist	0.0154	0.0024		
gas oil	0.0858	0.0343	0.3900	
vac resid	0.1981	0.0605	1.2000	
	mass % N:	0.0973		
	mass % N:			
	(from tot)	0.0887		
	error %	-9.6931		

	Hydrogen m% of cut	Hydrogen m% of whole	Carbon m% of cut	Carbon m% of whole
naptha	14.7200	2.0975	85.4000	12.1692
mid dist	12.5600	1.9181	86.6600	13.2345
gas oil	11.5700	4.6231	86.9100	34.7273
vac resid	9.2500	2.8232	82.5700	25.2010
	Mass % H:	11.4620	mass % N:	85.3320
	Mass % H:		mass % N:	
	(from total)	11.1400	(from tot)	85.1800
	error %	-2.8902	error %	-0.1785

Product Gas Analysis by GC-FID

component	response factor	area	mol %
c1	5.577E-07	2.499E+06	1.3937
c2	2.696E-07	2.306E+06	0.6217
1-c2	2.719E-07	7.116E+03	0.0019
c3	1.893E-07	2.726E+06	0.5160
1-c3	1.937E-07	7.364E+04	0.0143
i-c4	1.482E-07	5.140E+05	0.0910
c4	1.433E-07	1.449E+06	0.2076
1-c4	1.467E-07	6.331E+04	0.0093
2-c4,trans	1.412E-07	2.023E+04	0.0029
2-c4,cis	1.403E-07	1.277E+04	0.0018
i-c5	1.098E-07	5.435E+05	0.0597
c5	1.098E-07	6.124E+05	0.0672
1-c5	1.124E-07	9.398E+03	0.0011
2-c5	1.124E-07	1.848E+04	0.0021
i-c6	9.013E-08	2.758E+05	0.0249
c6	9.242E-08	1.260E+05	0.0116
1-c6	9.461E-08	2.014E+05	0.0191
		Total:(mol%)	3.0458

	sept 23,92	430 C	800 mL/hr	13.7 MPa	
				78 g cat	
	Liquid			Gas	
	feed			Feed	
vlt esso	mL/hr	800.000	H2 init	meter read	49.540
temp correct	mL/hr	884.800	H2 final	meter read	56.250
bitumen rate	g/hr	816.670	time	min	5.348
residence t	hr	0.469	H2	slm	6.223
			H	mol/hr	31.506

	Product			Product	
init mass	g	6834.000	o.g. init	meter read	0.000
final mass	g	7020.000	o.g. final	meter read	6.500
corrected	g	7010.000	time	min	5.348
time	hr	0.229	o.g.	slm	4.825
rate	g/hr	768.223	corrected	slm	
sulfur	mass %	1.880	o.g.	mol/hr	12.214
nitrogen	mass %	0.376	H2S+NH4+H2	mol/hr	11.830
carbon	mass %	85.620			
hydrogen	mass %	11.300			

Product by mass balance

Product Boiling Cuts					
naptha	mass %	7.905	H2S	mol/hr	0.757
mid dist	mass %	27.343	NH4	mol/hr	0.052
gas oil	mass %	35.719	H2	mol/hr	11.431
vac resid	mass %	29.033	H2S+NH4+H2	mol/hr	12.241
			error	%	-3.472
	MCR				
residue	mass %	33.540	carbon bal		
whole prod.	mass %	9.738	error	%	0.657

Product Composition

	sulfur		nitrogen	
	m% of cut	m% of whole	m% of cut	m% of whole
naptha	0.2027	0.016	0.0292	0.0023
mid dist	0.6248	0.171	0.1137	0.0311
gas oil	1.5361	0.549	0.3386	0.1209
vac resid	3.7800	1.097	0.8360	0.2427
	mass % S:	1.833	mass % N:	0.3971
	mass % S:		mass % N:	
	(from tot)	1.880	(from tot)	0.3760
	error %	2.501	error %	-5.6003

	N as carbazol,m%	N as carb m% of whole	S as Sulfide,m%	S as Sulfide m% of whole
naptha	0.0000	0.0000	0.0800	0.0063
mid dist	0.0244	0.0067	0.1800	0.0492
gas oil	0.1059	0.0378	0.2900	0.1036
vac resid	0.1754	0.0509	1.5900	0.4616
	mass % N:	0.0954	Mass % S:	0.6208
	mass % N: (from tot)	0.0909	Mass % S: (from tot)	0.5000
	error %	-5.0267	error %	-24.1502

	Hydrogen m% of cut	Hydrogen m% of whole	Carbon m% of cut	Carbon m% of whole
naptha	14.5000	1.1463	85.4600	6.7559
mid dist	12.4400	3.4015	87.0400	23.7992
gas oil	11.3300	4.0469	87.0400	31.0897
vac resid	9.1400	2.6536	82.9300	24.0771
	Mass % H:	11.2483	mass % N:	85.7218
	Mass % H: (from total)	11.3000	mass % N: (from tot)	85.6200
	error %	0.4577	error %	-0.1189

component	Gas Analysis by GC-FID		
	response factor	area	mol %
c1	5.5770E-07	2.5430E+06	1.4182
c2	2.6960E-07	2.3990E+06	0.6468
1-c2	2.7190E-07	3.7020E+04	0.0101
c3	1.8930E-07	2.7940E+06	0.5289
1-c3	1.9370E-07	7.8160E+04	0.0151
i-c4	1.4820E-07	6.1710E+05	0.0915
c4	1.4330E-07	1.5160E+06	0.2172
1-c4	1.4670E-07	6.3720E+04	0.0093
2-c4,trans	1.4120E-07	2.1930E+04	0.0031
2-c4,cis	1.4030E-07	1.3810E+04	0.0019
i-c5	1.0980E-07	5.6250E+05	0.0618
c5	1.0980E-07	6.5300E+05	0.0717
1-c5	1.1240E-07	1.0000E+04	0.0011
2-c5	1.1240E-07	0.0000E+00	0.0000
i-c6	9.0130E-08	2.3980E+05	0.0216
c6	9.2420E-08	1.4790E+05	0.0137
1-c6	9.4610E-08	3.2850E+05	0.0311
		Total:(mol%)	3.1431

	oct 30 92	430 C	730 mL/h	13.7 MPa 78 g cat	
	Liquid		Gas		
	feed		Feed		
vlt esso	mL/hr	724.000	H2 init	meter read	3530.000
temp correct	mL/hr	800.744	H2 final	meter read	3544.000
bitumen rate	g/hr	739.087	time	min	13.155
residence t	hr	0.518	H2	slm	5.279
			H	mol/hr	26.724
	Product		Product		
init mass	g	6825.000	o.g. init	meter read	3222.830
final mass	g	7385.600	o.g. final	meter read	3236.260
corrected	g	7395.000	time	min	13.155
time	hr	0.821	o.g.	slm	4.053
rate	g/hr	694.081	corrected	slm	
sulfur	mass %	1.680	o.g.	mol/hr	10.260
nitrogen	mass %	0.380	H2S+NH4+H2	mol/hr	9.873
carbon	mass %	85.800			
hydrogen	mass %	11.460			

Product by mass balance

Product Boiling Cuts					
naptha	mass %	9.507	H2S	mol/hr	0.729
mid dist	mass %	24.973	NH4	mol/hr	0.046
gas oil	mass %	38.046	H2	mol/hr	8.823
vac resid	mass %	27.474	H2S+NH4+H2	mol/hr	9.598
			error	%	2.787
	MCR				
residue	mass %	31.070	carbon bal		
whole prod.	mass %	8.536	error	%	0.496

Product Composition

	sulfur	sulfur	nitrogen	nitrogen
	m% of cut	m% of whole	m% of cut	m% of whole
naptha	0.2130	0.020	0.0200	0.0019
mid dist	0.4330	0.108	0.1020	0.0255
gas oil	1.3500	0.514	0.3100	0.1179
vac resid	3.5300	0.970	0.8560	0.2352
	mass % S:	1.612	mass % N:	0.3805
	mass % S:		mass % N:	
	(from tot)	1.680	(from tot)	0.3800
	error %	4.058	error %	-0.1298

	N as carbazol,m%	N as carb m% of whole	S as Sulfide,m%	S as Sulfide m% of whole
naptha	0.0018	0.0002		
mid dist	0.0199	0.0050		
gas oil	0.1036	0.0394		
vac resid	0.1943	0.0534		
	mass % N:	0.0979	Mass % S:	0.0000
	mass % N: (from tot)	0.0962	Mass % S: (from tot)	
	error %	-1.8433	error %	ERR
	Hydrogen m% of cut	Hydrogen m% of whole	Carbon m% of cut	Carbon m% of whole
naptha	14.6100	1.3889	85.7600	8.1530
mid dist	12.5200	3.1267	86.8600	21.6918
gas oil	11.2900	4.2954	86.6700	32.9745
vac resid	9.5700	2.6293	82.6300	22.7017
	Mass % H:	11.4402	mass % N:	85.5210
	Mass % H: (from total)	11.4600	mass % N: (from tot)	85.8000
	error %	0.1724	error %	0.3252

component	Gas Analysis by GC-FID		
	response factor	area	mol %
c1	5.5770E-07	3.1550E+06	1.7595
c2	2.6960E-07	2.8870E+06	0.7783
1-c2	2.7190E-07	0.0000E+00	0.0000
c3	1.8930E-07	3.3750E+06	0.6389
1-c3	1.9370E-07	7.7820E+04	0.0151
i-c4	1.4820E-07	7.4520E+05	0.1104
c4	1.4330E-07	1.7380E+06	0.2491
1-c4	1.4670E-07	5.5520E+04	0.0081
2-c4,trans	1.4120E-07	1.7360E+04	0.0025
2-c4,cis	1.4030E-07	1.1140E+04	0.0016
i-c5	1.0980E-07	6.1410E+05	0.0674
c5	1.0980E-07	6.8460E+05	0.0752
1-c5	1.1240E-07	7.2360E+03	0.0008
2-c5	1.1240E-07	3.8830E+03	0.0004
i-c6	9.0130E-08	3.0340E+05	0.0273
c6	9.2420E-08	1.3030E+05	0.0120
1-c6	9.4610E-08	2.0920E+05	0.0198
		Total:(mol%)	3.7665

	sept 28,92	430 C	675 mL/hr	13.7 MPa	
				78 g cat	
	Liquid		Gas		
	feed		Feed		
vlt esso	mL/hr	675.000	H2 init	meter read	405.5000
temp correct	mL/hr	746.550	H2 final	meter read	410.8000
bitumen rate	g/hr	689.066	time	min	3.7410
residence t	hr	0.556	H2	slm	7.0270
			H	mol/hr	35.5749

	Product		Product		
init mass	g		o.g. init	meter read	372.2700
final mass	g		o.g. final	meter read	377.7600
corrected	g		time	min	3.7410
time	hr		o.g.	slm	5.8261
rate	g/hr	644.832	corrected	slm	
sulfur	mass %	1.750	o.g.	mol/hr	14.7475
nitrogen	mass %	0.364	H2S+NH4+H2	mol/hr	14.3646
carbon	mass %	86.540			
hydrogen	mass %	11.440			

Product by mass balance

Product Boiling Cuts					
naptha	mass %	9.049	H2S	mol/hr	0.6668
mid dist	mass %	29.218	NH4	mol/hr	0.0507
gas oil	mass %	35.483	H2	mol/hr	13.6368
vac resid	mass %	26.250	H2S+NH4+H2	mol/hr	14.3543
			error	%	0.0716
	MCR				
residue	mass %	31.070	carbon bal		
whole prod.	mass %	8.536	error	%	-0.1934

Product Composition

	sulfur	sulfur	nitrogen	nitrogen
	m% of cut	m% of whole	m% of cut	m% of whole
naptha	0.2216	0.020	0.0182	0.0016
mid dist	0.4279	0.125	0.0998	0.0292
gas oil	1.2894	0.458	0.3178	0.1128
vac resid	3.5068	0.921	0.8286	0.2175
	mass % S:	1.523	mass % N:	0.3611
	mass % S:		mass % N:	
	(from tot)	1.750	(from tot)	0.3639
	error %	12.965	error %	0.7759

	N as carbazol,m%	N as carb m% of whole	S as Sulfide,m%	S as Sulfide m% of whole
naptha	0.0020	0.0002		
mid dist	0.0202	0.0059		
gas oil	0.1027	0.0364		
vac resid	0.1981	0.0520		
	mass % N:	0.0945	Mass % S:	0.0000
	mass % N: (from tot)	0.0926	Mass % S: (from tot)	
	error %	-2.0494	error %	ERR
	Hydrogen m% of cut	Hydrogen m% of whole	Carbon m% of cut	Carbon m% of whole
naptha	14.7800	1.3375	85.0600	7.6973
mid dist	12.6400	3.6932	87.2100	25.4811
gas oil	11.4700	4.0699	87.1200	30.9128
vac resid	9.0300	2.3703	82.6900	21.7059
	Mass % H:	11.4709	mass % N:	85.7970
	Mass % H: (from total)	11.4400	mass % N: (from tot)	86.5400
	error %	-0.2700	error %	0.8585

component	Gas Analysis by GC-FID		
	response factor	area	mol %
c1	5.5770E-07	2.0040E+06	1.1176
c2	2.6960E-07	1.9850E+06	0.5352
1-c2	2.7190E-07	5.7890E+04	0.0157
c3	1.8930E-07	2.3830E+06	0.4511
1-c3	1.9370E-07	6.7420E+04	0.0131
i-c4	1.4820E-07	5.3690E+05	0.0796
c4	1.4330E-07	1.3590E+06	0.1947
1-c4	1.4670E-07	5.8880E+04	0.0086
2-c4,trans	1.4120E-07	1.9800E+04	0.0028
2-c4,cis	1.4030E-07	1.2750E+04	0.0018
i-c5	1.0980E-07	5.0990E+05	0.0560
c5	1.0980E-07	5.9640E+05	0.0655
1-c5	1.1240E-07	9.0360E+03	0.0010
2-c5	1.1240E-07	6.5860E+03	0.0007
i-c6	9.0130E-08	2.7720E+05	0.0250
c6	9.2420E-08	1.1780E+05	0.0109
1-c6	9.4610E-08	1.8310E+05	0.0173
		Total:(mol%)	2.5966

	oct. 8 92	430 C	500 mL/h	13.7 MPa 78 g cat	
	Liquid			Gas	
	feed			Feed	
vlt esso	mL/hr	503.000	H2 init	meter read	0.0000
temp correct	mL/hr	556.318	H2 final	meter read	11.0000
bitumen rate	g/hr	513.482	time	min	7.7932
residence t	hr	0.746	H2	slm	7.0010
			H	mol/hr	35.4431

	Product			Product	
init mass	g	6957.900	o.g. init	meter read	0.0000
final mass	g	7305.500	o.g. final	meter read	12.5000
corrected	g	7298.000	time	min	7.7932
time	hr	0.710	o.g.	slm	6.3677
rate	g/hr	478.825	corrected	slm	
sulfur	mass %	1.140	o.g.	mol/hr	16.1186
nitrogen	mass %	0.321	H2S+NH4+H2	mol/hr	15.7075
carbon	mass %	86.320			
hydrogen	mass %	11.560			

Product by mass balance

Product Boiling Cuts					
naptha	mass %	7.918	H2S	mol/hr	0.5889
mid dist	mass %	36.496	NH4	mol/hr	0.0529
gas oil	mass %	32.555	H2	mol/hr	13.9121
vac resid	mass %	23.031	H2S+NH4+H2	mol/hr	14.5539
			error	%	7.3447
	MCR				
residue	mass %	32.360	carbon bal		
whole prod.	mass %	7.453	error	%	-0.4082

Product Composition

	sulfur	sulfur	nitrogen	nitrogen
	m% of cut	m% of whole	m% of cut	m% of whole
naptha	0.1063	0.008	0.0138	0.0011
mid dist	0.3237	0.118	0.1053	0.0384
gas oil	1.0034	0.327	0.3369	0.1097
vac resid	2.9908	0.689	0.8217	0.1892
	mass % S:	1.142	mass % N:	0.3384
	mass % S:		mass % N:	
	(from tot)	1.140	(from tot)	0.3211
	error %	-0.178	error %	-5.4024

	N as carbazol,m%	N as carb m% of whole	S as Sulfide,m%	S as Sulfide m% of whole
naptha	0.0000	0.0000		
mid dist	0.0238	0.0087		
gas oil	0.1161	0.0378		
vac resid	0.2124	0.0489		
	mass % N:	0.0954	Mass % S:	0.0000
	mass % N: (from tot)	0.0888	Mass % S: (from tot)	
	error %	-7.4129	error %	ERR

	Hydrogen m% of cut	Hydrogen m% of whole	Carbon m% of cut	Carbon m% of whole
naptha	14.6600	1.1608	85.5800	6.7763
mid dist	12.5900	4.5948	87.0300	31.7621
gas oil	11.3100	3.6820	87.1300	28.3654
vac resid	9.3600	2.1557	82.0200	18.8900
	Mass % H:	11.5933	mass % N:	85.7939
	Mass % H: (from total)	11.5600	mass % N: (from tot)	86.3200
	error %	-0.2880	error %	0.6095

component	Gas Analysis by GC-FID		
	response factor	area	mol %
c1	5.5770E-07	1.9400E+06	1.0819
c2	2.6960E-07	1.9655E+06	0.5299
1-c2	2.7190E-07	5.8955E+04	0.0160
c3	1.8930E-07	2.3250E+06	0.4401
1-c3	1.9370E-07	5.7470E+04	0.0111
i-c4	1.4820E-07	5.2420E+05	0.0777
c4	1.4330E-07	1.3420E+06	0.1923
1-c4	1.4670E-07	5.4830E+04	0.0080
2-c4,trans	1.4120E-07	2.3340E+04	0.0033
2-c4,cis	1.4030E-07	1.4720E+04	0.0021
i-c5	1.0980E-07	4.9725E+05	0.0546
c5	1.0980E-07	6.0005E+05	0.0659
1-c5	1.1240E-07	7.1080E+03	0.0008
2-c5	1.1240E-07	1.1664E+05	0.0131
i-c6	9.0130E-08	2.6195E+05	0.0236
c6	9.2420E-08	1.0868E+05	0.0100
1-c6	9.4610E-08	2.1080E+05	0.0199
		Total:(mol%)	2.5505

	oct 18 92	430 C	430 mL/h	13.7 MPa	
				78 g cat	
	Liquid			Gas	
	feed		Feed		
vlt esso	mL/hr	426.000	H2 init	meter read	1388.8800
temp correct	mL/hr	471.156	H2 final	meter read	1398.5000
bitumen rate	g/hr	434.877	time	min	9.2510
residence t	hr	0.880	H2	slm	5.1578
			H	mol/hr	26.1121

	Product			Product	
init mass	g	6896.000	o.g. init	meter read	1210.9000
final mass	g	7241.800	o.g. final	meter read	1222.6800
corrected	g	7255.000	time	min	9.2510
time	hr	0.897	o.g.	slm	5.0553
rate	g/hr	400.393	corrected	slm	4.7000
sulfur	mass %	1.180	o.g.	mol/hr	11.8971
nitrogen	mass %	0.327	H2S+NH4+H2	mol/hr	11.5992
carbon	mass %	86.660			
hydrogen	mass %	11.700			

Product by mass balance

Product Boiling Cuts					
naptha	mass %	12.799	H2S	mol/hr	0.4956
mid dist	mass %	33.053	NH4	mol/hr	0.0444
gas oil	mass %	32.423	H2	mol/hr	10.0047
vac resid	mass %	21.726	H2S+NH4+H2	mol/hr	10.5447
			error	%	9.0910
	MCR				
residue	mass %	32.370	carbon bal		
whole prod.	mass %	7.033	error	%	0.7996

Product Composition

	sulfur	sulfur	nitrogen	nitrogen
	m% of cut	m% of whole	m% of cut	m% of whole
naptha	0.1044	0.013	0.0254	0.0033
mid dist	0.3160	0.104	0.1077	0.0356
gas oil	0.9293	0.301	0.3291	0.1067
vac resid	3.0060	0.653	0.8032	0.1745
	mass % S:	1.072	mass % N:	0.3201
	mass % S:		mass % N:	
	(from tot)	1.180	(from tot)	0.3266
	error %	9.137	error %	2.0050

	N as carbazol,m%	N as carb m% of whole	S as Sulfide,m%	S as Sulfide m% of whole
naptha	0.0031	0.0004		
mid dist	0.0259	0.0085		
gas oil	0.1185	0.0384		
vac resid	0.2170	0.0471		
	mass % N:	0.0945	Mass % S:	0.0000
	mass % N: (from tot)	0.0919	Mass % S: (from tot)	
	error %	-2.8138	error %	ERR

	Hydrogen m% of cut	Hydrogen m% of whole	Carbon m% of cut	Carbon m% of whole
naptha	14.5700	1.8648	85.9800	11.0045
mid dist	12.5900	4.1613	87.0800	28.7823
gas oil	11.3500	3.6800	87.1400	28.2533
vac resid	9.2300	2.0053	82.0500	17.8258
	Mass % H:	11.7114	mass % N:	85.8659
	Mass % H: (from total)	11.7000	mass % N: (from tot)	86.6600
	error %	-0.0974	error %	0.9164

component	Gas Analysis by GC-FID		
	response factor	area	mol %
c1	5.5770E-07	1.8760E+06	1.0462
c2	2.6960E-07	1.9460E+06	0.5246
1-c2	2.7190E-07	6.0020E+04	0.0163
c3	1.8930E-07	2.2670E+06	0.4291
1-c3	1.9370E-07	4.7520E+04	0.0092
i-c4	1.4820E-07	5.1150E+05	0.0758
c4	1.4330E-07	1.3250E+06	0.1899
1-c4	1.4670E-07	5.0780E+04	0.0074
2-c4,trans	1.4120E-07	2.6880E+04	0.0038
2-c4,cis	1.4030E-07	1.6690E+04	0.0023
i-c5	1.0980E-07	4.8460E+05	0.0532
c5	1.0980E-07	6.0370E+05	0.0663
1-c5	1.1240E-07	5.1800E+03	0.0006
2-c5	1.1240E-07	2.2670E+05	0.0255
i-c6	9.0130E-08	2.4670E+05	0.0222
c6	9.2420E-08	9.9560E+04	0.0092
1-c6	9.4610E-08	2.3850E+05	0.0226
		Total:(mol%)	2.5044

	oct 21 92	430 C	430 mL/h	13.7 MPa 78 g cat	
	Liquid		Gas		
	feed		Feed		
vlt esso	mL/hr	435.000	H2 init	meter read	2094.6000
temp correct	mL/hr	481.110	H2 final	meter read	2103.3000
bitumen rate	g/hr	444.065	time	min	8.5775
residence t	hr	0.862	H2	slm	5.0308
			H	mol/hr	25.4691

	Product		Product		
init mass	g	6852.300	o.g. init	meter read	1926.4800
final mass	g	7207.200	o.g. final	meter read	1936.2600
corrected	g	7189.000	time	min	8.5775
time	hr	0.813	o.g.	slm	4.5266
rate	g/hr	414.115	corrected	slm	
sulfur	mass %	1.060	o.g.	mol/hr	11.4581
nitrogen	mass %	0.323	H2S+NH4+H2	mol/hr	11.0929
carbon	mass %	86.510			
hydrogen	mass %	11.600			

Product by mass balance

Product Boiling Cuts					
naptha	mass %	10.996	H2S	mol/hr	0.5196
mid dist	mass %	30.437	NH4	mol/hr	0.0451
gas oil	mass %	37.607	H2	mol/hr	9.3106
vac resid	mass %	20.960	H2S+NH4+H2	mol/hr	9.8753
			error	%	10.9759
	MCR				
residue	mass %	33.430	carbon bal		
whole prod.	mass %	7.007	error	%	-0.7052

Product Composition

	sulfur	sulfur	nitrogen	nitrogen
	m% of cut	m% of whole	m% of cut	m% of whole
naptha	0.1522	0.017	0.0146	0.0016
mid dist	0.2369	0.072	0.0921	0.0280
gas oil	0.9648	0.363	0.3244	0.1220
vac resid	2.9960	0.628	0.9484	0.1988
	mass % S:	1.080	mass % N:	0.3504
	mass % S:		mass % N:	
	(from tot)	1.060	(from tot)	0.3233
	error %	-1.852	error %	-8.3881

	N as carbazol,m%	N as carb m% of whole	S as Sulfide,m%	S as Sulfide m% of whole
naptha	0.0025	0.0003		
mid dist	0.0178	0.0054		
gas oil	0.1097	0.0413		
vac resid	0.2150	0.0451		
	mass % N:	0.0920	Mass % S:	0.0000
	mass % N: (from tot)	0.0919	Mass % S: (from tot)	
	error %	-0.1142	error %	ERR
	Hydrogen m% of cut	Hydrogen m% of whole	Carbon m% of cut	Carbon m% of whole
naptha	14.7800	1.6251	86.7600	9.5397
mid dist	12.7200	3.8716	86.7700	26.4106
gas oil	11.4400	4.3023	87.7700	33.0079
vac resid	9.2700	1.9430	82.5400	17.3002
	Mass % H:	11.7420	mass % C:	86.2584
	Mass % H: (from total)	11.6000	mass % C: (from tot)	86.5100
	error %	-1.2243	error %	0.2909

component	Gas Analysis by GC-FID		
	response factor	area	mol %
c1	5.5770E-07	2.4800E+06	1.3831
c2	2.6960E-07	2.4010E+06	0.6473
1-c2	2.7190E-07	0.0000E+00	0.0000
c3	1.8930E-07	2.9250E+06	0.5537
1-c3	1.9370E-07	5.4380E+04	0.0105
i-c4	1.4820E-07	6.5500E+05	0.0971
c4	1.4330E-07	1.6710E+06	0.2395
1-c4	1.4670E-07	4.7410E+04	0.0070
2-c4,trans	1.4120E-07	1.4360E+04	0.0020
2-c4,cis	1.4030E-07	9.2180E+03	0.0013
i-c5	1.0980E-07	6.1090E+05	0.0671
c5	1.0980E-07	7.2800E+05	0.0799
1-c5	1.1240E-07	4.5910E+03	0.0005
2-c5	1.1240E-07	3.6860E+04	0.0041
i-c6	9.0130E-08	4.2910E+05	0.0387
c6	9.2420E-08	2.9410E+05	0.0272
1-c6	9.4610E-08	3.0270E+05	0.0286
		Total:(mol%)	3.1876

	Nov 2 92	430 C	400 mL/h	13.7 MPa	
				78 g cat	
	Liquid			Gas	
	feed			Feed	
vlt esso	mL/hr	404.000	H2 init	meter read	4084.3000
temp correct	mL/hr	446.824	H2 final	meter read	4089.9000
bitumen rate	g/hr	412.419	time	min	10.0452
residence t	hr	0.928	H2	slm	2.7651
			H	mol/hr	13.9986

	Product			Product	
init mass	g	6905.100	o.g. init	meter read	3715.5200
final mass	g	7179.900	o.g. final	meter read	3721.4200
corrected	g	7183.000	time	min	10.0452
time	hr	0.721	o.g.	slm	2.3318
rate	g/hr	385.501	corrected	slm	2.1000
sulfur	mass %	1.350	o.g.	mol/hr	5.3157
nitrogen	mass %	0.340	H2S+NH4+H2	mol/hr	5.0534
carbon	mass %	86.080			
hydrogen	mass %	11.600			

Product by mass balance

Product Boiling Cuts					
naptha	mass %	13.575	H2S	mol/hr	0.4474
mid dist	mass %	30.336	NH4	mol/hr	0.0372
gas oil	mass %	35.228	H2	mol/hr	4.1252
vac resid	mass %	20.861	H2S+NH4+H2	mol/hr	4.6099
			error	%	8.7770
	MCR				
residue	mass %	33.280	carbon bal		
whole prod.	mass %	6.943	error	%	0.3987

Product Composition

	sulfur	sulfur	nitrogen	nitrogen
	m% of cut	m% of whole	m% of cut	m% of whole
naptha	0.0987	0.013	0.0197	0.0027
mid dist	0.2690	0.082	0.1050	0.0319
gas oil	1.1000	0.388	0.3510	0.1236
vac resid	3.0000	0.626	0.8440	0.1761
	mass % S:	1.108	mass % N:	0.3342
	mass % S:		mass % N:	
	(from tot)	1.350	(from tot)	0.3400
	error %	17.900	error %	1.6921

	N as carbazol,m%	N as carb m% of whole	S as Sulfide,m%	S as Sulfide m% of whole
naptha	0.0023	0.0003		
mid dist	0.0214	0.0065		
gas oil	0.1237	0.0436		
vac resid	0.2221	0.0463		
	mass % N:	0.0967	Mass % S:	0.0000
	mass % N: (from tot)	0.0889	Mass % S: (from tot)	
	error %	-8.8049	error %	ERR

	Hydrogen m% of cut	Hydrogen m% of whole	Carbon m% of cut	Carbon m% of whole
naptha	14.4000	1.9548	85.6900	11.6321
mid dist	12.4200	3.7678	86.7600	26.3196
gas oil	11.4400	4.0301	87.7600	30.9159
vac resid	9.1300	1.9046	82.5700	17.2253
	Mass % H:	11.6572	mass % C:	86.0929
	Mass % H: (from total)	11.6000	mass % C: (from tot)	86.0800
	error %	-0.4932	error %	-0.0150

component	Gas Analysis by GC-FID		
	response factor	area	mol %
c1	5.5770E-07	4.4820E+06	2.4996
c2	2.6960E-07	3.7870E+06	1.0210
1-c2	2.7190E-07	2.0380E+04	0.0055
c3	1.8930E-07	4.0820E+06	0.7727
1-c3	1.9370E-07	4.4970E+04	0.0087
i-c4	1.4820E-07	8.5520E+05	0.1267
c4	1.4330E-07	1.9270E+06	0.2761
1-c4	1.4670E-07	2.9680E+04	0.0044
2-c4,trans	1.4120E-07	9.7960E+03	0.0014
2-c4,cis	1.4030E-07	5.7920E+03	0.0008
i-c5	1.0980E-07	6.3690E+05	0.0699
c5	1.0980E-07	6.8860E+05	0.0756
1-c5	1.1240E-07	2.5280E+03	0.0003
2-c5	1.1240E-07	5.0070E+04	0.0056
i-c6	9.0130E-08	2.2780E+05	0.0205
c6	9.2420E-08	1.2810E+05	0.0118
1-c6	9.4610E-08	3.6060E+05	0.0341
		Total:(mol%)	4.9349

	Nov 5 92	430 C	400 mL/h	13.7 MPa 78 g cat	
	Liquid		Gas		
	feed		Feed		
vlt esso	mL/hr	398.000	H2 init	meter read	4692.6000
temp correct	mL/hr	440.188	H2 final	meter read	4721.5000
bitumen rate	g/hr	406.294	time	min	30.0100
residence t	hr	0.942	H2	slm	4.7765
			H	mol/hr	24.1817

	Product		Product		
init mass	g	6976.100	o.g. init	meter read	4361.0300
final mass	g	7296.400	o.g. final	meter read	4399.0800
corrected	g	7285.000	time	min	30.0100
time	hr	0.816	o.g.	slm	5.0336
rate	g/hr	378.740	corrected	slm	4.2000
sulfur	mass %	1.260	o.g.	mol/hr	10.6315
nitrogen	mass %	0.309	H2S+NH4+H2	mol/hr	10.3436
carbon	mass %	86.230			
hydrogen	mass %	11.730			

Product by mass balance

Product Boiling Cuts					
naptha	mass %	11.798	H2S	mol/hr	0.4518
mid dist	mass %	29.112	NH4	mol/hr	0.0451
gas oil	mass %	38.622	H2	mol/hr	8.8974
vac resid	mass %	20.468	H2S+NH4+H2	mol/hr	9.3944
			error	%	9.1768
	MCR				
residue	mass %	33.130	carbon bal		
whole prod.	mass %	6.781	error	%	0.0604

Product Composition

	sulfur	sulfur	nitrogen	nitrogen
	m% of cut	m% of whole	m% of cut	m% of whole
naptha	0.1310	0.015	0.0155	0.0018
mid dist	0.2190	0.064	0.0969	0.0282
gas oil	0.9320	0.360	0.3330	0.1286
vac resid	2.8700	0.587	0.8310	0.1701
	mass % S:	1.027	mass % N:	0.3287
	mass % S:		mass % N:	
	(from tot)	1.260	(from tot)	0.3090
	error %	18.524	error %	-6.3878

	N as carbazol,m%	N as carb m% of whole	S as Sulfide,m%	S as Sulfide m% of whole
naptha	0.0000	0.0000	0.0800	0.0094
mid dist	0.0199	0.0058	0.4100	0.1194
gas oil	0.1183	0.0457	0.2500	0.0966
vac resid	0.2050	0.0420	1.6000	0.3275
	mass % N:	0.0934	Mass % S:	0.5528
	mass % N: (from tot)	0.0921	Mass % S: (from tot)	0.5100
	error %	-1.4216	error %	-8.3995

	Hydrogen m% of cut	Hydrogen m% of whole	Carbon m% of cut	Carbon m% of whole
naptha	14.6600	1.7296	85.3200	10.0662
mid dist	12.5400	3.6506	86.9200	25.3037
gas oil	11.2800	4.3566	86.8600	33.5474
vac resid	9.2700	1.8974	81.8500	16.7529
	Mass % H:	11.6342	mass % C:	85.6703
	Mass % H: (from total)	11.7300	mass % C: (from tot)	86.2300
	error %	0.8169	error %	0.6490

component	Gas Analysis by GC-FID		
	response factor	area	mol %
c1	5.5770E-07	2.1260E+06	1.1857
c2	2.6960E-07	2.0360E+06	0.5489
1-c2	2.7190E-07	6.3560E+03	0.0017
c3	1.8930E-07	2.4730E+06	0.4681
1-c3	1.9370E-07	5.0040E+04	0.0097
i-c4	1.4820E-07	7.9580E+05	0.1179
c4	1.4330E-07	1.3810E+06	0.1979
1-c4	1.4670E-07	3.9990E+04	0.0059
2-c4,trans	1.4120E-07	1.3760E+04	0.0019
2-c4,cis	1.4030E-07	8.9320E+03	0.0013
i-c5	1.0980E-07	4.9990E+05	0.0549
c5	1.0980E-07	5.9530E+05	0.0654
1-c5	1.1240E-07	0.0000E+00	0.0000
2-c5	1.1240E-07	0.0000E+00	0.0000
i-c6	9.0130E-08	2.0770E+05	0.0187
c6	9.2420E-08	1.4200E+05	0.0131
1-c6	9.4610E-08	1.7700E+05	0.0167
		Total:(mol%)	2.7079

	oct 24 92	430 C	350 mL/h	13.7 MPa	
				78 g cat	
			Liquid	Gas	
	feed			Feed	
vlt esso	mL/hr	351.000	H2 init	meter read	2763.4000
temp correct	mL/hr	388.206	H2 final	meter read	2771.7500
bitumen rate	g/hr	358.314	time	min	9.3638
residence t	hr	1.068	H2	slm	4.4230
			H	mol/hr	22.3918

	Product		Product		
init mass	g	6939.700	o.g. init	meter read	2580.7100
final mass	g	7246.400	o.g. final	meter read	2590.8400
corrected	g	7243.000	time	min	9.3638
time	hr	0.913	o.g.	slm	4.2948
rate	g/hr	332.114	corrected	slm	4.0000
sulfur	mass %	1.120	o.g.	mol/hr	10.1252
nitrogen	mass %	0.308	H2S+NH4+H2	mol/hr	9.8153
carbon	mass %	86.260			
hydrogen	mass %	11.660			

Product by mass balance

Product Boiling Cuts					
naptha	mass %	12.158	H2S	mol/hr	0.4137
mid dist	mass %	33.824	NH4	mol/hr	0.0405
gas oil	mass %	35.019	H2	mol/hr	8.4010
vac resid	mass %	19.000	H2S+NH4+H2	mol/hr	8.8552
			error	%	9.7810
	MCR				
residue	mass %	32.840	carbon bal		
whole prod.	mass %	6.240	error	%	0.0409

Product Composition

	sulfur	sulfur	nitrogen	nitrogen
	m% of cut	m% of whole	m% of cut	m% of whole
naptha	0.1730	0.021	0.0128	0.0016
mid dist	0.2230	0.075	0.1010	0.0342
gas oil	0.8610	0.302	0.3390	0.1187
vac resid	2.7100	0.515	0.8470	0.1609
	mass % S:	0.913	mass % N:	0.3154
	mass % S:		mass % N:	
	(from tot)	1.120	(from tot)	0.3080
	error %	18.494	error %	-2.3897

	N as carbazol,m%	N as carb m% of whole	S as Sulfide,m%	S as Sulfide m% of whole
naptha	0.0029	0.0003		
mid dist	0.0208	0.0070		
gas oil	0.1228	0.0430		
vac resid	0.2282	0.0434		
	mass % N:	0.0937	Mass % S:	0.0000
	mass % N:		Mass % S:	
	(from tot)	0.0896	(from tot)	
	error %	-4.6520	error %	ERR
	Hydrogen m% of cut	Hydrogen m% of whole	Carbon m% of cut	Carbon m% of whole
naptha	14.7000	1.7872	85.3200	10.3730
mid dist	12.6800	4.2889	87.0600	29.4470
gas oil	11.1600	3.9081	87.2000	30.5362
vac resid	9.4400	1.7936	82.9200	15.7547
	Mass % H:	11.7777	mass % C:	86.1109
	Mass % H:		mass % C:	
	(from total)	11.6600	(from tot)	86.2600
	error %	-1.0095	error %	0.1729

component	Gas Analysis by GC-FID		mol %
	response factor	area	
c1	5.5770E-07	2.3560E+06	1.3139
c2	2.6960E-07	2.3500E+06	0.6336
1-c2	2.7190E-07	1.6500E+04	0.0045
c3	1.8930E-07	2.8170E+06	0.5333
1-c3	1.9370E-07	5.1950E+04	0.0101
i-c4	1.4820E-07	6.3470E+05	0.0941
c4	1.4330E-07	1.6540E+06	0.2370
1-c4	1.4670E-07	4.3400E+04	0.0064
2-c4,trans	1.4120E-07	1.2870E+04	0.0018
2-c4,cis	1.4030E-07	8.2520E+03	0.0012
i-c5	1.0980E-07	6.0190E+05	0.0661
c5	1.0980E-07	7.1840E+05	0.0789
1-c5	1.1240E-07	0.0000E+00	0.0000
2-c5	1.1240E-07	0.0000E+00	0.0000
i-c6	9.0130E-08	3.6580E+05	0.0330
c6	9.2420E-08	2.2780E+05	0.0211
1-c6	9.4610E-08	2.7710E+05	0.0262
		Total:(mol%)	3.0609

	Dec 2 92	430 C	300 mL/h	13.7 MPa	
				78 g cat	
	Liquid			Gas	
	feed			Feed	
vlt esso	mL/hr	300.000	H2 init	meter read	7027.6000
temp correct	mL/hr	331.800	H2 final	meter read	7032.2900
bitumen rate	g/hr	306.251	time	min	6.5020
residence t	hr	1.250	H2	slm	3.5777
			H	mol/hr	18.1126
	Product			Product	
init mass	g	7099.800	o.g. init	meter read	6735.5000
final mass	g	7305.500	o.g. final	meter read	6745.4000
corrected	g	7345.000	time	min	6.5020
time	hr	0.862	o.g.	slm	6.0448
rate	g/hr	284.300	corrected	slm	3.1000
sulfur	mass %	1.456	o.g.	mol/hr	7.8470
nitrogen	mass %	0.418	H2S+NH4+H2	mol/hr	7.5580
carbon	mass %	86.010			
hydrogen	mass %	11.440			

Product by mass balance

Product Boiling Cuts					
naptha	mass %	13.642	H2S	mol/hr	0.3236
mid dist	mass %	35.671	NH4	mol/hr	0.0121
gas oil	mass %	33.343	H2	mol/hr	6.9800
vac resid	mass %	17.344	H2S+NH4+H2	mol/hr	7.3157
			error	%	3.2061
	MCR				
residue	mass %	33.180	carbon bal		
whole prod.	mass %	5.755	error	%	0.0531

Product Composition

	sulfur	sulfur	nitrogen	nitrogen
	m% of cut	m% of whole	m% of cut	m% of whole
naptha	0.0964	0.013	0.0219	0.0030
mid dist	0.4070	0.145	0.1390	0.0496
gas oil	1.5000	0.500	0.4070	0.1357
vac resid	5.9700	1.035	1.8600	0.3226
	mass % S:	1.694	mass % N:	0.5109
	mass % S:		mass % N:	
	(from tot)	1.460	(from tot)	0.4180
	error %	-16.020	error %	-22.2173

	N as carbazol,m%	N as carb m% of whole	S as Sulfide,m%	S as Sulfide m% of whole
naptha	0.0028	0.0004		
mid dist	0.0254	0.0090		
gas oil	0.1449	0.0483		
vac resid	0.2680	0.0465		
	mass % N:	0.1042	Mass % S:	0.0000
	mass % N: (from tot)	0.0951	Mass % S: (from tot)	
	error %	-9.5667	error %	ERR
	Hydrogen m% of cut	Hydrogen m% of whole	Carbon m% of cut	Carbon m% of whole
naptha	14.7700	2.0149	84.6500	11.5477
mid dist	12.5400	4.4732	86.9500	31.0163
gas oil	10.9500	3.6511	86.8900	28.9720
vac resid	9.1500	1.5869	85.7200	14.8669
	Mass % H:	11.7261	mass % C:	86.4029
	Mass % H: (from total)	11.4400	mass % C: (from tot)	86.0100
	error %	-2.5009	error %	-0.4568

component	Gas Analysis by GC-FID		
	response factor	area	mol %
c1	5.5770E-07	2.9640E+06	1.6530
c2	2.6960E-07	2.8520E+06	0.7689
1-c2	2.7190E-07	1.3210E+05	0.0359
c3	1.8930E-07	3.2850E+06	0.6219
1-c3	1.9370E-07	6.7300E+04	0.0130
i-c4	1.4820E-07	7.1980E+05	0.1067
c4	1.4330E-07	1.7940E+06	0.2571
1-c4	1.4670E-07	4.8370E+04	0.0071
2-c4,trans	1.4120E-07	1.9340E+04	0.0027
2-c4,cis	1.4030E-07	1.2570E+04	0.0018
i-c5	1.0980E-07	6.4120E+05	0.0704
c5	1.0980E-07	7.5580E+05	0.0830
1-c5	1.1240E-07	7.5040E+03	0.0008
2-c5	1.1240E-07	6.9820E+03	0.0008
i-c6	9.0130E-08	2.5660E+05	0.0231
c6	9.2420E-08	1.4840E+05	0.0137
1-c6	9.4610E-08	2.4450E+05	0.0231
		Total:(mol%)	3.6831

	Dec 2 92	430 C	250 mL/h	13.7 MPa	
				78 g cat	
	Liquid			Gas	
	feed			Feed	
vit esso	mL/hr	249.000	H2 init	meter read	0.0000
temp correct	mL/hr	275.394	H2 final	meter read	3.7200
bitumen rate	g/hr	254.189	time	min	6.2130
residence t	hr	1.506	H2	slm	2.9698
			H	mol/hr	15.0348
	Product			Product	
init mass	g	7241.800	o.g. init	meter read	0.0000
final mass	g	7411.000	o.g. final	meter read	3.7100
corrected	g	7434.000	time	min	6.2130
time	hr	0.825	o.g.	slm	2.3706
rate	g/hr	233.105	corrected	slm	
sulfur	mass %	1.330	o.g.	mol/hr	6.0008
nitrogen	mass %	0.386	H2S+NH4+H2	mol/hr	5.7434
carbon	mass %	86.600			
hydrogen	mass %	11.730			

Product by mass balance

Product Boiling Cuts					
naptha	mass %	18.915	H2S	mol/hr	0.2791
mid dist	mass %	36.849	NH4	mol/hr	0.0163
gas oil	mass %	29.507	H2	mol/hr	5.5528
vac resid	mass %	14.729	H2S+NH4+H2	mol/hr	5.8482
			error	%	-1.8252
	MCR				
residue	mass %	37.050	carbon bal		
whole prod.	mass %	5.457	error	%	0.4216

Product Composition

	sulfur	sulfur	nitrogen	nitrogen
	m% of cut	m% of whole	m% of cut	m% of whole
naptha	0.0964	0.018	0.0257	0.0049
mid dist	0.3190	0.118	0.1380	0.0509
gas oil	1.2500	0.369	0.4290	0.1266
vac resid	2.7400	0.404	0.9210	0.1357
	mass % S:	0.908	mass % N:	0.3180
	mass % S:		mass % N:	
	(from tot)	1.320	(from tot)	0.3860
	error %	31.198	error %	17.6295

	N as carbazol,m%	N as carb m% of whole	S as Sulfide,m%	S as Sulfide m% of whole
naptha	0.0041	0.0008		
mid dist	0.0322	0.0118		
gas oil	0.1612	0.0476		
vac resid	0.2480	0.0365		
	mass % N:	0.0967	Mass % S:	0.0000
	mass % N: (from tot)	0.0921	Mass % S: (from tot)	
	error %	-4.9751	error %	ERR
	Hydrogen m% of cut	Hydrogen m% of whole	Carbon m% of cut	Carbon m% of whole
naptha	14.7100	2.7824	85.2500	16.1253
mid dist	12.4200	4.5766	87.3600	32.1909
gas oil	10.8000	3.1868	87.1300	25.7099
vac resid	8.7200	1.2843	84.1200	12.3897
	Mass % H:	11.8302	mass % C:	86.4158
	Mass % H: (from total)	11.7300	mass % C: (from tot)	86.6000
	error %	-0.8540	error %	0.2127

component	Gas Analysis by GC-FID		mol %
	response factor	area	
c1	5.5770E-07	3.5670E+06	1.9893
c2	2.6960E-07	3.3410E+06	0.9007
1-c2	2.7190E-07	6.2630E+04	0.0170
c3	1.8930E-07	3.8090E+06	0.7210
1-c3	1.9370E-07	5.4960E+04	0.0106
i-c4	1.4820E-07	8.2300E+05	0.1220
c4	1.4330E-07	2.0310E+06	0.2910
1-c4	1.4670E-07	3.7570E+04	0.0055
2-c4,trans	1.4120E-07	1.4740E+04	0.0021
2-c4,cis	1.4030E-07	9.5600E+03	0.0013
i-c5	1.0980E-07	6.9340E+05	0.0761
c5	1.0980E-07	8.1540E+05	0.0895
1-c5	1.1240E-07	5.0050E+03	0.0006
2-c5	1.1240E-07	1.0210E+03	0.0001
i-c6	9.0130E-08	2.6290E+05	0.0237
c6	9.2420E-08	1.5180E+05	0.0140
1-c6	9.4610E-08	2.5270E+05	0.0239
		Total:(mol%)	4.2887

	N as carbazol,m%	N as carb m% of whole	S as Sulfide,m%	S as Sulfide m% of whole
naptha	0.0023	0.0004	0.0000	0.0000
mid dist	0.0208	0.0079	0.0000	0.0000
gas oil	0.1531	0.0469	0.1900	0.0582
vac resid	0.2390	0.0290	1.4900	0.1808
	mass % N:	0.0843	Mass % S:	0.2390
	mass % N: (from tot)	0.0841	Mass % S: (from tot)	0.1700
	error %	-0.2056	error %	-40.5991
	Hydrogen m% of cut	Hydrogen m% of whole	Carbon m% of cut	Carbon m% of whole
naptha	14.6200	2.7950	85.4000	16.3267
mid dist	12.6000	4.8016	87.1800	33.2222
gas oil	11.1800	3.4256	87.8300	26.9112
vac resid	9.5900	1.1637	83.8000	10.1686
	Mass % H:	12.1858	mass % C:	86.6287
	Mass % H: (from total)	11.6300	mass % C: (from tot)	86.4600
	error %	-4.7794	error %	-0.1951

component	Gas Analysis by GC-FID		mol %
	response factor	area	
c1	5.5770E-07	2.6210E+06	1.4617
c2	2.6960E-07	2.5900E+06	0.6983
1-c2	2.7190E-07	5.2260E+04	0.0142
c3	1.8930E-07	3.1280E+06	0.5921
1-c3	1.9370E-07	2.8390E+04	0.0055
i-c4	1.4820E-07	6.7500E+05	0.1000
c4	1.4330E-07	1.6780E+06	0.2405
1-c4	1.4670E-07	1.8680E+04	0.0027
2-c4,trans	1.4120E-07	6.5160E+03	0.0009
2-c4,cis	1.4030E-07	3.8890E+03	0.0005
i-c5	1.0980E-07	5.5210E+05	0.0606
c5	1.0980E-07	6.2270E+05	0.0684
1-c5	1.1240E-07	1.3070E+03	0.0001
2-c5	1.1240E-07	0.0000E+00	0.0000
i-c6	9.0130E-08	1.9320E+05	0.0174
c6	9.2420E-08	1.0560E+05	0.0098
1-c6	9.4610E-08	1.5520E+05	0.0147
		Total:(mol%)	3.2875

	Dec 9 92	410 C	400 mL/h	13.7 MPa	
				78 g cat	
	Liquid			Gas	
	feed			Feed	
vlt esso	mL/hr	401.000	H2 init	meter read	7698.900
temp correct	mL/hr	443.506	H2 final	meter read	7708.200
bitumen rate	g/hr	409.356	time	min	9.649
residence t	hr	0.935	H2	slm	4.781
			H	mol/hr	24.204
	Product			Product	
init mass	g	7179.900	o.g. init	meter read	8192.570
final mass	g	7509.300	o.g. final	meter read	8218.420
corrected	g	7467.000	time	min	9.649
time	hr	0.743	o.g.	slm	10.636
rate	g/hr	386.251	corrected	slm	4.600
sulfur	mass %	1.760	o.g.	mol/hr	11.644
nitrogen	mass %	0.393	H2S+NH4+H2	mol/hr	11.488
carbon	mass %	85.800			
hydrogen	mass %	11.280			
			Product by mass balance		

Product Boiling Cuts

			H2S	mol/hr	0.393
naptha	mass %	9.806	NH4	mol/hr	0.021
mid dist	mass %	18.207	H2	mol/hr	10.005
gas oil	mass %	39.093	H2S+NH4+H2	mol/hr	10.420
vac resid	mass %	32.895	error	%	9.297
	MCR				
residue	mass %	27.460	carbon bal		
whole prod.	mass %	9.033	error	%	0.383

Product Composition

	sulfur	sulfur	nitrogen	nitrogen
	m% of cut	n% of whole	m% of cut	m% of whole
naptha	0.159	0.016	0.033	0.003
mid dist	0.359	0.065	0.084	0.015
gas oil	1.080	0.422	0.268	0.105
vac resid	2.380	0.783	0.814	0.268
	mass % S:	1.286	mass % N:	0.391
	mass % S:		mass % N:	
	(from tot)	1.760	(from tot)	0.393
	error %	26.929	error %	0.483

	N as carbazol,m%	N as carb m% of whole	S as Sulfide,m%	S as Sulfide m% of whole
naptha	0.000	0.000		0.000
mid dist	0.016	0.003		0.000
gas oil	0.088	0.034		0.000
vac residu	0.258	0.085		0.000
	mass % N:	0.122	Mass % S:	0.000
	mass % N:		Mass % S:	
	(from tot)	0.088	(from tot)	
	error %	-38.331	error %	ERR

	Hydrogen m% of cut	Hydrogen m% of whole	Carbon m% of cut	Carbon m% of whole
naptha	1.426E+01	1.398E+00	8.543E+01	8.377E+00
mid dist	12.480	2.272	86.800	15.804
gas oil	11.620	4.543	87.350	34.148
vac resid	9.660	3.178	86.000	28.290
	Mass % H:	11.391	mass % N:	86.618
	Mass % H:		mass % N:	
	(from total)	11.280	(from tot)	85.800
	error %	-0.981	error %	-0.953

component	Gas Analysis by GC-FID		
	response factor	area	mol %
c1	5.577E-07	1.013E+06	0.565
c2	2.696E-07	1.014E+06	0.273
1-c2	2.719E-07	6.928E+04	0.019
c3	1.893E-07	1.214E+06	0.230
1-c3	1.937E-07	1.599E+04	0.003
i-c4	1.482E-07	2.724E+05	0.040
c4	1.433E-07	7.360E+05	0.105
1-c4	1.467E-07	1.593E+04	0.002
2-c4,trans	1.412E-07	6.029E+03	0.001
2-c4,cis	1.403E-07	3.639E+03	0.001
i-c5	1.098E-07	2.936E+05	0.032
c5	1.098E-07	3.524E+05	0.039
1-c5	1.124E-07	0.000E+00	0.000
2-c5	1.124E-07	1.621E+03	0.000
i-c6	9.013E-08	1.293E+05	0.012
c6	9.242E-08	7.226E+04	0.007
1-c6	9.461E-08	1.204E+05	0.011
		Total:(mol%)	1.340

	Dec 9 92	420 C	400 mL/h	13.7 MPa 78 g cat	
	Liquid		Gas		
	feed		Feed		
vlt esso	mL/hr	399.000	H2 init	meter read	7698.900
temp correct	mL/hr	441.294	H2 final	meter read	7708.200
bitumen rate	g/hr	407.314	time	min	9.649
residence t	hr	0.940	H2	slm	4.781
			H	mol/hr	24.204

	Product		Product		
init mass	g	7349.200	o.g. init	meter read	8192.570
final mass	g	7607.600	o.g. final	meter read	8218.420
corrected	g	7624.000	time	min	9.649
time	hr	0.722	o.g.	slm	10.636
rate	g/hr	380.710	corrected	slm	4.300
sulfur	mass %	1.600	o.g.	mol/hr	10.885
nitrogen	mass %	0.383	H2S+NH4+H2	mol/hr	10.676
carbon	mass %	86.570			
hydrogen	mass %	11.660			

Product by mass balance

Product Boiling Cuts

			H2S	mol/hr	0.412
naptha	mass %	10.756	NH4	mol/hr	0.025
mid dist	mass %	23.770	H2	mol/hr	9.307
gas oil	mass %	39.887	H2S+NH4+H2	mol/hr	9.744
vac resid	mass %	25.587	error	%	8.732
	MCR				
residue	mass %	27.560	carbon bal		
whole prod.	mass %	7.052	error	%	0.025

Product Composition

	sulfur	sulfur	nitrogen	nitrogen
	m% of cut	n% of whole	m% of cut	m% of whole
naptha	0.123	0.013	0.022	0.002
mid dist	0.281	0.067	0.090	0.021
gas oil	0.994	0.396	0.301	0.120
vac resid	3.010	0.770	0.732	0.187
	mass % S:	1.247	mass % N:	0.331
	mass % S:		mass % N:	
	(from tot)	1.600	(from tot)	0.383
	error %	22.082	error %	13.573

Sulfide data collected by:
Colin Winklmeier

	N as carbazol,m%	N as carb m% of whole	S as Sulfide,m%	S as Sulfide m% of whole
naptha	0.003	0.000		0.000
mid dist	0.018	0.004		0.000
gas oil	0.103	0.041		0.000
vac resid	0.242	0.062	0.930	0.238
	mass % N:	0.108	Mass % S:	0.238
	mass % N: (from tot)	0.085	Mass % S: (from tot)	
	error %	-26.893	error %	ERR
	Hydrogen m% of cut	Hydrogen m% of whole	Carbon m% of cut	Carbon m% of whole
naptha	1.452E+01	1.562E+00	8.500E+01	9.142E+00
mid dist	12.530	2.978	87.430	20.782
gas oil	11.470	4.575	86.890	34.658
vac resid	9.610	2.459	83.600	21.391
	Mass % H:	11.574	mass % C:	85.973
	Mass % H: (from total)	11.660	mass % C: (from tot)	86.570
	error %	0.737	error %	0.689

component	Gas Analysis by GC-FID		
	response factor	area	mol %
c1	5.577E-07	1.461E+06	0.815
c2	2.696E-07	1.467E+06	0.396
1-c2	2.719E-07	7.076E+04	0.019
c3	1.893E-07	1.758E+06	0.333
1-c3	1.937E-07	3.011E+04	0.006
i-c4	1.482E-07	3.948E+05	0.059
c4	1.433E-07	1.026E+06	0.147
1-c4	1.467E-07	2.757E+04	0.004
2-c4,trans	1.412E-07	1.021E+04	0.001
2-c4,cis	1.403E-07	6.446E+03	0.001
i-c5	1.098E-07	3.975E+05	0.044
c5	1.098E-07	4.682E+05	0.051
1-c5	1.124E-07	2.299E+03	0.000
2-c5	1.124E-07	2.095E+03	0.000
i-c6	9.013E-08	1.683E+05	0.015
c6	9.242E-08	9.546E+04	0.009
1-c6	9.461E-08	1.578E+05	0.015
		Total:(mol%)	1.915

	dec 13 92	440 C	400 mL/hr	13.7 MPa	
				78 g cat	
	Liquid			Gas	
	feed			Feed	
vlt esso	mL/hr	402.000	H2 init	meter read	8557.350
temp correct	mL/hr	444.612	H2 final	meter read	8565.000
bitumen rate	g/hr	410.377	time	min	7.939
residence t	hr	0.933	H2	slm	4.779
			H	mol/hr	24.195
	Product			Product	
init mass	g	6994.300	o.g. init	meter read	390.500
final mass	g	7296.400	o.g. final	meter read	413.230
corrected	g	7262.000	time	min	7.939
time	hr	0.709	o.g.	slm	11.366
rate	g/hr	377.641	corrected	slm	3.900
sulfur	mass %	0.984	o.g.	mol/hr	9.872
nitrogen	mass %	0.329	H2S+NH4+H2	mol/hr	9.428
carbon	mass %	86.460			
hydrogen	mass %	11.910			

Product by mass balance

Product Boiling Cuts					
			H2S	mol/hr	0.491
naptha	mass %	18.182	NH4	mol/hr	0.041
mid dist	mass %	37.651	H2	mol/hr	8.355
gas oil	mass %	31.331	H2S+NH4+H2	mol/hr	8.887
vac resid	mass %	12.836	error	%	5.738
	MCR				
residue	mass %	25.010	carbon bal		
whole prod.	mass %	3.210	error	%	0.007

Product Composition

	sulfur	sulfur	nitrogen	nitrogen
	m% of cut	n% of whole	m% of cut	m% of whole
naptha	0.135	0.025	0.014	0.002
mid dist	0.209	0.079	0.103	0.039
gas oil	0.901	0.282	0.404	0.127
vac resid	3.060	0.393	0.750	0.096
	mass % S:	0.778	mass % N:	0.264
	mass % S:		mass % N:	
	(from tot)	0.984	(from tot)	0.329
	error %	20.904	error %	19.727

	N as carbazol,m%	N as carb m% of whole	S as Sulfide,m%	S as Sulfide m% of whole
naptha	0.003	0.001		0.000
mid dist	0.021	0.008		0.000
gas oil	0.164	0.051		0.000
vac resid	0.170	0.022		0.000
	mass % N:	0.082	Mass % S:	0.000
	mass % N:		Mass % S:	
	(from tot)	0.088	(from tot)	
	error %	7.053	error %	ERR

	Hydrogen m% of cut	Hydrogen m% of whole	Carbon m% of cut	Carbon m% of whole
naptha	1.475E+01	2.682E+00	8.444E+01	1.535E+01
mid dist	12.500	4.706	86.960	32.741
gas oil	11.010	3.450	87.520	27.421
vac resid	9.900	1.271	83.960	10.777
	Mass % H:	12.109	mass % C:	86.292
	Mass % H:		mass % C:	
	(from total)	11.910	(from tot)	86.460
	error %	-1.667	error %	0.194

component	Gas Analysis by GC-FID		mol %
	response factor	area	
c1	5.577E-07	3.639E+06	2.029
c2	2.696E-07	3.449E+06	0.930
1-c2	2.719E-07	2.604E+05	0.071
c3	1.893E-07	4.016E+06	0.760
1-c3	1.937E-07	7.606E+04	0.015
i-c4	1.482E-07	8.520E+05	0.126
c4	1.433E-07	2.179E+06	0.312
1-c4	1.467E-07	5.568E+04	0.008
2-c4,trans	1.412E-07	2.012E+04	0.003
2-c4,cis	1.403E-07	1.323E+04	0.002
i-c5	1.098E-07	7.183E+05	0.079
c5	1.098E-07	8.536E+05	0.094
1-c5	1.124E-07	8.164E+03	0.001
2-c5	1.124E-07	1.025E+04	0.001
i-c6	9.013E-08	2.739E+05	0.025
c6	9.242E-08	1.591E+05	0.015
1-c6	9.461E-08	2.604E+05	0.025
		Total:(mol%)	4.495

	Dec 13 92	450 C	400 mL/h	13.7 MPa	
				78 g cat	
	Liquid		Gas		
	feed			Feed	
vlt esso	mL/hr	399.000	H2 init	meter read	8869.200
temp correct	mL/hr	441.294	H2 final	meter read	8877.800
bitumen rate	g/hr	407.314	time	min	8.925
residence t	hr	0.940	H2	slm	4.780
			H	mol/hr	24.197

	Product		Product		
init mass	g	7056.100	o.g. init	meter read	1322.630
final mass	g	7269.100	o.g. final	meter read	1357.350
corrected	g	7252.000	time	min	8.925
time	hr	0.532	o.g.	slm	15.445
rate	g/hr	367.968	corrected	slm	3.800
sulfur	mass %	0.931	o.g.	mol/hr	9.619
nitrogen	mass %	0.329	H2S+NH4+H2	mol/hr	8.996
carbon	mass %	86.860			
hydrogen	mass %	12.110			

Product by mass balance

Product Boiling Cuts

			H2S	mol/hr	0.495
naptha	mass %	23.236	NH4	mol/hr	0.043
mid dist	mass %	44.034	H2	mol/hr	7.866
gas oil	mass %	24.956	H2S+NH4+H2	mol/hr	8.404
vac resid	mass %	7.774	error	%	6.582
	MCR				
residue	mass %	52.050	carbon bal		
whole prod.	mass %	4.046	error	%	0.037

Product Composition

	sulfur		nitrogen	
	m% of cut	n% of whole	m% of cut	m% of whole
naptha	0.139	0.032	0.018	0.004
mid dist	0.317	0.140	0.146	0.064
gas oil	1.260	0.314	0.554	0.138
vac resid	2.620	0.204	1.110	0.086
	mass % S:	0.690	mass % N:	0.293
	mass % S:		mass % N:	
	(from tot)	0.931	(from tot)	0.000
	error %	25.885	error %	ERR

	N as carbazol,m%	N as carb m% of whole	S as Sulfide,m%	S as Sulfide m% of whole
naptha	0.003	0.001		0.000
mid dist	0.031	0.014		0.000
gas oil	0.232	0.058		0.000
vac resid	0.034	0.003		0.000
	mass % N:	0.075	Mass % S:	0.000
	mass % N:		Mass % S:	
	(from tot)	0.097	(from tot)	
	error %	22.918	error %	ERR
	Hydrogen m% of cut	Hydrogen m% of whole	Carbon m% of cut	Carbon m% of whole
naptha	1.475E+01	3.427E+00	8.493E+01	1.973E+01
mid dist	12.460	5.487	87.680	38.609
gas oil	10.320	2.575	88.010	21.964
vac resid	7.660	0.595	84.060	6.535
	Mass % H:	12.085	mass % C:	86.842
	Mass % H:		mass % C:	
	(from total)	12.110	(from tot)	86.860
	error %	0.207	error %	0.021

component	Gas Analysis by GC-FID		
	response factor	area	mol %
c1	5.577E-07	5.398E+06	3.010
c2	2.696E-07	5.073E+06	1.368
1-c2	2.719E-07	6.724E+04	0.018
c3	1.893E-07	5.813E+06	1.100
1-c3	1.937E-07	1.603E+05	0.031
i-c4	1.482E-07	1.154E+06	0.171
c4	1.433E-07	2.974E+06	0.426
1-c4	1.467E-07	1.022E+05	0.015
2-c4,trans	1.412E-07	4.034E+04	0.006
2-c4,cis	1.403E-07	2.694E+04	0.004
i-c5	1.098E-07	9.532E+05	0.105
c5	1.098E-07	1.156E+06	0.127
1-c5	1.124E-07	1.810E+04	0.002
2-c5	1.124E-07	1.580E+04	0.002
i-c6	9.013E-08	3.582E+05	0.032
c6	9.242E-08	2.279E+05	0.021
1-c6	9.461E-08	3.582E+05	0.034
		Total:(mol%)	6.472

	Supt 10 92	400 C	500 mL/h	13.7 MPa no catalyst	
	Liquid		Gas		
	feed		Feed		
vlt esso	mL/hr	500.000	H2 init	meter read	0.000
temp correct	mL/hr	553.000	H2 final	meter read	0.000
bitumen rate	g/hr	510.419	time	min	0.000
residence t	hr	0.750	H2	slm	5.250
			H	mol/hr	26.579

	Product		Product		
init mass	g	6701.200	o.g. init	meter read	0.000
final mass	g	0.000	o.g. final	meter read	0.000
corrected	g	7151.000	time	min	0.000
time	hr	0.910	o.g.	slm	5.000
rate	g/hr	494.117	corrected	slm	
sulfur	mass %	3.920	o.g.	mol/hr	12.657
nitrogen	mass %	0.412	H2S+NH4+H2	mol/hr	12.576
carbon	mass %	84.140			
hydrogen	mass %	10.540			

Product by mass balance

Product Boiling Cuts					
naptha	mass %	4.511	H2S	mol/hr	0.150
mid dist	mass %	17.952	NH4	mol/hr	0.016
gas oil	mass %	41.658	H2	mol/hr	12.499
vac resid	mass %	35.880	H2S+NH4+H2	mol/hr	12.666
			error	%	-0.719
	MCR				
residue	mass %	33.840	carbon bal		
whole prod.	mass %	12.142	error	%	0.445

Product Composition

	sulfur		nitrogen	
	m% of cut	m% of whole	m% of cut	m% of whole
naptha	1.514	0.068	0.018	0.001
mid dist	2.533	0.455	0.051	0.009
gas oil	3.229	1.345	0.241	0.100
vac resid	5.227	1.875	0.900	0.323
	mass % S:	3.743	mass % N:	0.433
	mass % S:		mass % N:	
	(from tot)	3.920	(from tot)	0.412
	error %	4.508	error %	-5.259

	N as carbazol,m%	N as carb m% of whole	S as Sulfide,m%	S as Sulfide m% of whole
naptha	0.002	0.000		0.000
mid dist	0.007	0.001		0.000
gas oil	0.057	0.024		0.000
vac resid	0.157	0.056		0.000
	mass % N:	0.082	Mass % S:	0.000
	mass % N:		Mass % S:	
	(from tot)	0.079	(from tot)	
	error %	-3.786	error %	ERR

	Hydrogen m% of cut	Hydrogen m% of whole	Carbon m% of cut	Carbon m% of whole
naptha	1.432E+01	6.459E-01	8.527E+01	3.846E+00
mid dist	12.450	2.235	84.900	15.241
gas oil	11.220	4.674	85.260	35.518
vac resid	8.860	3.179	81.850	29.367
	Mass % H:	10.734	mass % C:	83.972
	Mass % H:		mass % C:	
	(from total)	10.540	(from tot)	84.140
	error %	-1.839	error %	0.199

component	Gas Analysis by GC-FID		
	response factor	area	mol %
c1	5.577E-07	4.216E+05	2.351E-01
c2	2.696E-07	4.274E+05	1.152E-01
1-c2	2.719E-07	6.382E+04	1.735E-02
c3	1.893E-07	4.388E+05	8.306E-02
1-c3	1.937E-07	1.352E+05	2.619E-02
i-c4	1.482E-07	7.978E+04	1.182E-02
c4	1.433E-07	2.858E+05	4.096E-02
1-c4	1.467E-07	1.203E+05	1.765E-02
2-c4,trans	1.412E-07	3.338E+04	4.713E-03
2-c4,cis	1.403E-07	2.264E+04	3.176E-03
i-c5	1.098E-07	1.312E+05	1.441E-02
c5	1.098E-07	2.025E+05	2.223E-02
1-c5	1.124E-07	3.874E+04	4.354E-03
2-c5	1.124E-07	2.691E+04	3.025E-03
i-c6	9.013E-08	1.382E+05	1.246E-02
c6	9.242E-08	1.210E+05	1.118E-02
1-c6	9.461E-08	1.399E+05	1.324E-02
		Total:(mol%)	6.362E-01

	Jan 26 93	420 C	400 mL/h	13.7 MPa no catalyst	
	Liquid		Gas		
	feed		Feed		
vlt esso	mL/hr	400.000	H2 init	meter read	2043.800
temp correct	mL/hr	442.400	H2 final	meter read	2052.000
bitumen rate	g/hr	408.335	time	min	8.495
residence t	hr	0.938	H2	slm	4.788
			H	mol/hr	24.240
	Product		Product		
init mass	g	7083.400	o.g. init	meter read	1986.410
final mass	g	7349.200	o.g. final	meter read	1996.730
corrected	g	7355.000	time	min	8.495
time	hr	0.696	o.g.	slm	4.823
rate	g/hr	390.228	corrected	slm	
sulfur	mass %	3.733	o.g.	mol/hr	12.209
nitrogen	mass %	0.474	H2S+NH4+H2	mol/hr	11.997
carbon	mass %	84.290			
hydrogen	mass %	10.470			

Product by mass balance

Product Boiling Cuts					
naptha	mass %	11.078	H2S	mol/hr	0.149
mid dist	mass %	21.467	NH4	mol/hr	-0.003
gas oil	mass %	35.850	H2	mol/hr	11.454
vac resid	mass %	31.605	H2S+NH4+H2	mol/hr	11.601
			error	%	3.306
	MCR				
residue	mass %	38.630	carbon bal		
whole prod.	mass %	12.209	error	%	0.474

Product Composition

	sulfur	sulfur	nitrogen	nitrogen
	m% of cut	m% of whole	m% of cut	m% of whole
naptha	1.480	0.164	0.036	0.004
mid dist	2.840	0.610	0.097	0.021
gas oil	3.490	1.251	0.348	0.125
vac resid	5.020	1.587	1.020	0.322
	mass % S:	3.611	mass % N:	0.472
	mass % S:		mass % N:	
	(from tot)	3.733	(from tot)	0.474
	error %	3.269	error %	0.409

	N as carbazol,m%	N as carb m% of whole	S as Sulfide,m%	S as Sulfide m% of whole
naptha	0.005	0.001		0.000
mid dist	0.018	0.004		0.000
gas oil	0.099	0.035		0.000
vac resid	0.188	0.059		0.000
	mass % N:	0.099	Mass % S:	0.000
	mass % N: (from tot)	0.096	Mass % S: (from tot)	
	error %	-3.892	error %	ERR

	Hydrogen m% of cut	Hydrogen m% of whole	Carbon m% of cut	Carbon m% of whole
naptha	1.358E+01	1.504E+00	8.435E+01	9.344E+00
mid dist	11.940	2.563	85.530	18.361
gas oil	10.740	3.850	85.610	30.691
vac resid	8.770	2.772	82.740	26.150
	Mass % H:	10.690	mass % C:	84.546
	Mass % H: (from total)	10.470	mass % C: (from tot)	84.290
	error %	-2.097	error %	-0.304

component	Gas Analysis by GC-FID		
	response factor	area	mol %
c1	5.577E-07	1.381E+06	0.770
c2	2.696E-07	1.222E+06	0.329
1-c2	2.719E-07	1.088E+05	0.030
c3	1.893E-07	1.311E+06	0.248
1-c3	1.937E-07	2.709E+05	0.052
i-c4	1.482E-07	2.772E+05	0.041
c4	1.433E-07	7.322E+05	0.105
1-c4	1.467E-07	1.944E+05	0.029
2-c4,trans	1.412E-07	6.912E+04	0.010
2-c4,cis	1.403E-07	4.717E+04	0.007
i-c5	1.098E-07	2.929E+05	0.032
c5	1.098E-07	3.593E+05	0.039
1-c5	1.124E-07	4.693E+04	0.005
2-c5	1.124E-07	2.746E+04	0.003
i-c6	9.013E-08	1.260E+05	0.011
c6	9.242E-08	9.922E+04	0.009
1-c6	9.461E-08	1.359E+05	0.013
		Total:(mol%)	1.734

	Jan 26 93	430 C	400 mL/h	13.7 MPa no catalyst	
	Liquid		Gas		
	feed		Feed		
vlt esso	mL/hr	400.000	H2 init	meter read	1749.100
temp correct	mL/hr	442.400	H2 final	meter read	1758.000
bitumen rate	g/hr	408.335	time	min	9.221
residence t	hr	0.938	H2	slm	4.788
			H	mol/hr	24.237

	Product		Product		
init mass	g	7037.900	o.g. init	meter read	1637.590
final mass	g	7401.900	o.g. final	meter read	1648.900
corrected	g	7390.000	time	min	9.221
time	hr	0.913	o.g.	slm	
rate	g/hr	385.580	corrected	slm	3.836
sulfur	mass %	3.621	o.g.	mol/hr	9.711
nitrogen	mass %	0.479	H2S+NH4+H2	mol/hr	9.414
carbon	mass %	84.800			
hydrogen	mass %	11.660			

Product by mass balance

Product Boiling Cuts					
naptha	mass %	9.638	H2S	mol/hr	0.168
mid dist	mass %	32.922	NH4	mol/hr	-0.002
gas oil	mass %	33.908	H2	mol/hr	9.154
vac resid	mass %	23.532	H2S+NH4+H2	mol/hr	9.320
			error	%	0.997
	MCR				
residue	mass %	46.510	carbon bal		
whole prod.	mass %	10.945	error	%	0.467

Product Composition

	sulfur	sulfur	nitrogen	nitrogen
	m% of cut	m% of whole	m% of cut	m% of whole
naptha	0.984	0.095	0.024	0.002
mid dist	2.580	0.849	0.100	0.033
gas oil	3.520	1.194	0.379	0.129
vac resid	4.910	1.155	1.160	0.273
	mass % S:	3.293	mass % N:	0.437
	mass % S:		mass % N:	
	(from tot)	3.621	(from tot)	0.479
	error %	9.052	error %	8.808

	N as carbazol,m%	N as carb m% of whole	S as Sulfide,m%	S as Sulfide m% of whole
naptha	0.005	0.000	0.000	0.000
mid dist	0.016	0.005	0.340	0.112
gas oil	0.135	0.046	0.480	0.163
vac resid	0.253	0.060	0.980	0.231
	mass % N:	0.111	Mass % S:	0.505
	mass % N: (from tot)	0.102	Mass % S: (from tot)	0.790
	error %	-8.598	error %	36.037

	Hydrogen m% of cut	Hydrogen m% of whole	Carbon m% of cut	Carbon m% of whole
naptha	1.455E+01	1.402E+00	8.454E+01	8.148E+00
mid dist	12.100	3.984	85.350	28.099
gas oil	10.410	3.530	85.440	28.971
vac resid	8.090	1.904	84.150	19.803
	Mass % H:	10.819	mass % C:	85.020
	Mass % H: (from total)	11.660	mass % C: (from tot)	84.800
	error %	7.209	error %	-0.260

component	Gas Analysis by GC-FID		mol %
	response factor	area	
c1	5.577E-07	2.577E+06	1.437
c2	2.696E-07	2.177E+06	0.587
1-c2	2.719E-07	1.120E+05	0.030
c3	1.893E-07	2.290E+06	0.433
1-c3	1.937E-07	3.659E+05	0.071
i-c4	1.482E-07	4.980E+05	0.074
c4	1.433E-07	1.235E+06	0.177
1-c4	1.467E-07	2.434E+05	0.036
2-c4,trans	1.412E-07	1.015E+05	0.014
2-c4,cis	1.403E-07	6.858E+04	0.010
i-c5	1.098E-07	4.896E+05	0.054
c5	1.098E-07	6.009E+05	0.066
1-c5	1.124E-07	6.862E+04	0.008
2-c5	1.124E-07	4.647E+04	0.005
i-c6	9.013E-08	2.030E+05	0.018
c6	9.242E-08	1.523E+05	0.014
1-c6	9.461E-08	2.242E+05	0.021
		Total:(mol%)	3.056

Aug 19 92 440 C 545 mL/h 13.7 MPa
no catalyst

This reactor run was done by SCL, supervised by Dr. Edward Chan

Liquid			Gas		
	feed			Feed	
vlt esso	mL/hr	500.000	H2 init	meter read	0.000
temp correct	mL/hr	553.000	H2 final	meter read	0.000
bitumen rate	g/hr	510.419	time	min	0.000
residence t	hr	0.750	H2	slm	5.320
			H	mol/hr	26.933
Product			Product		
init mass	g		o.g. init	meter read	0.000
final mass	g		o.g. final	meter read	0.000
corrected	g		time	min	0.000
time	hr		o.g.	slm	
rate	g/hr	480.000	corrected	slm	5.510
sulfur	mass %	3.570	o.g.	mol/hr	13.947
nitrogen	mass %	0.382	H2S+NH4+H2	mol/hr	13.516
carbon	mass %	85.010			
hydrogen	mass %	10.600			

Product by mass balance

Product Boiling Cuts					
naptha	mass %	12.509	H2S	mol/hr	0.220
mid dist	mass %	28.329	NH4	mol/hr	0.031
gas oil	mass %	34.715	H2	mol/hr	12.125
vac resid	mass %	24.447	H2S+NH4+H2	mol/hr	12.376
			error	%	8.430
MCR					
residue	mass %	47.930	carbon bal		
whole prod.	mass %	11.717	error	%	0.221

Product Composition

	sulfur	sulfur	nitrogen	nitrogen
	m% of cut	m% of whole	m% of cut	m% of whole
naptha	1.157	0.145	0.015	0.002
mid dist	2.666	0.755	0.080	0.023
gas oil	3.815	1.324	0.345	0.120
vac resid	5.487	1.341	1.102	0.269
	mass % S:	3.566	mass % N:	0.414
	mass % S:		mass % N:	
	(from tot)	3.570	(from tot)	0.382
	error %	0.120	error %	-8.410

	N as carbazol,m%	N as carb m% of whole	S as Sulfide,m%	S as Sulfide m% of whole
naptha	0.000	0.000		0.000
mid dist	0.011	0.003		0.000
gas oil	0.099	0.034		0.000
vac resid	0.214	0.052		0.000
	mass % N:	0.090	Mass % S:	0.000
	mass % N: (from tot)	0.086	Mass % S: (from tot)	
	error %	-5.009	error %	ERR
	Hydrogen m% of cut	Hydrogen m% of whole	Carbon m% of cut	Carbon m% of whole
naptha	1.401E+01	1.752E+00	8.466E+01	1.059E+01
mid dist	12.100	3.428	85.030	24.088
gas oil	10.080	3.499	84.830	29.449
vac resid	7.560	1.848	83.290	20.362
	Mass % H:	10.528	mass % C:	84.489
	Mass % H: (from total)	10.600	mass % C: (from tot)	85.010
	error %	0.681	error %	0.613

component	Gas Analysis by GC-FID		
	response factor	area	mol %
c1	5.577E-07	2.491E+06	1.389
c2	2.696E-07	2.279E+06	0.614
1-c2	2.719E-07	1.395E+05	0.038
c3	1.893E-07	2.351E+06	0.445
1-c3	1.937E-07	5.071E+05	0.098
i-c4	1.482E-07	4.957E+05	0.073
c4	1.433E-07	1.200E+06	0.172
1-c4	1.467E-07	3.534E+05	0.052
2-c4,trans	1.412E-07	1.280E+05	0.018
2-c4,cis	1.403E-07	9.026E+04	0.013
i-c5	1.098E-07	4.555E+05	0.050
c5	1.098E-07	5.799E+05	0.064
1-c5	1.124E-07	9.952E+04	0.011
2-c5	1.124E-07	1.274E+05	0.014
i-c6	9.013E-08	2.446E+05	0.022
c6	9.242E-08	1.480E+05	0.014
1-c6	9.461E-08	8.500E+04	0.008
		Total:(mol%)	3.096

	Jan 21 93	430 C	400 mL/h	1485 psig 78 g cat	
				Liquid	Gas
	feed			Feed	
vlt esso	mL/hr	405.000	H2 init	meter read	1128.900
temp correct	mL/hr	447.930	H2 final	meter read	1142.000
bitumen rate	g/hr	413.439	time	min	13.570
residence t	hr	0.926	H2	slm	4.788
			H	mol/hr	24.241

	Product			Product	
init mass	g	7019.700	o.g. init	meter read	1112.390
final mass	g	7401.900	o.g. final	meter read	1126.600
corrected	g	7369.000	time	min	13.570
time	hr	0.910	o.g.	slm	4.216
rate	g/hr	383.715	corrected	slm	
sulfur	mass %	1.210	o.g.	mol/hr	10.672
nitrogen	mass %	0.382	H2S+NH4+H2	mol/hr	10.355
carbon	mass %	86.670			
hydrogen	mass %	11.660			

	Product Boiling Cuts			Product by mass balance	
naptha	mass %	13.445	H2S	mol/hr	0.466
mid dist	mass %	32.929	NH4	mol/hr	0.026
gas oil	mass %	34.751	H2	mol/hr	9.078
vac resid	mass %	18.875	H2S+NH4+H2	mol/hr	9.571
			error	%	7.573
	MCR				
residue	mass %	31.400	carbon bal		
whole prod.	mass %	5.927	error	%	-0.130

	Product Composition			
	sulfur	sulfur	nitrogen	nitrogen
	m% of cut	m% of whole	m% of cut	m% of whole
naptha	0.118	0.016	0.020	0.003
mid dist	0.264	0.087	0.116	0.038
gas oil	0.971	0.337	0.364	0.126
vac resid	2.700	0.510	0.885	0.167
	mass % S:	0.950	mass % N:	0.334
	mass % S:		mass % N:	
	(from tot)	1.210	(from tot)	0.382
	error %	21.500	error %	12.469

	N as carbazol,m%	N as carb m% of whole	S as Sulfide,m%	S as Sulfide m% of whole
naptha	0.002	0.000	0.000	0.000
mid dist	0.024	0.008	0.170	0.056
gas oil	0.134	0.047	0.230	0.080
vac resid	0.245	0.046	0.710	0.134
	mass % N:	0.101	Mass % S:	0.270
	mass % N: (from tot)	0.090	Mass % S: (from tot)	0.150
	error %	-12.605	error %	-79.946

	Hydrogen m% of cut	Hydrogen m% of whole	Carbon m% of cut	Carbon m% of whole
naptha	14.660	1.971	85.330	11.472
mid dist	12.510	4.119	87.560	28.833
gas oil	11.230	3.903	87.400	30.372
vac resid	9.320	1.759	85.900	16.214
	Mass % H:	11.752	mass % N:	86.891
	Mass % H: (from total)	11.660	mass % N: (from tot)	86.670
	error %	0.784	error %	0.255

component	Gas Analysis by GC-FID		
	response factor	area	mol %
c1	5.577E-07	2.427E+06	1.354
c2	2.696E-07	2.236E+06	0.603
1-c2	2.719E-07	2.066E+04	0.006
c3	1.893E-07	2.668E+06	0.505
1-c3	1.937E-07	6.268E+04	0.012
i-c4	1.482E-07	5.747E+05	0.085
c4	1.433E-07	1.478E+06	0.212
1-c4	1.467E-07	5.239E+04	0.008
2-c4,trans	1.412E-07	1.709E+04	0.002
2-c4,cis	1.403E-07	1.128E+04	0.002
i-c5	1.098E-07	5.216E+05	0.057
c5	1.098E-07	6.342E+05	0.070
1-c5	1.124E-07	7.428E+03	0.001
2-c5	1.124E-07	1.602E+04	0.002
i-c6	9.013E-08	2.235E+05	0.020
c6	9.242E-08	1.265E+05	0.012
1-c6	9.461E-08	2.116E+05	0.020
		Total:(mol%)	2.969

	Jan 6 93	430 C	400 mL/h 78 g cat	13.7 MPa 925 um ground	
	Liquid		Gas		
	feed			Feed	
vlt esso	mL/hr	405.000	H2 init	meter read	361.320
temp correct	mL/hr	447.930	H2 final	meter read	367.600
bitumen rate	g/hr	413.439	time	min	6.515
residence t	hr	0.926	H2	slm	4.781
			H	mol/hr	24.205
	Product		Product		
init mass	g	7118.000	o.g. init	meter read	370.750
final mass	g	7536.600	o.g. final	meter read	377.350
corrected	g	7470.000	time	min	6.515
time	hr	0.917	o.g.	slm	4.022
rate	g/hr	383.862	corrected	slm	
sulfur	mass %	0.982	c.g.	mol/hr	10.180
nitrogen	mass %	0.327	H2S+NH4+H2	mol/hr	9.845
carbon	mass %	86.760			
hydrogen	mass %	11.720			
	Product by mass balance				
	Product Boiling Cuts				
naptha	mass %	22.786	H2S	mol/hr	0.494
mid dist	mass %	22.920	NH4	mol/hr	0.041
gas oil	mass %	35.928	H2	mol/hr	8.820
vac resid	mass %	18.366	H2S+NH4+H2	mol/hr	9.354
			error	%	4.982
	MCR				
residue	mass %	38.870	carbon bal		
whole prod.	mass %	7.139	error	%	-0.409
	Product Composition				
	sulfur	sulfur	nitrogen	nitrogen	
	m% of cut	m% of whole	m% of cut	m% of whole	
naptha	0.042	0.010	0.014	0.003	
mid dist	0.185	0.042	0.103	0.024	
gas oil	0.879	0.316	0.353	0.127	
vac resid	2.650	0.487	0.884	0.162	
	mass % S:	0.855	mass % N:	0.316	
	mass % S:		mass % N:		
	(from tot)	0.982	(from tot)	0.327	
	error %	12.980	error %	3.357	

	N as carbazol,m%	N as carb m% of whole	S as Sulfide,m%	S as Sulfide m% of whole
naptha	0.002	0.000		0.000
mid dist	0.020	0.005		0.000
gas oil	0.130	0.047		0.000
vac resid	0.245	0.045		0.000
	mass % N:	0.097	Mass % S:	0.000
	mass % N:		Mass % S:	
	(from tot)	0.086	(from tot)	
	error %	-12.769	error %	ERR

	Hydrogen m% of cut	Hydrogen m% of whole	Carbon m% of cut	Carbon m% of whole
naptha	14.760	3.363	85.680	19.523
mid dist	12.690	2.908	87.400	20.032
gas oil	11.290	4.056	87.180	31.322
vac resid	8.720	1.601	82.680	15.185
	Mass % H:	11.930	mass % C:	86.062
	Mass % H:		mass % C:	
	(from total)	11.720	(from tot)	86.760
	error %	1.757	error %	-0.811

component	Gas Analysis by GC-FID		
	response factor	area	mol %
c1	5.577E-07	2.685E+06	1.497
c2	2.696E-07	2.532E+06	0.683
1-c2	2.719E-07	0.000E+00	0.000
c3	1.893E-07	2.975E+06	0.563
1-c3	1.937E-07	3.360E+04	0.007
i-c4	1.482E-07	6.606E+05	0.098
c4	1.433E-07	1.674E+06	0.240
1-c4	1.467E-07	2.592E+04	0.004
2-c4,trans	1.412E-07	9.348E+03	0.001
2-c4,cis	1.403E-07	5.865E+03	0.001
i-c5	1.098E-07	6.019E+05	0.066
c5	1.098E-07	7.190E+05	0.079
1-c5	1.124E-07	0.000E+00	0.000
2-c5	1.124E-07	1.630E+03	0.000
i-c6	9.013E-08	2.433E+05	0.022
c6	9.242E-08	1.366E+05	0.013
1-c6	9.461E-08	2.289E+05	0.022
		Total:(mol%)	3.295

	Jan 19 93	430 C	400 mL/h 78 g cat	13.7 MPa 600 um ground	
	Liquid		Gas		
	feed		Feed		
vlt esso	mL/hr	408.000	H2 init	meter read	384.430
temp correct	mL/hr	451.248	H2 final	meter read	391.340
bitumen rate	g/hr	416.502	time	min	7.158
residence t	hr	0.919	H2	slm	4.788
			H	mol/hr	24.242

	Product		Product		
init mass	g	7179.900	o.g. init	meter read	405.600
final mass	g	7500.200	o.g. final	meter read	413.200
corrected	g	7515.000	time	min	7.158
time	hr	0.868	o.g.	slm	4.215
rate	g/hr	385.870	corrected	slm	
sulfur	mass %	1.098	o.g.	mol/hr	10.670
nitrogen	mass %	0.349	H2S+NH4+H2	mol/hr	10.208
carbon	mass %	86.360			
hydrogen	mass %	11.720			

Product by mass balance

Product Boiling Cuts					
naptha	mass %	16.334	H2S	mol/hr	0.484
mid dist	mass %	34.361	NH4	mol/hr	0.036
gas oil	mass %	33.350	H2	mol/hr	8.521
vac resid	mass %	15.956	H2S+NH4+H2	mol/hr	9.040
			error	%	11.442
	MCR				
residue	mass %	28.910	carbon bal		
whole prod.	mass %	4.613	error	%	-0.604

Product Composition

	sulfur	sulfur	nitrogen	nitrogen
	m% of cut	m% of whole	m% of cut	m% of whole
naptha	0.042	0.007	0.015	0.002
mid dist	0.207	0.071	0.117	0.040
gas oil	1.000	0.334	0.378	0.126
vac resid	2.530	0.404	0.869	0.139
	mass % S:	0.815	mass % N:	0.307
	mass % S:		mass % N:	
	(from tot)	1.100	(from tot)	0.349
	error %	25.897	error %	11.933

	N as carbazol,m%	N as carb m% of whole	S as Sulfide,m%	S as Sulfide m% of whole
naptha	0.002	0.000		0.000
mid dist	0.024	0.008		0.000
gas oil	0.142	0.047		0.000
vac resid	0.250	0.040		0.000
	mass % N:	0.096	Mass % S:	0.000
	mass % N: (from tot)	0.085	Mass % S: (from tot)	
	error %	-13.426	error %	ERR

	Hydrogen m% of cut	Hydrogen m% of whole	Carbon m% of cut	Carbon m% of whole
naptha	14.760	2.411	85.590	13.980
mid dist	12.510	4.299	86.890	29.856
gas oil	11.150	3.719	87.400	29.148
vac resid	9.510	1.517	85.880	13.703
	Mass % H:	11.945	mass % C:	86.687
	Mass % H: (from total)	11.720	mass % C: (from tot)	86.360
	error %	1.886	error %	0.377

Gas Analysis by GC-FID

component	response factor	area	mol %
c1	5.577E-07	3.644E+06	2.032
c2	2.696E-07	3.278E+06	0.884
1-c2	2.719E-07	4.769E+04	0.013
c3	1.893E-07	3.768E+06	0.713
1-c3	1.937E-07	3.861E+04	0.007
i-c4	1.482E-07	8.220E+05	0.122
c4	1.433E-07	2.080E+06	0.298
1-c4	1.467E-07	2.771E+04	0.004
2-c4,trans	1.412E-07	1.127E+04	0.002
2-c4,cis	1.403E-07	7.284E+03	0.001
i-c5	1.098E-07	8.372E+05	0.092
c5	1.098E-07	8.776E+05	0.096
1-c5	1.124E-07	0.000E+00	0.000
2-c5	1.124E-07	1.956E+03	0.000
i-c6	9.013E-08	2.733E+05	0.025
c6	9.242E-08	1.636E+05	0.015
1-c6	9.461E-08	2.731E+05	0.026
		Total:(mol%)	4.330

Appendix B
Metals Content

Metals Accumulation

Fe	Si	Al	Co	Ni	Mg
352.24	954.56	676.69	1.43	85.78	40.94
V	Na	Mo	Ca	Ti	Mn
227.61	60.02	10.76	104.32	124.72	11.72
Cd	Cr	Cu	P	Zn	Pb
0.00	1.31	0.63	0.00	2.13	0.00

Fe	Si	Al	Co	Ni	Mg
0.51	0.00	0.00	0.00	14.44	-
V	Na	Mo	Ca	Ti	Mn
24.33	0.00	0.00	0.58	0.43	0.00
Cd	Cr	Cu	P	Zn	Pb
-	-	-	0.00	0.00	0.00

- indicates intensity below calibration curve range

Summing the metals which could end up in the catalyst (Ni and V) and doing a balance for the 400 ml/h run (3HPP0014) gives an estimated metals laydown of 0.11 g/h. For the 6 h needed to reach the midpoint of the product collection, this gives an accumulation of approximately 0.64 g of metal. The added catalyst (Criterion HDS-1443) had a total of 8.6 g of Ni and Mo. The thermal run done at the same conditions

(3HPP0026) gave an accumulation of approximately 0.40 g of Ni and V, indicating a relatively insignificant metal accumulation on the catalyst of 0.24 g by difference. The other elements would be expected to be associated with clays, some of which were observed on the sides of the product collection drum.

Appendix C
Arrhenius Plots

